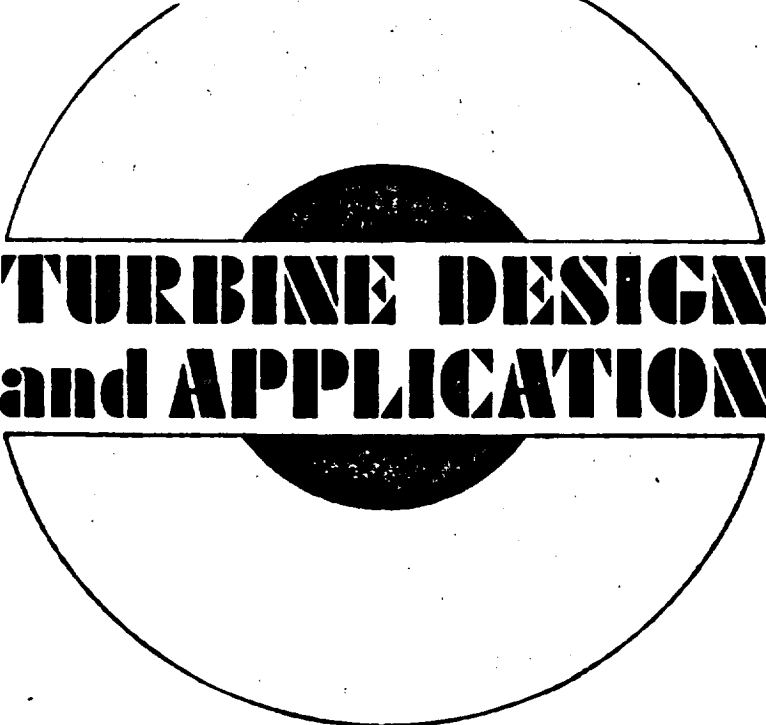


VOLUME ONE

NASA SP-290

N72-26685
thru
N72-26688
Unclass
31362

H1/28

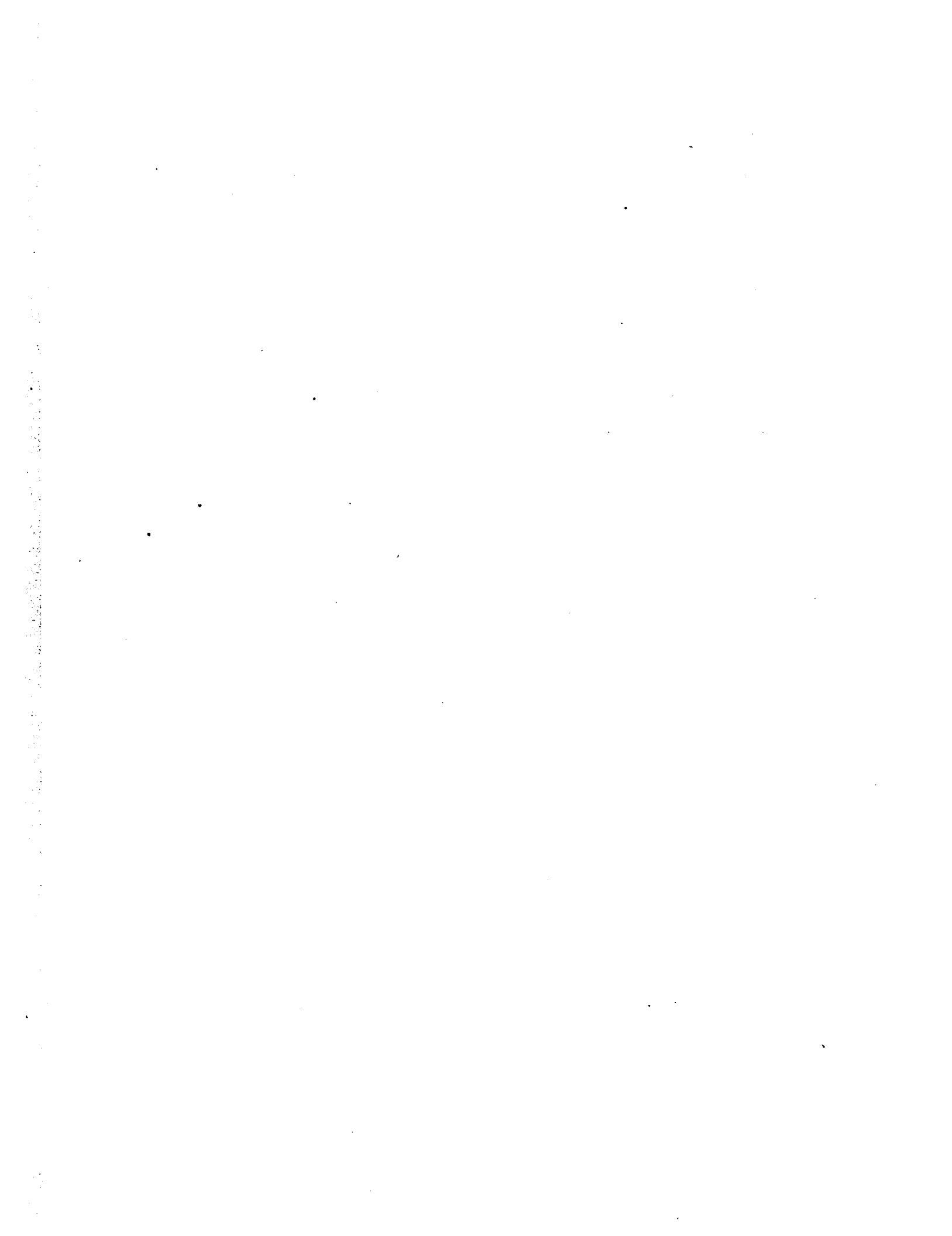


**TURBINE DESIGN
and APPLICATION**

REPRODUCED BY
U.S. DEPARTMENT OF COMMERCE
NATIONAL TECHNICAL
INFORMATION SERVICE
SPRINGFIELD, VA. 22161

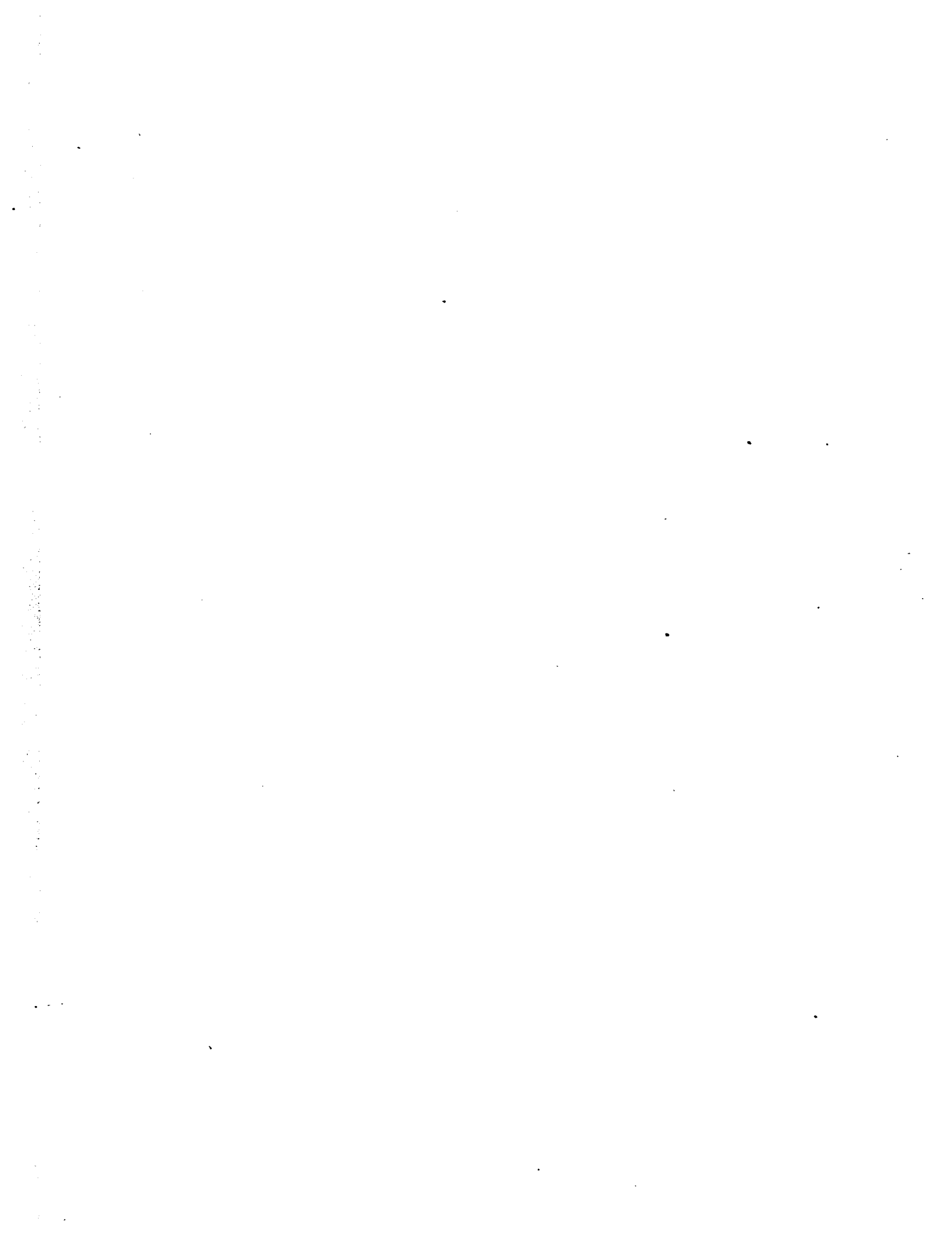


NATIONAL AERONAUTICS AND SPACE ADMINISTRATION



N O T I C E

THIS DOCUMENT HAS BEEN REPRODUCED FROM THE BEST COPY FURNISHED US BY THE SPONSORING AGENCY. ALTHOUGH IT IS RECOGNIZED THAT CERTAIN PORTIONS ARE ILLEGIBLE, IT IS BEING RELEASED IN THE INTEREST OF MAKING AVAILABLE AS MUCH INFORMATION AS POSSIBLE.



NASA SP-290

TURBINE DESIGN and APPLICATION

VOLUME ONE

Edited by Arthur J. Glassman
Lewis Research Center



Scientific and Technical Information Office 1972
NATIONAL AERONAUTICS AND SPACE ADMINISTRATION
Washington, D.C.

For sale by the Superintendent of Documents
U.S. Government Printing Office, Washington, D.C. 20402
Stock Number 3300-0418
Library of Congress Catalog Card Number 79-185105

PREFACE

NASA has an interest in turbines related primarily to aeronautics and space applications. Airbreathing turbine engines provide jet and turboshaft propulsion, as well as auxiliary power for aircraft. Propellant-driven turbines provide rocket propulsion and auxiliary power for spacecraft. Closed-cycle turbine engines using inert gases, organic fluids, and metal fluids are being studied for providing long-duration electric power for spacecraft.

In view of the turbine-system interest and efforts at Lewis Research Center, a course entitled "Turbine Design and Application" was presented during 1968-69 as part of the In-House Graduate Study Program. The course was prepared and presented primarily by members of the Turbodrives Branch, Fluid System Components Division, and consisted of 25 lectures covering all aspects of turbine technology. In particular, the course material covered thermodynamic and fluid-dynamic concepts, fundamental turbine concepts, velocity diagrams, losses, blade aerodynamic design, mechanical design, operation, performance, and requirements and problems associated with various applications. Much of the material referred primarily to axial-flow turbines, with radial-inflow turbines covered as a specific topic.

The notes written and used for the course are being revised and edited for publication. Such a publication can serve as a foundation for an introductory turbine course, a means for self-study, or a reference for selected topics. This volume presents the material covered in the first six lectures of the course. The three chapters of this volume cover thermodynamic and fluid-dynamic concepts, fundamental turbine concepts, and velocity diagram design.

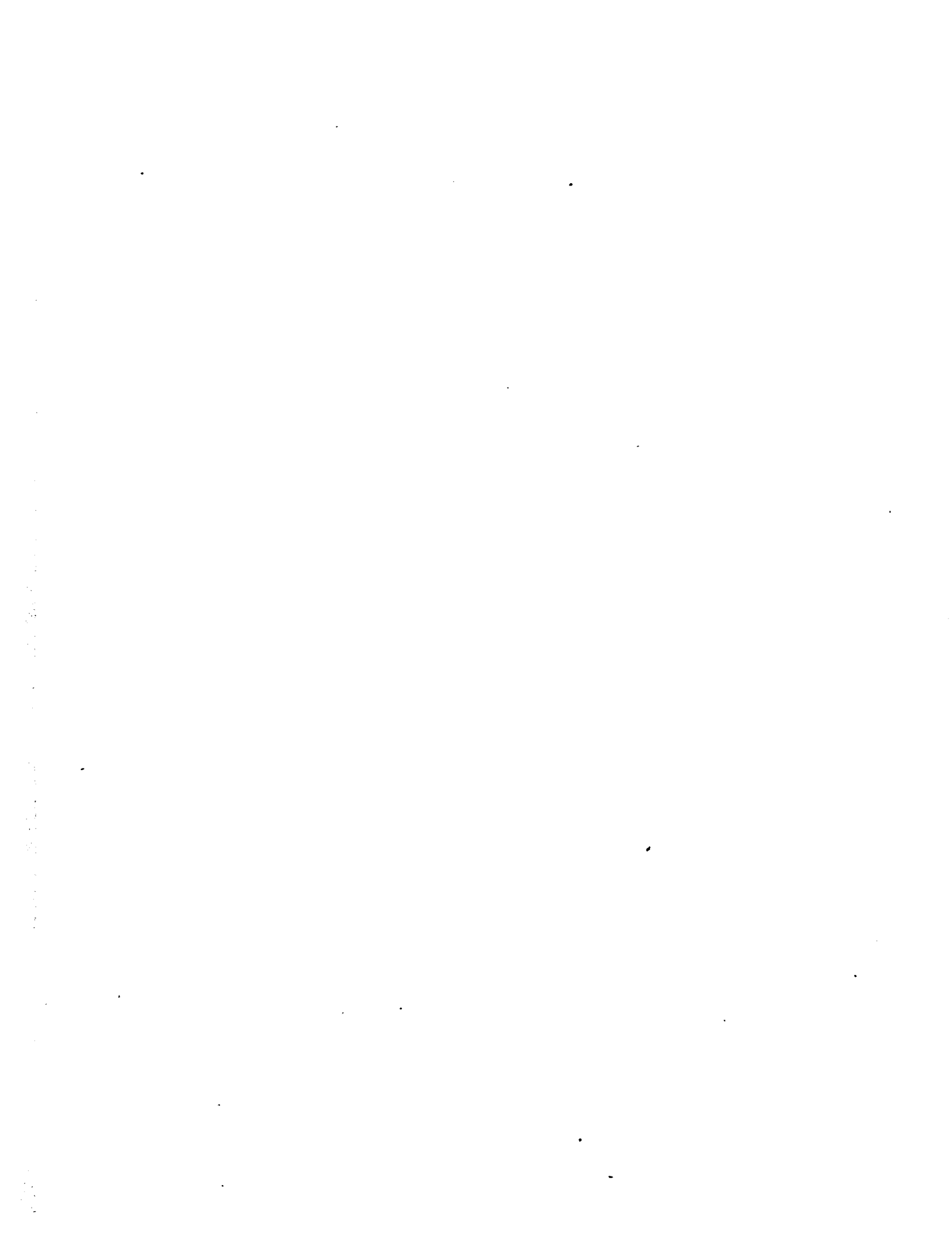
ARTHUR J. GLASSMAN

PRECEDING PAGE BLANK NOT FILMED

CONTENTS

CHAPTER	PAGE
<i>PREFACE</i>	iii
1 <i>THERMODYNAMIC AND FLUID-DYNAMIC CONCEPTS</i> by Arthur J. Glassman.....	1
BASIC CONCEPTS AND RELATIONS.....	1
APPLICATION TO FLOW WITH VARYING AREA.....	14
REFERENCES.....	19
SYMBOLS.....	20
2 <i>BASIC TURBINE CONCEPTS</i> by Arthur J. Glassman....	21
TURBINE FLOW AND ENERGY TRANSFER.....	21
DIMENSIONLESS PARAMETERS.....	45
REFERENCES.....	62
SYMBOLS.....	63
GLOSSARY.....	65
3 <i>VELOCITY DIAGRAMS</i> by Warren J. Whitney and Warner L. Stewart.....	69
MEAN-SECTION DIAGRAMS.....	70
RADIAL VARIATION OF DIAGRAMS.....	84
COMPUTER PROGRAMS FOR VELOCITY-DIAGRAM STUDIES.....	95
REFERENCES.....	96
SYMBOLS.....	98

Preceding page blank



CHAPTER 1

Thermodynamic and Fluid-Dynamic Concepts

By Arthur J. Glassman

This chapter is intended to review some of the fundamental concepts of thermodynamics and compressible fluid mechanics. These are the concepts needed to analyze and understand the flow and energy-transfer processes occurring in a turbine. A more complete treatment of these subjects can be found in reference 1 and in many textbooks. Flow is assumed to be steady and one-dimensional for the purposes of this chapter.

Any consistent set of units will satisfy the equations presented. Two commonly used consistent sets of units and constant values are given after the symbol definitions. These are the SI units and the U.S. customary units. A single set of equations covers both sets of units by including all constants required for the U.S. customary units and defining as unity those not required for the SI units.

BASIC CONCEPTS AND RELATIONS

Equation of State

Before we can get very far with any kind of calculation involving gases, we must know how pressure, volume, and temperature are interrelated. The study of gases has resulted in certain laws and generalizations concerning their behavior. In discussing these laws of behavior, gases are referred to as being either ideal or real. The

TURBINE DESIGN AND APPLICATION

ideal gas is only hypothetical and obeys various simplified laws that the real gas can only approach under certain conditions.

The ideal gas equation of state is

$$pv = \frac{R^*}{M_w} T \quad (1-1)$$

where

p absolute pressure, N/m²; lb/ft²

v specific volume, m³/kg; ft³/lb

R^* universal gas constant, 8314 J/(kg mole)(K); 1545 (ft)(lb)/(lb mole)(°R)

M_w molecular weight, kg/(kg mole); lb/(lb mole)

T absolute temperature, K; °R

The quantity R^*/M_w is often used as a single quantity such that

$$R = \frac{R^*}{M_w} \quad (1-2)$$

where R is the gas constant, in J/(kg)(K) or (ft)(lb)/(lb)(°R).

Density is often used instead of specific volume in the ideal gas law. Thus,

$$p = \frac{1}{v} RT = \rho RT \quad (1-3)$$

where ρ is density, in kg/m³ or lb/ft³.

In general, a real gas will approximate ideal behavior at low pressures or high temperatures, conditions under which the free space within the gas is large and the attractive forces between molecules are small. For gases which are above their critical temperatures, the ideal gas law may be accurate to within 5 percent up to pressures as high as 50 atmospheres, while for gases below their critical temperatures, deviations of 2 to 3 percent may appear at 1 atmosphere pressure.

Deviations of real gases from ideal behavior have resulted in the proposal of several hundred equations of state to express the p - v - T relation. None of these have been found universally satisfactory, and most are applicable only to a single gas over a limited range of temperature and pressure. Even the most useful of these equations are cumbersome to use and cannot be justified unless a high degree of accuracy is required.

The similarity in behavior of substances at equal values of reduced temperature (ratio of temperature, T , to critical temperature, T_c) and reduced pressure (ratio of pressure, p , to critical pressure, p_c) forms the basis of a relatively simple method for estimating real gas behavior. The method of general correlation is to incorporate a

THERMODYNAMIC AND FLUID-DYNAMIC CONCEPTS

correction term, called the compressibility factor, into the ideal gas law:

$$p = z\rho RT \quad (1-4)$$

where z is the compressibility factor.

The compressibility factor is a function of reduced temperature and reduced pressure, and is assumed to be independent of the nature of the gas. Values of compressibility factor as a function of reduced temperature and reduced pressure are presented in many texts and other sources. One of the charts from reference 2 is reproduced here as figure 1-1. This type of correlation is derived from an average of data for a large number of gases and is not in rigorous agreement with all the data for any one gas. The compressibility-factor correlation may be extended to gas mixtures if pseudocritical temperatures and pressures are used to calculate reduced temperatures and pressures. The pseudocritical properties are approximated by using the molal averages of the critical properties of the components.

Examination of figure 1-1 shows that there is a large region of state conditions where use of the ideal gas law would result in a large error. Fortunately, the conditions that we are concerned with in our calculations do not usually fall within this region. However, we should never take for granted that the ideal gas law is always valid. A quick determination of the compressibility factor can show the approximate error associated with use of the ideal gas law.

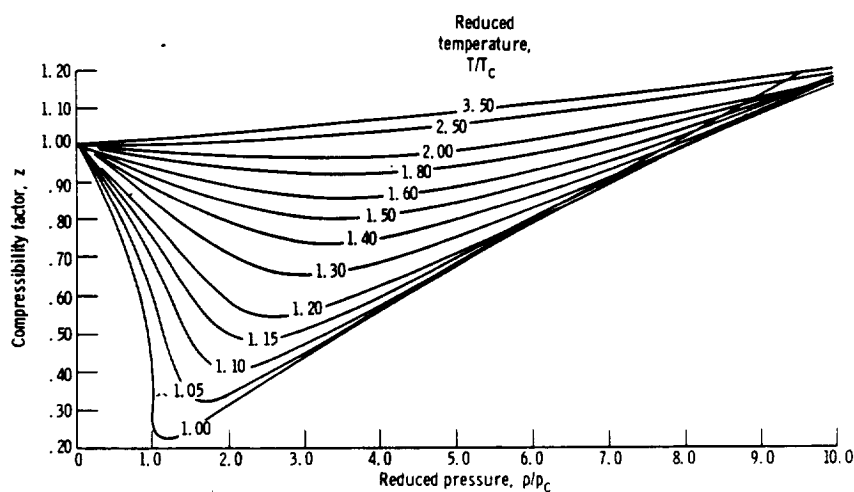


FIGURE 1-1.—Effect of reduced pressure and reduced temperature on compressibility factor. (Curves from ref. 2.)

Relation of Energy Change to State Conditions

In a flow process, the energy term associated with work and heat is the enthalpy h . For a one-phase system of constant chemical composition, enthalpy can be expressed as a function of temperature and pressure:

$$h = \text{fcn}(T, p) \quad (1-5)$$

where h is specific enthalpy, in J/kg or Btu/lb. A differential change in enthalpy can be expressed as

$$dh = \left(\frac{\partial h}{\partial T} \right)_p dT + \left(\frac{\partial h}{\partial p} \right)_T dp \quad (1-6)$$

The partial derivatives can be expressed in terms of determinable properties as follows. By definition,

$$c_p = \left(\frac{\partial h}{\partial T} \right)_p \quad (1-7)$$

where c_p is heat capacity at constant pressure, in J/(kg)(K) or Btu/(lb)(°R). One of the basic differential equations of thermodynamics is

$$dh = T ds + \frac{1}{J} v dp \quad (1-8)$$

where s is specific entropy, in J/(kg)(K) or Btu/(lb)(°R), and J is a conversion constant, 1 or 778 (ft)(lb)/Btu. Therefore, the partial derivative with respect to pressure at constant temperature is, as determined from equation (1-8),

$$\left(\frac{\partial h}{\partial p} \right)_T = T \left(\frac{\partial s}{\partial p} \right)_T + \frac{1}{J} v \quad (1-9)$$

One of the Maxwell relations states that

$$\left(\frac{\partial s}{\partial p} \right)_T = -\frac{1}{J} \left(\frac{\partial v}{\partial T} \right)_p \quad (1-10)$$

Substituting equations (1-7), (1-9), and (1-10) into equation (1-6) yields

$$dh = c_p dT + \frac{1}{J} \left[v - T \left(\frac{\partial v}{\partial T} \right)_p \right] dp \quad (1-11)$$

Equation (1-11) is the rigorous equation for a differential enthalpy change in terms of the state conditions, and the enthalpy change between two states is calculated rigorously as

$$\Delta h = \int_{T_1}^{T_2} c_p dT + \frac{1}{J} \int_{p_1}^{p_2} \left[v - T \left(\frac{\partial v}{\partial T} \right)_p \right] dp \quad (1-12)$$

If we now assume that the gas behaves according to the ideal gas law, we can set

$$v = \frac{RT}{p} \quad (1-13)$$

and

$$\left(\frac{\partial v}{\partial T} \right)_p = \frac{R}{p} \quad (1-14)$$

By using these last two equations in equation (1-12), the effect of pressure on enthalpy change is reduced to zero, and there remains

$$\Delta h = \int_{T_1}^{T_2} c_p dT \quad (1-15)$$

Empirical equations for c_p as a function of T are available in handbooks and textbooks for most gases of interest. If, for example,

$$c_p = a + bT + cT^2 \quad (1-16)$$

then integration of equation (1-15) yields

$$\Delta h = a(T_2 - T_1) + \frac{b}{2} (T_2^2 - T_1^2) + \frac{c}{3} (T_2^3 - T_1^3) \quad (1-17)$$

Although one might not want to use this type of expression for hand calculations, there is no reason to avoid it for computer calculations.

If it can be assumed that c_p is constant between temperatures T_1 and T_2 , then equation (1-15) becomes

$$\Delta h = c_p (T_2 - T_1) \quad (1-18)$$

This assumption is an excellent one for monatomic gases; for other gases, there is a significant variation in c_p with T . However, the use of some average value for c_p will give an approximation that should be within a few percent of the true value.

Relation of State Conditions for Constant Entropy Process

In a turbine, the heat loss is normally small, and the flow process usually can be assumed to be adiabatic. For adiabatic flow with no loss, there is no change in entropy. Therefore, the constant-entropy (isentropic) process is the ideal process for flow in the various parts of the turbine (inlet manifold, stator, rotor, and exit diffuser) as well as for the overall turbine. Actual conditions within and across the

TURBINE DESIGN AND APPLICATION

turbine are usually determined from isentropic process calculations in conjunction with some efficiency or loss term. It is, therefore, necessary to be able to relate state conditions for an isentropic process.

For a one-phase system of constant chemical composition, entropy can be expressed as a function of temperature and pressure

$$s = \text{fcn}(T, p) \quad (1-19)$$

and a differential change in entropy can be expressed as

$$ds = \left(\frac{\partial s}{\partial T} \right)_p dT + \left(\frac{\partial s}{\partial p} \right)_T dp \quad (1-20)$$

From equations (1-8) and (1-7), we get

$$\left(\frac{\partial s}{\partial T} \right)_p = \frac{1}{T} \left(\frac{\partial h}{\partial T} \right)_p = \frac{c_p}{T} \quad (1-21)$$

Substituting equations (1-21) and (1-10) into equation (1-20) yields

$$ds = \frac{c_p}{T} dT - \frac{1}{J} \left(\frac{\partial v}{\partial T} \right)_p dp \quad (1-22)$$

For a constant-entropy process, $ds=0$ and

$$\int_{T_1}^{T_2} \frac{c_p}{T} dT = \frac{1}{J} \int_{p_1}^{p_2} \left(\frac{\partial v}{\partial T} \right)_p dp \quad (1-23)$$

Equation (1-23) is the rigorous, but not particularly useful, expression relating temperature and pressure conditions for an isentropic process.

If we assume ideal-gas-law behavior and substitute equation (1-14) into equation (1-23) and perform the integration, we get

$$\int_{T_1}^{T_2} \frac{c_p}{T} dT = \frac{1}{J} R \ln \frac{p_2}{p_1} \quad (1-24)$$

By using a relation such as equation (1-16), integration yields

$$\frac{1}{J} R \ln \frac{p_2}{p_1} = a \ln \frac{T_2}{T_1} + b(T_2 - T_1) + \frac{c}{2} (T_2^2 - T_1^2) \quad (1-25)$$

Like equation (1-17), equation (1-25) also is more suitable for use in a computer calculation than in a hand calculation.

With the additional assumption that c_p is constant between temperatures T_1 and T_2 , equation (1-24) becomes

THERMODYNAMIC AND FLUID-DYNAMIC CONCEPTS

$$Jc_p \ln \frac{T_2}{T_1} = R \ln \frac{p_2}{p_1} \quad (1-26)$$

and

$$\frac{p_2}{p_1} = \left(\frac{T_2}{T_1} \right)^{Jc_p/R} \quad (1-27)$$

But

$$\frac{Jc_p}{R} = \frac{\gamma}{\gamma - 1} \quad (1-28)$$

where γ is the ratio of heat capacity at constant pressure to heat capacity at constant volume. Substitution of equation (1-28) into equation (1-27) yields the more familiar form

$$\frac{p_2}{p_1} = \left(\frac{T_2}{T_1} \right)^{\gamma/(\gamma-1)} \quad (1-29)$$

Where specific heat ratio γ is not constant, the use of an average value should give a reasonable approximation.

Conservation of Mass

The rate of mass flow through an area A can be expressed as

$$w = \rho AV \quad (1-30)$$

where

w rate of mass flow, kg/sec; lb/sec

A flow area, m²; ft²

V fluid velocity, m/sec; ft/sec

For a steady flow (and nonnuclear) process, the rate of mass flow across any section of the flow path must equal the rate of mass flow across any other section. That is,

$$\rho_1 A_1 V_1 = \rho_2 A_2 V_2 \quad (1-31)$$

This expresses the principle of conservation of mass, and equation (1-31) is referred to as the continuity equation.

Newton's Second Law of Motion

All conservation equations, theorems, etc., dealing with momentum are consequences of Newton's Second Law of Motion, which states that an unbalanced force that acts on a body will cause it to accelerate in the direction of the unbalanced force in such a manner that the force is proportional to the product of the mass and acceleration of the body.

TURBINE DESIGN AND APPLICATION

Thus,

$$F = \frac{m}{g} a \quad (1-32)$$

where

F unbalanced force, N; lbf

m mass, kg; lbm

a acceleration, m/sec²; ft/sec²

g conversion constant, 1; 32.17 (lbm)(ft)/(lbf)(sec²)

But

$$a = \frac{dV}{dt} \quad (1-33)$$

where t is time, in seconds. Substituting equation (1-33) into equation (1-32) yields

$$F = \frac{m}{g} \frac{dV}{dt} \quad (1-34a)$$

Since the mass is constant, equation (1-34a) can also be written as

$$F = \frac{1}{g} \frac{d(mV)}{dt} \quad (1-34b)$$

Equation (1-34b) specifies that the unbalanced force acting on the fluid is equal to the rate of change of momentum (mV) with time. Since mass per increment of time is the mass flow rate, equation (1-34a) can also be written as

$$F = \frac{w}{g} dV \quad (1-35)$$

A useful relation, sometimes called the equation of motion, can be derived from second-law considerations. Consider an element of fluid as indicated in figure 1-2. Gravitational forces are assumed negligible. A frictional resistance (force) is indicated as R_f . The element of fluid is subjected to fluid-pressure and boundary-surface-pressure forces acting in the downstream direction and fluid-pressure and friction forces acting in the upstream direction. Therefore, the net force in the downstream direction is

$$F = pA + \left(p + \frac{dp}{2}\right)dA - (p + dp)(A + dA) - dR_f \quad (1-36)$$

Expanding, simplifying, and dropping second-order differentials yields

$$F = -Adp - dR_f \quad (1-37)$$

THERMODYNAMIC AND FLUID-DYNAMIC CONCEPTS

The mass of the element is

$$m = \rho A dx \quad (1-38)$$

Substituting equation (1-38) into equation (1-34) yields

$$F = \frac{\rho A dx}{g} \frac{dV}{dt} \quad (1-39)$$

Since

$$V = \frac{dx}{dt} \quad (1-40)$$

equation (1-39) can be written in the form

$$F = \frac{\rho A V}{g} dV \quad (1-41)$$

Equating (1-37) with (1-41) now yields

$$F = -Adp - dR_f = \frac{\rho A}{g} V dV \quad (1-42)$$

and

$$\frac{dp}{\rho} + \frac{V dV}{g} + \frac{dR_f}{\rho A} = 0 \quad (1-43)$$

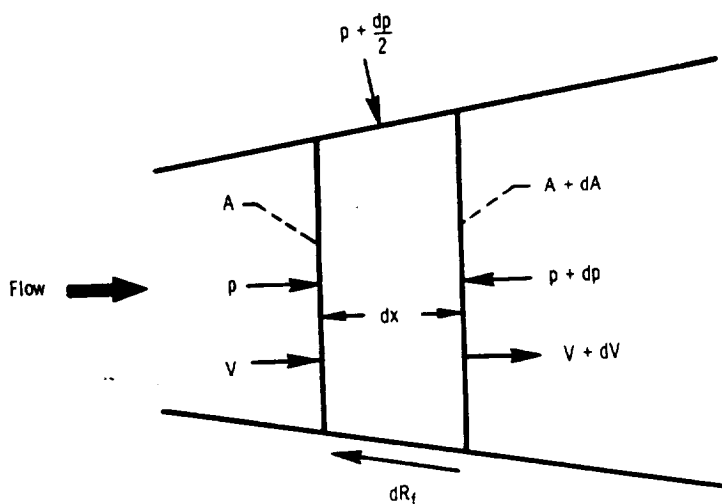


FIGURE 1-2.—Forces on an element of fluid.

If we now let

$$Jdq_f = \frac{dR_f}{\rho A} \quad (1-44)$$

where q_f is heat produced by friction, in J/kg or Btu/lb, we have

$$\frac{dp}{\rho} + \frac{VdV}{g} + Jdq_f = 0 \quad (1-45)$$

For isentropic flow, $dq_f = 0$.

Conservation of Energy

For a steady-flow (and nonnuclear) process, the energy entering a system or part of a system must equal the energy leaving that system or part of that system. If we can neglect chemical energy, electrical energy, etc., we still have to consider internal energy u , flow energy pv , kinetic energy $V^2/2g$, potential energy Z , heat q , and mechanical work W_s . Thus,

$$u_1 + \frac{p_1 v_1}{J} + \frac{V_1^2}{2gJ} + \frac{Z_1}{J} + q = u_2 + \frac{p_2 v_2}{J} + \frac{V_2^2}{2gJ} + \frac{Z_2}{J} + W_s \quad (1-46)$$

where

- u specific internal energy, J/kg; Btu/lb
- Z specific potential energy, J/kg; (ft) (lbf)/lbm
- q heat added to system, J/kg; Btu/lb
- W_s mechanical work done by system, J/kg; Btu/lb

For a gas system, the potential energy can be neglected. In addition, by definition

$$h = u + \frac{pv}{J} \quad (1-47)$$

Thus, equation (1-46) reduces to

$$h_1 + \frac{V_1^2}{2gJ} + q = h_2 + \frac{V_2^2}{2gJ} + W_s \quad (1-48)$$

Equation (1-48) is the basic form of the steady-flow energy balance as we will be using it.

Total Conditions

The sum of the enthalpy and the kinetic energy is always appearing in flow problems, and it is convenient to use it as a single quantity. Thus,

$$h' \equiv h + \frac{V^2}{2gJ} \quad (1-49)$$

where h' is total enthalpy, in J/kg or Btu/lb.

The concept of total enthalpy leads us to the concept of total temperature. Total temperature can be defined as the temperature that corresponds to the total enthalpy. The total-temperature concept is most useful when ideal-gas-law behavior and constant heat capacity can be assumed. In that case, according to equation (1-15),

$$h' - h = c_p(T' - T) \quad (1-50)$$

where T' is total temperature, in K or °R. Combining equation (1-50) with equation (1-49) yields

$$T' = T + \frac{V^2}{2gc_p} \quad (1-51)$$

The total temperature T' can be thought of as the temperature attained when a gas at static temperature T and velocity V is brought to rest adiabatically. Thus, total temperature is also called stagnation temperature, and these two terms are used interchangeably.

The total, or stagnation, pressure can be regarded as the pressure of a fluid brought to rest isentropically from a velocity V and static pressure p . Since the relation between p' and p is isentropic, we can use equation (1-29) to write

$$\frac{p'}{p} = \left(\frac{T'}{T}\right)^{\gamma/(\gamma-1)} \quad (1-52)$$

where p' is total pressure, in N/m² or lb/ft².

With regard to the above-defined total conditions, certain points should be emphasized. The concept of total enthalpy is general, and its use involves no assumptions other than those associated with the energy balance as we have considered it. Total temperature, as will be seen, is a very useful convenience for easing the burden of calculation, but it is rigorous only for ideal-gas-law behavior and constant heat capacity. For systems involving chemical reaction or a phase change, the use of total temperature is not recommended. Total pressure, in addition to the assumptions associated with total temperature, involves an isentropic path between the static and total conditions.

Flow Process With No Heat and No Work

Let us now, in terms of total conditions, examine a process that occurs with neither heat transfer (adiabatic process) nor mechanical work. This process is the one that occurs (neglecting heat losses) in each part of the turbine (including the rotor, at constant radius, when

TURBINE DESIGN AND APPLICATION

the velocities are expressed relative to the moving blade).

Substitution of equation (1-49) into equation (1-48) and rearrangement yields

$$h_2' - h_1' = q - W, \quad (1-53)$$

The energy balance now looks something like the First Law of Thermodynamics for a flow process, as we were first exposed to it in college. If we set q and W , equal to zero, we get

$$h_2' = h_1' \quad (1-54)$$

Therefore, for adiabatic flow with no work, total enthalpy remains constant. Further, from equations (1-18) and (1-50), it can be shown that total temperature also remains constant.

$$T_2' = T_1' \quad (1-55)$$

Note that the process does not have to be isentropic in order for total enthalpy and total temperature to remain constant.

Total pressure is another matter. From equations (1-22), (1-52), and (1-55) and the ideal-gas-law and constant-heat-capacity assumptions, it can be shown that for adiabatic flow with no work,

$$e^{Jds/R} = \frac{p_1'}{p_2'} \quad (1-56)$$

Only for isentropic flow ($ds=0$), therefore, does total pressure remain constant. For flow with loss ($ds>0$), there is a decrease in total pressure.

Speed of Sound and Velocity Ratios

An important characteristic of gases is the speed of pressure-wave propagation or, as otherwise called, the speed of sound. From small-pressure-disturbance theory

$$a = \sqrt{g \left(\frac{\partial p}{\partial \rho} \right)}, \quad (1-57)$$

where a is speed of sound, in m/sec or ft/sec.

From the ideal gas law and isentropic process relations, this reduces to

$$a = \sqrt{\gamma g R T} \quad (1-58)$$

The ratio of fluid velocity V to sound velocity a is an important factor in determining the flow characteristics of a gas. This ratio is called the Mach number M :

$$M = \frac{V}{a} \quad (1-59)$$

Mach number is a useful parameter not only for identifying flow-behavior regimes, but also for simplifying and generalizing certain expressions. Consider the relation of total temperature to static temperature, given in equation (1-51). Combining equations (1-58), (1-59), and (1-28) with equation (1-51) yields

$$\frac{T'}{T} = 1 + \frac{\gamma-1}{2} M^2 \quad (1-60)$$

Another velocity ratio often used is the ratio of fluid velocity to critical velocity

$$\frac{V}{V_{cr}} = \frac{V}{a_{cr}} \quad (1-61)$$

where V_{cr} is critical velocity, in m/sec or ft/sec, and a_{cr} is speed of sound at critical condition, in m/sec or ft/sec. The critical velocity is equal to the velocity of sound at the critical condition. The critical condition is that condition where $M=1$. Consequently, from equation (1-60), at the critical condition

$$T_{cr} = \frac{2}{\gamma+1} T' \quad (1-62)$$

and substitution of equation (1-62) into equation (1-58) yields

$$a_{cr} = \sqrt{\frac{2\gamma}{\gamma+1} gRT'} \quad (1-63)$$

Thus, in any flow process with constant total temperature (no heat and no work), the value of the critical velocity ($V_{cr} = a_{cr}$) remains constant for the entire process, while the value of the speed of sound (a) changes as the static temperature changes.

The ratio of fluid velocity to critical velocity is sometimes called the critical velocity ratio. Its use is often preferred over Mach number because the critical velocity ratio is directly proportional to velocity, while Mach number is not (since there is a square root of static temperature in the denominator).

The relation between static and total temperature in terms of the critical velocity ratio results from combining equations (1-61), (1-63), (1-28), and (1-51).

$$\frac{T}{T'} = 1 - \frac{\gamma-1}{\gamma+1} \left(\frac{V}{V_{cr}} \right)^2 \quad (1-64)$$

APPLICATION TO FLOW WITH VARYING AREA

The equations already presented are sufficient to analyze completely the flow through turbine passages, provided that there are no losses (flow is isentropic). Although there are losses in a turbine, we can use the loss-free process to learn something about the behavior of the flow in the varying-area passages (stator, rotor, and exit diffuser) of the turbine.

Effect of Flow Regime

We are going to examine the relations among pressure, velocity, area change, and Mach number. Proper manipulation of the previously presented equations yields the following equation for isentropic flow:

$$-(1-M^2) \frac{dV}{V} = \frac{1-M^2}{\gamma M^2} \frac{dp}{p} = \frac{dA}{A} \quad (1-65)$$

Equation (1-65) shows that (1) for all Mach numbers the change in velocity is opposite to the change in pressure and (2) the directions of the changes in velocity and pressure with changes in area depend on whether the Mach number is less than 1 (subsonic flow), equal to 1 (sonic flow), or greater than 1 (supersonic flow). By way of definition, let us specify that a nozzle is a varying-area passage in which static pressure decreases and a diffuser is a varying-area passage in which static pressure increases.

Let us examine the various cases from equation (1-65):

A. Subsonic flow ($M < 1$):1. Increasing pressure ($dp > 0$):

Velocity decreases ($dV < 0$) and area increases ($dA > 0$).

This is the subsonic diffuser.

2. Decreasing pressure ($dp < 0$):

Velocity increases ($dV > 0$) and area decreases ($dA < 0$).

This is the subsonic nozzle.

B. Supersonic flow ($M > 1$):1. Increasing pressure ($dp > 0$):

Velocity decreases ($dV < 0$) and area decreases ($dA < 0$).

This is the supersonic diffuser.

2. Decreasing pressure ($dp < 0$):

Velocity increases ($dV > 0$) and area increases ($dA > 0$).

This is the supersonic nozzle.

C. Sonic flow ($M = 1$):

Both increasing ($dp > 0$) and decreasing ($dp < 0$) pressure.

Area change must equal zero ($dA = 0$). Thus, the sonic, or critical, condition can occur only at the inlet, exit, or minimum-area section of a varying-area passage.

You may also want to note that in order to cross the critical condition ($M=1$) going either up or down in velocity, the flow passage must have a decreasing-area portion followed by an increasing-area portion.

Flow in Nozzles

Since we are concerned primarily with nozzle flow rather than diffuser flow in turbines, we will narrow the discussion to flow in nozzles. We will further limit the discussion to the case where the flow entering the nozzle is subsonic, since this is the case of most interest.

Convergent nozzle.—Let us first consider the simple convergent nozzle. This corresponds to the case A2 mentioned previously. Assume the nozzle is supplied with gas from a reservoir (zero velocity) where the gas is maintained at a static (and total) pressure p' and a static (and total) temperature T' . The exhaust, or outside, static pressure is designated as p_e and the static pressure right at the nozzle exit (in the throat) is designated as p_t . When p_e is a little less than p' , flow commences and the throat pressure p_t is equal to p_e . As p_e is progressively lowered, flow rate and velocity both increase, with p_t still equal to p_e . At some value of p_e , the velocity at the throat becomes equal to sonic velocity, and $M=1$ at the throat.

What happens if p_e is now lowered further? We have seen that a Mach number greater than 1 cannot be attained in a convergent nozzle. Therefore, the flow at the throat remains in the critical condition ($M=1$) no matter how much p_e is lowered. The static pressure in the throat remains at the critical pressure, which according to equations (1-62) and (1-29) is

$$p_t = p_{cr} = p' \left(\frac{2}{\gamma + 1} \right)^{\gamma/(\gamma-1)} \quad (1-66)$$

Once p_e is reduced below p_{cr} , the exhaust pressure has no effect on the flow within the nozzle. The gas expands from p' to $p_t = p_{cr}$ within the nozzle and then expands further from p_t to p_e outside the nozzle. The expansion process from p_t to p_e occurs with shocks (which occur with an increase in entropy and will be discussed a little later), and the isentropic equations are not valid for this part of the process.

The fact that the throat condition remains constant for nozzle pressure ratios (p'/p_e) greater than or equal to the critical pressure ratio (p'/p_{cr}) means that the nozzle mass flow rate also remains constant under these conditions. Thus, for a fixed upstream state, the mass flow rate reaches a maximum value when M becomes 1 at the throat and thereafter remains constant no matter to what value the exhaust pressure is reduced. The fact that this condition corresponds to maximum flow can be proven mathematically. A nozzle in

TURBINE DESIGN AND APPLICATION

this condition is said to be choked.

Convergent-divergent nozzle.—Let us now consider the somewhat more involved case of the convergent-divergent nozzle. Again, assume the nozzle to be supplied with gas from the same reservoir maintained at pressure p' and temperature T' . Figure 1-3, showing plots of pressure ratio against nozzle length, will supplement this discussion. If the exhaust pressure p_e is a little less than p' (curve AB in fig. 1-3), flow commences with the lowest pressure occurring at the throat ($p_t < p_e$). In this case, the divergent section of the passage is acting as a subsonic diffuser. As p_e is progressively lowered (curve AC in fig. 1-3), the pressure p_t at the throat decreases and the velocity increases. Eventually, at some particular value of p_e , the throat velocity becomes equal to the sonic velocity, or $M_t=1$ (curve AD in fig. 1-3). Note that p_e is still higher than p_t , and the gas still diffuses subsonically

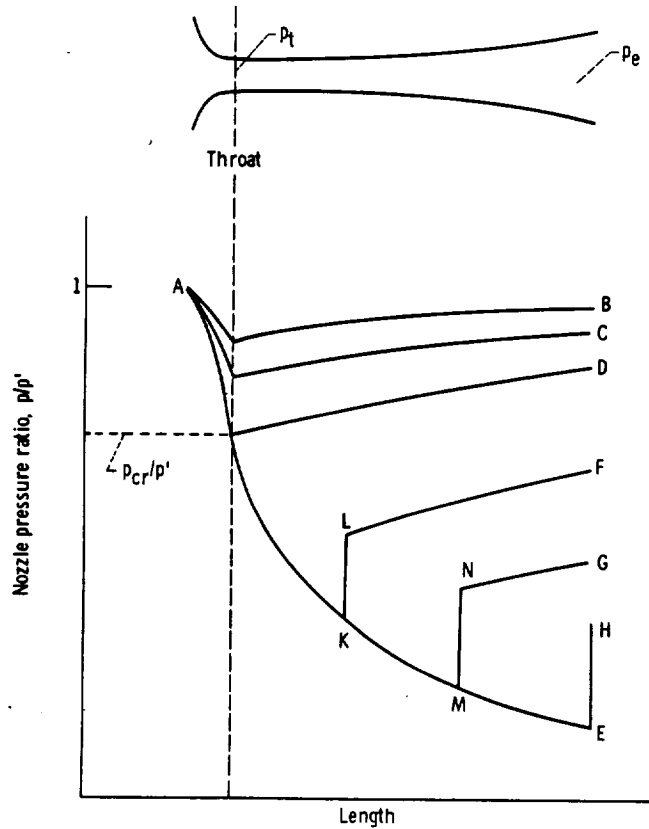


FIGURE 1-3.—Nozzle flow processes.

in the divergent section. Since the throat condition is now critical (with $p_t = p_{cr} < p_e$), we see that the nozzle pressure ratio (p'/p_e) required to achieve the critical condition in a convergent-divergent nozzle is less than the nozzle pressure ratio ($p'/p_e = p'/p_{cr}$) required to achieve the critical condition in a simple convergent nozzle.

If p_e is again lowered, the throat must remain at the critical condition because equation (1-65) showed us that the throat is the only place where the critical condition can exist. Thus, as with the convergent nozzle, the throat state remains constant, and the mass flow must remain constant at its maximum value. As long as the critical condition is maintained at the throat, the nozzle is choked and the convergent part of the nozzle continues to behave independently of the conditions beyond the throat.

If the flow is to be supersonic and isentropic throughout the divergent part of the nozzle, then for any given ratio of throat area to discharge area, only one exhaust pressure p_e will satisfy the conservation of mass and energy, as well as the isentropic process, relations. This case is represented in figure 1-3 by curve AE, which shows pressure falling continuously. It is unreasonable to assume that flow is impossible between the values of p_e that allow either isentropic subsonic diffusion to some $p_e > p_t$ (curve AD, fig. 1-3) or isentropic supersonic expansion to some $p_e < p_t$ (curve AE, fig. 1-3). The flow that does take place, therefore, cannot be isentropic.

Observing the gas flow under these nonisentropic conditions by optical means reveals that surfaces of abrupt density changes occur in the flow. These apparent discontinuities in the flow are shock waves. Shock waves are of very small thickness, and the fluid state changes may be considered as occurring instantaneously. Total temperature across a shock remains constant but, even though there is a rise in static pressure, there is a loss in total pressure because the process occurs with an increase in entropy. Shocks may be strong or weak. Strong shocks occur normal to the flow (and are thus called normal shocks) and result in subsonic velocities downstream of the shock. Weak shocks occur at some small angle with respect to the flow direction (and are thus called oblique shocks), and the velocity downstream of the shock remains supersonic, but the Mach number is less than that upstream of the shock.

Let us now complete the discussion of convergent-divergent nozzles for the region of pressure ratios between points D and E in figure 1-3. If the exhaust pressure p_e is reduced a little below the value at point D, a normal shock occurs at some point in the divergent part of the nozzle, and the pressure rises instantaneously to a value such that isentropic subsonic diffusion occurs from the shock plane to the nozzle

exit. The flow process in this case is illustrated by the path AKLF, with AK being an isentropic expansion, KL being the normal shock, and LF being the isentropic diffusion. As p_e is reduced further, the normal shock moves toward the nozzle exit, and the flow process is represented by a path such as AMNG. At some value of p_e corresponding to point H, the normal shock will be right at the nozzle exit, and the flow path in the nozzle is AEH.

For values of p_e between points H and E, a normal shock cannot occur because it is too strong and would result in a static pressure higher than p_e . In this case, the weaker oblique shock occurs at the nozzle exit, with the shock becoming weaker as p_e approaches point E. When p_e corresponds to point E, as mentioned previously, the nozzle flow is again completely isentropic. For lower values of p_e , the final expansion from the nozzle-exit static pressure to p_e occurs outside the nozzle in a nonisentropic manner.

It should be pointed out that the previous discussion and the processes shown in figure 1-3 are idealized. In actuality, the shock effects do not occur exactly instantaneously and the pressure rise, although abrupt, takes place over a finite distance. Also, real-fluid considerations may produce effects that make the subsonic flow downstream of a shock different from isentropic. The general processes, however, are qualitatively similar to those shown in figure 1-3.

Thermodynamic-Property and Flow-Function Tables and Charts

In order to facilitate thermodynamic and flow calculations, many sets of tables and charts have been constructed and published in books and reports. Some of these are listed as references 3 to 7.

Thermodynamic properties of air and its combustion products as functions of temperature are presented in references 3 and 4. These charts and tables include the variation in heat capacity with temperature. The thermodynamic properties of air and also the individual components of air and its combustion products (nitrogen, oxygen, carbon dioxide, water vapor, and argon) are presented in references 4 and 5. Compressibility factors are also presented in reference 5. The properties presented in reference 5 include the effect of pressure, as well as temperature.

Isentropic compressible-flow functions (T/T' , p/p' , ρ/ρ' , A/A_{cr} , and others) as functions of Mach number are presented in references 4, 6, and 7 for various values of heat-capacity ratio. Also included are tables and charts for normal and oblique shock calculations. Reference 6 presents a listing of compressible flow function and shock function equations in terms of both Mach number and critical velocity ratio.

REFERENCES

1. KUNKLE, JOHN S.; WILSON, SAMUEL D.; AND COTA, RICHARD A.; ED: Compressed Gas Handbook. NASA SP-3045, 1969.
2. NELSON, L. C.; AND OBERT, E. F.: How to Use the New . . . Generalized Compressibility Charts. Chem. Eng., vol. 61, no. 7, July 1954, pp. 203-208.
3. ENGLISH, ROBERT E.; AND WACHTL, WILLIAM W.: Charts of Thermodynamic Properties of Air and Combustion Products from 300° to 3500° R. NACA TN 2071, 1950.
4. KEENAN, JOSEPH H.; AND KAYE, JOSEPH: Gas Tables. John Wiley and Sons, Inc., 1948.
5. HILSENRATH, JOSEPH; BECKETT, CHARLES W.; BENEDICT, WILLIAM S.; FANO, LILLA; HOGE, HAROLD J.; MASI, JOSEPH F.; NUTTALL, RALPH L.; TOULOUKIAN, YERAM S.; AND WOOLLEY, HAROLD W.: Tables of Thermal Properties of Gases Comprising Tables of Thermodynamics and Transport Properties of Air, Argon, Carbon Dioxide, Carbon Monoxide, Hydrogen, Nitrogen, Oxygen, and Steam. NBS Circular 564, National Bureau of Standards, Nov. 1, 1955.
6. AMES RESEARCH STAFF: Equations, Tables, and Charts for Compressible Flow. NACA Rep. 1135, 1953.
7. LEWIS LABORATORY COMPUTING STAFF: Tables of Various Mach Number Functions for Specific-Heat Ratios from 1.28 to 1.38. NACA TN 3981, 1957.

SYMBOLS

A	flow area, m^2 ; ft^2
a	{ acceleration, m/sec^2 ; ft/sec^2 speed of sound, m/sec ; ft/sec
a, b, c	general constants for polynomial, eq. (1-16)
c_p	heat capacity at constant pressure, $J/(kg)(K)$; $Btu/(lb)(^{\circ}R)$
F	unbalanced force, N ; lb
g	conversion constant, 1; 32.17 $(lbm)(ft)/(lbf)(sec^2)$
h	specific enthalpy, J/kg ; Btu/lb
J	conversion constant, 1; 778 $(ft)(lb)/Btu$
M	Mach number, defined by eq. (1-59)
M_w	molecular weight, $kg/(kg\ mole)$; $lb/(lb\ mole)$
m	mass, kg ; lb
p	absolute pressure, N/m^2 ; lb/ft^2
q	heat added to system, J/kg ; Btu/lb
q_f	heat produced by friction, J/kg ; Btu/lb
R	gas constant, $J/(kg)(K)$; $(ft)(lbf)/(lbm)(^{\circ}R)$
R_f	frictional resistance force, N ; lb
R^*	universal gas constant, 8314 $J/(kg\ mole)(K)$; 1545 $(ft)(lbf)/(lb\ mole)(^{\circ}R)$
s	specific entropy, $J/(kg)(K)$; $Btu/(lb)(^{\circ}R)$
T	absolute temperature, K ; $^{\circ}R$
t	time, sec
u	specific internal energy, J/kg ; Btu/lb
V	fluid absolute velocity, m/sec ; ft/sec
v	specific volume, m^3/kg ; ft^3/lb
W_s	mechanical work done by system, J/kg ; Btu/lb
w	mass flow rate, kg/sec ; lb/sec
x	length, m ; ft
Z	specific potential energy, J/kg ; $(ft)(lbf)/lbm$
z	compressibility factor, defined by eq. (1-4)
γ	ratio of heat capacity at constant pressure to heat capacity at constant volume
ρ	density, kg/m^3 ; lb/ft^3
Subscripts:	
c	critical state condition
cr	critical flow condition ($M=1$)
e	exhaust
t	throat
Superscript:	
'	absolute total state

CHAPTER 2

Basic Turbine Concepts

By Arthur J. Glassman

This chapter introduces turbine geometric, flow, energy-transfer, efficiency, and performance characteristics primarily by means of definitions, diagrams, and dimensionless parameters. Terms referring to the blades and blading geometry are defined in the GLOSSARY, at the end of this chapter.

TURBINE FLOW AND ENERGY TRANSFER

Analysis Coordinate System

An analysis of the flow and energy-transfer processes within a turbine requires some convenient coordinate system. For fluid flowing through a turning wheel, a logical system consists of one coordinate directed parallel to the axis of rotation, one coordinate directed radially through the axis of rotation, and one coordinate directed tangentially to the rotating wheel. These are the axial, radial, and tangential directions indicated in figure 2-1.

These three coordinates form three planes. Analysis of flow in the radial-axial plane depicts the circumferentially-averaged (or blade-to-blade average) radial and axial variation of the desired flow parameters. For many types of calculations, we can ignore the circumferential (or blade-to-blade) variation of parameter values and just use average values. Such a calculation is called an axisymmetric analysis.

Calculations made in the axial-tangential or radial-tangential planes are usually at some constant value (rather than for average conditions) of the third coordinate. Velocity diagram, as well as blade-to-blade velocity-variation, calculations are usually made in these planes. When

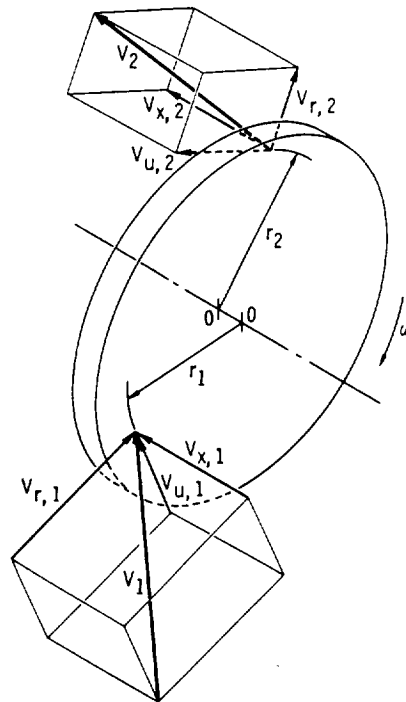


FIGURE 2-1.—Velocity components for a generalized rotor.

flow is predominantly radial, such as at the inlet to a radial-flow turbine, the radial-tangential plane is used. When flow is predominantly axial, such as in an axial-flow turbine, the axial-tangential plane is used.

Velocity Vectors and Diagrams

One of the most, if not the most, important variables that we will be concerned with in the analysis of turbine flow and energy transfer is the fluid velocity and its variation in the different coordinate directions. To assist us in making these analyses and in depicting blading shapes and types, we use velocity-vector diagrams.

For flow in and across the stators, the absolute velocities are of interest. For flow in and across the rotors, velocities must be considered relative to the rotating blade. In terms of relative velocities and other relative parameters to be discussed later in this chapter, flow in a rotating blade row can be analyzed in a manner similar to the analysis of flow in a stationary passage.

BASIC TURBINE CONCEPTS

Velocity-diagram calculations are made at locations upstream and downstream of the various blade rows or at just infinitesimal distances inside the blade rows. In making the velocity diagrams, the circumferential variations in flow are not considered. The velocity vectors represent the circumferential average of the flow.

The velocity diagram shows both the absolute and the relative velocities. In making the velocity diagram, note that

$$\text{Relative velocity} = \text{Absolute velocity} - \text{Blade velocity} \quad (2-1)$$

or

$$\vec{W} = \vec{V} - \vec{U} \quad (2-2)$$

where

\vec{W} relative velocity vector .

\vec{V} absolute velocity vector

\vec{U} blade velocity vector

Since blade velocity is always in the tangential direction, we need only consider the magnitude, that is, the blade speed. So, we can write

$$\vec{W} = \vec{V} - U \quad (2-3)$$

The velocity diagram in figure 2-2 represents equation (2-3) and also shows the components of the absolute and relative velocities. Assuming this velocity diagram to be drawn in an axial-tangential plane, the absolute and relative velocities can be expressed in terms of their

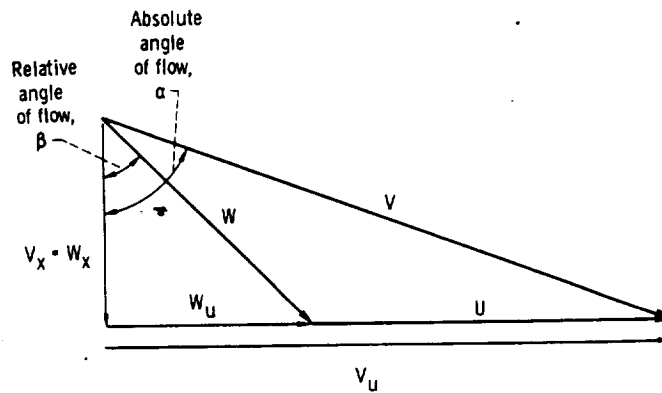


FIGURE 2-2.—Typical velocity-vector diagram having tangential components of absolute and relative velocities in the same direction.

TURBINE DESIGN AND APPLICATION

components in the axial and tangential directions as

$$V^2 = V_x^2 + V_u^2 \quad (2-4)$$

and

$$W^2 = W_x^2 + W_u^2 \quad (2-5)$$

where

V magnitude of \vec{V} , m/sec; ft/sec

V_x axial component of absolute velocity, m/sec; ft/sec

V_u tangential component of absolute velocity, m/sec; ft/sec

W magnitude of \vec{W} , m/sec; ft/sec

W_x axial component of relative velocity, m/sec; ft/sec

W_u tangential component of relative velocity, m/sec; ft/sec

If this diagram (fig. 2-2) were drawn in the radial-tangential plane, the values marked as axial components would be radial components. From figure 2-2, we see that we can write

$$W_u = V_u - U \quad (2-6)$$

A sign convention must be established for the angles and the tangential components of velocity, since not all velocity diagrams are of the exact same geometrical shape as the example diagram shown in figure 2-2. We could have, for example, the velocity diagram shown in figure 2-3. In this instance, the tangential components and flow angles of the absolute and relative velocities are directed in opposite directions, and it is not obvious that equation (2-6) is valid. Therefore, we will adopt and stick with the convention that

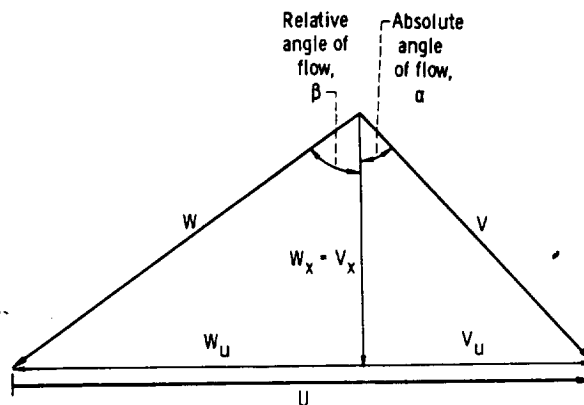


FIGURE 2-3.—Typical velocity-vector diagram having tangential components of absolute and relative velocities in opposite directions.

all angles and tangential components of velocity are positive if they are in the direction of the blade velocity and are negative if they are in the direction opposite to the blade velocity. With this convention, we can now see that equation (2-6) remains valid for the velocity diagram shown in figure 2-3, where a small positive value of V_u minus a larger positive value of U yields a negative value for W_u .

Not all turbine analysts use the above convention for all cases. Some use the above convention at a location immediately upstream of a rotor and then switch positive and negative directions at locations immediately downstream of a rotor. In many cases this avoids working with negative values. Also, many analysts work with angles defined with respect to the tangential direction rather than the axial direction as we are using. Therefore, if you should have occasion to use velocity-diagram information generated by someone else, make sure that you are aware of the convention used in generating this information.

Energy Transfer

The basic energy-transfer relation for all turbomachines is relatively simple and is only a form of Newton's Second Law of Motion as applied to a fluid traversing a rotor. Figure 2-1 represents a rotor of a generalized turbomachine, with 0-0 the axis of rotation and ω the angular velocity. Fluid enters the rotor at point 1, passes through the rotor by any path, and is discharged at point 2. The directions of the fluid at points 1 and 2 are at any arbitrary angle, and points 1 and 2 are at any radii r_1 and r_2 . A condition of steady state is assumed. Further, the velocity vectors at the inlet and the outlet are regarded as representing the average values for the mass of flow being considered.

The inlet and outlet velocity vectors can be resolved into the three mutually perpendicular components discussed previously. The change in magnitude of the axial velocity components through the rotor gives rise to an axial force, which must be taken by a thrust bearing. The change in magnitude of the radial velocity components gives rise to a radial bearing load. Neither the axial nor the radial velocity components have any effect on the angular motion of the rotor (except for the effect of bearing friction). It is the change in magnitude and radius of the tangential components of velocity that corresponds to a change in angular momentum of the fluid and results in the desired energy transfer.

Net rotor torque is equal to the difference between the inlet and outlet products of tangential force times radius, or

$$\tau = (F_u r)_1 - (F_u r)_2 \quad (2-7)$$

TURBINE DESIGN AND APPLICATION

where

τ net torque, N-m; lb-ft
 F_u tangential force, N; lb
 r radius, m; ft

Applying equation (1-34) in the tangential direction, integrating from $V=0$ at $t=0$ to $V=V$ at $t=t$, and setting $w=m/t$ yields

$$F_u = \frac{w}{g} V_u \quad (2-8)$$

where

w rate of mass flow, kg/sec; lb/sec
 g conversion constant, 1; 32.17 (lbm)(ft)/(lbf)(sec²)

Substituting equation (2-8) into (2-7) then yields

$$\tau = \frac{w}{g} V_{u,1} r_1 - \frac{w}{g} V_{u,2} r_2 = \frac{w}{g} (V_{u,1} r_1 - V_{u,2} r_2) \quad (2-9)$$

Power (rate of energy transfer) is equal to the product of torque and angular velocity:

$$P = \frac{\tau \omega}{J} = \frac{w}{gJ} \omega (r_1 V_{u,1} - r_2 V_{u,2}) \quad (2-10)$$

where

P net power, W; Btu/sec
 ω angular velocity, rad/sec
 J conversion constant, 1; 778 (ft)(lb)/Btu

Since

$$r\omega = U \quad (2-11)$$

we can write

$$P = \frac{w}{gJ} (U_1 V_{u,1} - U_2 V_{u,2}) \quad (2-12)$$

But

$$P = w \Delta h' \quad (2-13)$$

where h' is total enthalpy, in J/kg or Btu/lb. Substituting equation (2-13) into equation (2-12) yields

$$\Delta h' = \frac{1}{gJ} (U_1 V_{u,1} - U_2 V_{u,2}) \quad (2-14)$$

where $\Delta h'$ is here defined as $h'_1 - h'_2$.

Equation (2-14) is the basic work equation for all forms of turbomachines and is called the Euler equation. All the energy transfer between the fluid and the rotor must be accounted for by the difference between the two UV_u terms. The way equation (2-14) is stated, it

can be seen that $\Delta h'$ must be positive for a turbine. This is consistent with the energy balance, equation (1-46), where work done by the fluid is defined as positive.

It is useful to transform the Euler equation into another form. This will be done with the aid of figure 2-4, which shows an axial-flow turbine blade section along with the velocity diagrams for the inlet and outlet. The velocity diagrams are in axial-tangential planes. There is assumed to be no radial component of velocity at either the inlet or the outlet locations, although these locations are not necessarily at the same radius. Actually, the following derivation also can be made for a general three-dimensional case.

From equations (2-4) and (2-5), we get

$$V_z^2 = V^2 - V_u^2 \quad (2-15)$$

and

$$W_z^2 = W^2 - W_u^2 \quad (2-16)$$

Substituting equation (2-6) into (2-16) gives

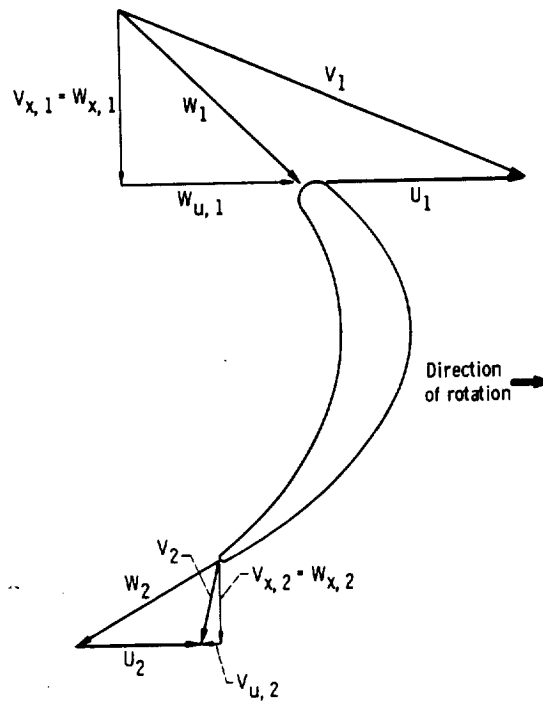


FIGURE 2-4.—Rotor section with inlet- and exit-velocity-vector diagrams.

$$W_x^2 = W^2 - (V_u - U)^2 \quad (2-17)$$

Since $V_x = W_x$, combining equations (2-15) and (2-17) yields

$$V^2 - V_u^2 = W^2 - V_u^2 + 2UV_u - U^2 \quad (2-18)$$

Therefore,

$$UV_u = \frac{1}{2}(V^2 + U^2 - W^2) \quad (2-19)$$

Now, adding subscripts for inlet and outlet yields

$$U_1 V_{u,1} = \frac{1}{2}(V_1^2 + U_1^2 - W_1^2) \quad (2-20)$$

$$U_2 V_{u,2} = \frac{1}{2}(V_2^2 + U_2^2 - W_2^2) \quad (2-21)$$

Inserting these values into the Euler equation (eq. (2-14)) finally yields

$$\Delta h' = \frac{1}{2gJ}(V_1^2 - V_2^2 + U_1^2 - U_2^2 + W_2^2 - W_1^2) \quad (2-22)$$

Equation (2-22) is an alternative form of the basic energy-transfer relation.

By definition,

$$\Delta h' = h'_1 - h'_2 = h_1 + \frac{V_1^2}{2gJ} - h_2 - \frac{V_2^2}{2gJ} \quad (2-23)$$

Therefore, comparison of equation (2-22) with equation (2-23) shows that

$$\Delta h = h_1 - h_2 = \frac{1}{2gJ}(U_1^2 - U_2^2 + W_2^2 - W_1^2) \quad (2-24)$$

Thus, the U^2 and W^2 terms of equation (2-22) represent the change in static enthalpy across the rotor, while the V^2 terms represent the change in absolute kinetic energy across the rotor. These three pairs of terms are sometimes referred to as the components of energy transfer.

Blade Loading

As mentioned previously, it is the change in the tangential momentum of the fluid that results in the transfer of energy from the fluid to the rotor. The following discussion and figure 2-5 concern the cause of this change in tangential momentum and the way in which the energy is actually transferred to the wheel.

As the fluid flows through the curved passage between each pair of blades, a centrifugal force acts on it in the direction of the pressure

BASIC TURBINE CONCEPTS

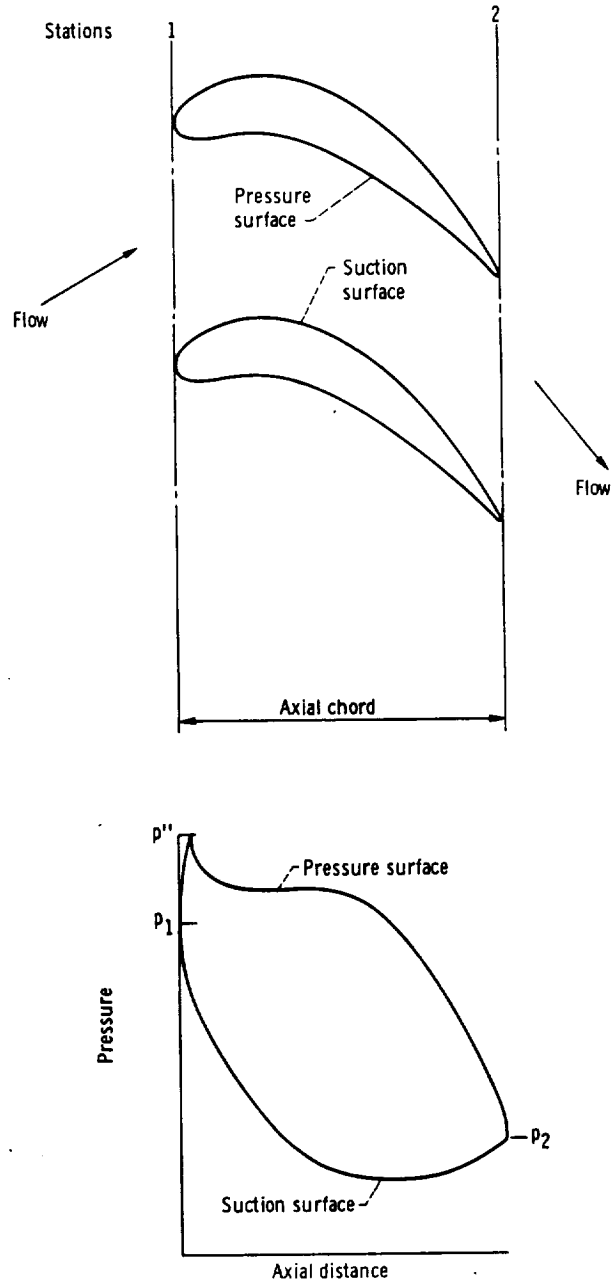


FIGURE 2-5.—Blade row with surface static-pressure distribution.

(concave) surface. Since the fluid is constrained and, therefore, not free to move in the direction of the centrifugal force, a pressure force must be established to balance the centrifugal force and turn the fluid through its curved path. The pressure force is directed normal to the flow and toward the suction (convex) surface. Thus, the pressure in the passage is highest at the pressure surface and lowest at the suction surface.

The resulting distribution of static pressure on the blade surfaces is illustrated in figure 2-5, where pressure is plotted against axial distance. At or near the blade leading edge there is a stagnation point where the velocity becomes zero and the pressure reaches its stagnation value. The stagnation point is the dividing point for the fluid flowing around to the two sides of the blade. From the stagnation point, the pressure along the blade surfaces decreases toward the blade trailing edge. On the suction surface, the static pressure will often decrease below the exit pressure and then increase back up to the exit pressure.

The pressure-distribution curve illustrated in figure 2-5 is called the blade-loading diagram. The area between the curves represents the blade force acting in the tangential direction.

Relative Conditions

Flow in a rotating passage can be analyzed in a manner similar to flow in a stationary passage by considering conditions relative to the moving passage. Let us first define relative total enthalpy in a manner similar to the definition of absolute total enthalpy.

$$h'' \equiv h + \frac{W^2}{2gJ} \quad (2-25)$$

where h'' is relative total enthalpy, in J/kg or Btu/lb. Now let us examine what happens to relative total enthalpy as the fluid flows through the rotor. If in equation (2-24) we substitute for W^2 according to equation (2-25), we get

$$h_2'' - h_1'' = \frac{U_2^2 - U_1^2}{2gJ} \quad (2-26)$$

Therefore, we see that the relative total enthalpy of the fluid flowing through the rotor changes only if there is a change in the blade speed. For purely axial flow, where there is no change in radius and, consequently, no change in blade speed, the relative total enthalpy remains constant for the rotor flow process.

We can also define a temperature that corresponds to relative total enthalpy. This is called the relative total temperature, T'' . When

ideal-gas-law behavior and constant heat capacity can be assumed, we can write

$$h'' - h = c_p(T'' - T) \quad (2-27)$$

where

c_p heat capacity at constant pressure, J/(kg)(K); Btu/(lb)(°R)
 T absolute temperature, K; °R

Combining equation (2-27) with equation (2-25) then yields

$$T'' = T + \frac{W^2}{2gJc_p} \quad (2-28)$$

From equation (1-51) and equation (2-28), we see that the absolute and relative total temperatures are related as follows:

$$T' - T'' = \frac{V^2 - W^2}{2gJc_p} \quad (2-29)$$

For the rotor flow process, we can write

$$h_2'' - h_1'' = c_p(T_2'' - T_1'') \quad (2-30)$$

Combining this with equation (2-26) shows that

$$T_2'' - T_1'' = \frac{U_2^2 - U_1^2}{2gJc_p} \quad (2-31)$$

Therefore, relative total temperature, like relative total enthalpy, depends only on blade speed and remains constant for purely axial flow through a rotor.

Relative total pressure can be defined as the pressure of a fluid brought to rest isentropically from a relative velocity W and a static pressure p . Therefore,

$$\frac{p''}{p} = \left(\frac{T''}{T}\right)^{\gamma/(\gamma-1)} \quad (2-32)$$

where

p'' relative total pressure, N/m²; lb/ft²

γ ratio of heat capacity at constant pressure to heat capacity at constant volume

From this equation and equation (1-52), we also see that

$$\frac{p''}{p'} = \left(\frac{T''}{T'}\right)^{\gamma/(\gamma-1)} \quad (2-33)$$

For the rotor flow process, relative total pressure can increase, decrease, or remain constant, depending on the change in relative total temperature and on the losses. For purely axial flow, relative total

TURBINE DESIGN AND APPLICATION

pressure will remain constant only if the flow is isentropic; otherwise, it must decrease.

We can define a relative Mach number M_{rel} as

$$M_{rel} = \frac{W}{a} \quad (2-34)$$

and a relative critical velocity as

$$W_{cr} = a_{cr,rel} = \sqrt{\frac{2\gamma}{\gamma+1} gRT''} \quad (2-35)$$

where

W_{cr} critical velocity, m/sec; ft/sec

$a_{cr,rel}$ speed of sound at relative critical condition, m/sec; ft/sec

R gas constant, J/(kg)(K); (ft)(lb)/(lb)(°R)

Then, in a manner similar to the way we derived equations (1-60) and (1-64), we can get

$$\frac{T''}{T} = 1 + \frac{\gamma-1}{2} M_{rel}^2 \quad (2-36)$$

and

$$\frac{T}{T''} = 1 - \frac{\gamma-1}{\gamma+1} \left(\frac{W}{W_{cr}} \right)^2 \quad (2-37)$$

Reaction

The fraction of total energy transfer (change in absolute total enthalpy) that is obtained by a change in static enthalpy is one important way of classifying a turbine stage. The change in kinetic energy as a fraction of the exit kinetic energy is one important way of classifying a blade row. The parameter used in both cases is the degree of reaction, or more simply, the reaction. Reaction is used for classifying types of velocity diagrams, and it is also an important parameter for correlating losses.

Stage reaction.—Stage reaction is defined as the change in static enthalpy across the rotor as a fraction of the change in absolute total enthalpy across the stage. Note that the change in absolute total enthalpy across the stage is the same as the change in absolute total enthalpy across the rotor, since total enthalpy remains constant through the stator. According to the above definition of stage reaction, we can write

$$R_{stg} = \frac{h_1 - h_2}{h_1' - h_2'} \quad (2-38)$$

where R_{stg} is stage reaction, and the subscripts 1 and 2 refer to conditions upstream and downstream of the rotor, respectively.

The preceding equation for reaction can be expressed in terms of velocities. Substituting equations (2-22) and (2-24) into equation (2-38) yields

$$R_{s,ig} = \frac{(U_1^2 - U_2^2) + (W_2^2 - W_1^2)}{(V_1^2 - V_2^2) + (U_1^2 - U_2^2) + (W_2^2 - W_1^2)} \quad (2-39)$$

Reaction can be positive, negative, or zero, depending on the values of $(U_1^2 - U_2^2)$ and $(W_2^2 - W_1^2)$.

Zero reaction is one important value that characterizes a particular stage design. If $R_{s,ig} = 0$, there is no change in static enthalpy in the rotor, and all the work done by the stage is a result of the change in absolute kinetic energy across the stage. This stage is called an impulse stage. In the general case where the fluid enters and leaves the rotor at different radii, an impulse stage may result from having a change of static enthalpy in one direction contributed by the centrifugal (U^2) effect and an equal change in the other direction contributed by the relative-velocity effect. For purely axial flow, any change in static enthalpy must be caused by a change of relative velocity only. Thus, an axial-flow impulse stage must have $W_1 = W_2$.

Some people define impulse on the basis of no change in static pressure in the rotor rather than no change in static enthalpy. This definition in terms of static pressure is approximately the same as that used herein. The difference is due to losses. For isentropic flow, the definitions exactly coincide.

Simple examples of impulse turbines are the child's pinwheel, the windmill, or the paddle wheel operated by the impingement of a fluid from a stationary nozzle. A simple example of a reaction turbine is the lawn sprinkler that ejects the water from nozzles, thus causing rotation.

Blade-row reaction.—Blade-row reaction is defined as the kinetic energy developed within the blade row as a fraction of the kinetic energy at the blade-row exit. These are the kinetic energies relative to that blade row. For a stator or axial-flow rotor, the change in kinetic energy corresponds to the change in static enthalpy. Therefore, blade-row reaction represents an effect similar to that represented by stage reaction.

For a stator blade row, reaction is defined as

$$R_{s,i} = \frac{V_1^2 - V_0^2}{V_1^2} = 1 - \frac{V_0^2}{V_1^2} \quad (2-40)$$

where $R_{s,i}$ is stator reaction. For a rotor blade row, reaction is defined as

$$R_{r,0} = \frac{W_2^2 - W_1^2}{W_2^2} = 1 - \frac{W_1^2}{W_2^2} \quad (2-41)$$

where $R_{r,0}$ is rotor reaction. The subscripts 0, 1, and 2 refer to conditions upstream of the stator, downstream of the stator, and downstream of the rotor, respectively.

In some literature, the blade-row reaction is defined in terms of velocities instead of kinetic energies. This definition is similar to equations (2-40) and (2-41) except that the velocities appear to the first power rather than squared (i.e., V rather than V^2).

Turbine Expansion Process

For all adiabatic expansion processes, the maximum energy transformation (development of kinetic energy) or energy transfer (development of mechanical work) for a given pressure ratio is obtained when the process is isentropic. This can be proven from the previously presented equations (but we will not do it here), and we will illustrate this fact graphically a little later in this discussion. With the ideal-gas-law and constant-heat-capacity assumptions, we have previously shown that energies and energy changes can be represented by temperatures and temperature changes. Therefore, with temperature, pressure, and entropy all being variables of interest, we can conveniently represent the ideal (isentropic) and actual expansion processes in a turbine by means of a temperature-entropy diagram.

The temperature-entropy diagram is a plot of temperature against entropy for lines of constant pressure. Since entropy increases with increasing temperature and decreasing pressure, as can be seen from

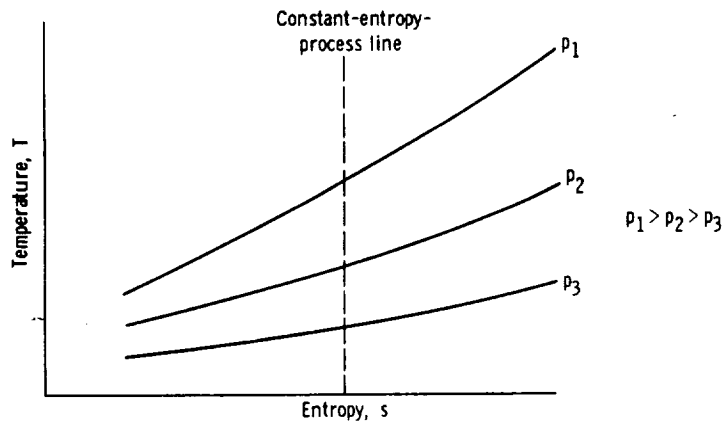
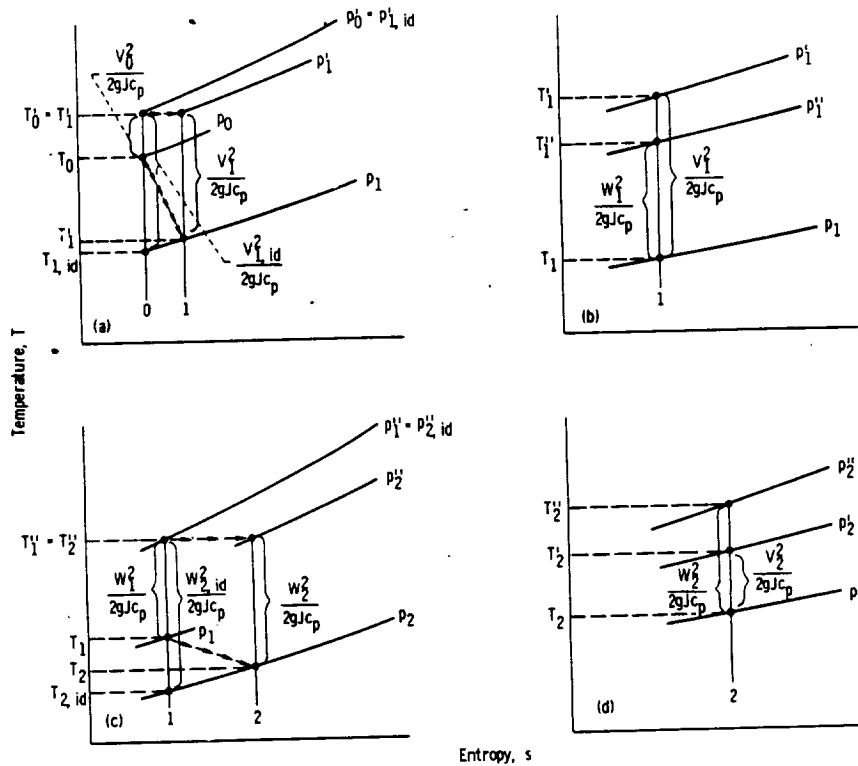


FIGURE 2-6.—Typical temperature-entropy diagram.

BASIC TURBINE CONCEPTS

the discussion of the constant-entropy-process thermodynamics in chapter 1, a temperature-entropy, or T - s , diagram looks like the example shown in figure 2-6. A constant-entropy process is represented by a vertical line. At increasing values of temperature and entropy, the pressure curves diverge; therefore, at increasing values of constant entropy, the temperature difference between any two given pressure curves is also increasing.

For the purposes of clarity, the turbine expansion process will be divided into four steps, with each shown in a separate T - s diagram. These four diagrams will then be combined into a single diagram. The four diagrams represent the stator expansion process (fig. 2-7(a)), the relation between absolute and relative conditions at the stator



- (a) Expansion process across stator.
- (c) Expansion process across rotor.

- (b) Relation between absolute and relative conditions at stator exit.
- (d) Relation between relative and absolute conditions at rotor exit.

FIGURE 2-7.—Temperature-entropy diagrams for flow-process steps of an axial-flow turbine.

exit (fig. 2-7(b)), the rotor expansion process relative to the moving blades (fig. 2-7(c)), and the relation between relative and absolute conditions at the rotor exit (fig. 2-7(d)).

Figure 2-7(a) shows the expansion process across the stator. The four constant-pressure curves represent the static and absolute total pressures before and after the expansion. The kinetic energy at each state is represented by the vertical distance between the static state point and the total state point in accordance with equation (1-51). If the expansion process were isentropic, the final state would be that indicated by the subscript $1,id$. The actual process proceeds from state 0 to state 1 with a small increase in entropy, as indicated by the small arrows. It can be noted that the kinetic energy developed by the actual process is less than would be developed by the ideal process.

As mentioned previously, we analyze flow through the rotor in terms of relative conditions. Figure 2-7(b) shows the relation between the absolute and relative total states at the stator exit. These states are related isentropically, and the absolute and relative kinetic energies and total temperatures are indicated in the figure.

The expansion process across the rotor is shown in figure 2-7(c) in terms of the relative conditions. The four constant-pressure curves represent the static and relative total pressures before and after the expansion. For simplicity, axial flow is assumed, so that $T_1' = T_2''$. If the expansion were isentropic, the final state would be that indicated by the subscript $2,id$. The actual process proceeds from state 1 to state 2, as indicated by the small arrows, with an increase in entropy. Here again it can be noted that the relative kinetic energy developed by the actual process is less than would be developed by an ideal process.

The relation between the relative and absolute total states at the rotor exit is shown in figure 2-7(d). These states are related isentropically, and the relative and absolute kinetic energies at the stage exit are indicated.

The four diagrams of figure 2-7 are now combined into one diagram shown as figure 2-8. The static, absolute total, and relative total state processes for the turbine expansion are indicated by the arrows through the appropriate state points. For the time being, ignore the enthalpy differences indicated on the right of the figure. Note that the point $(p_2, T_{2,id})$, which is on the state 1 constant-entropy line in figure 2-7(c), is not the same point as indicated in figure 2-8, where it is on the state 0 constant-entropy line. In figure 2-7(c), the subscript $2,id$ refers to the ideal expansion across the rotor alone. In figure 2-8, the subscript $2,id$ refers to the ideal expansion across the entire stage (both stator and rotor). The meaning of the subscript $2,id$

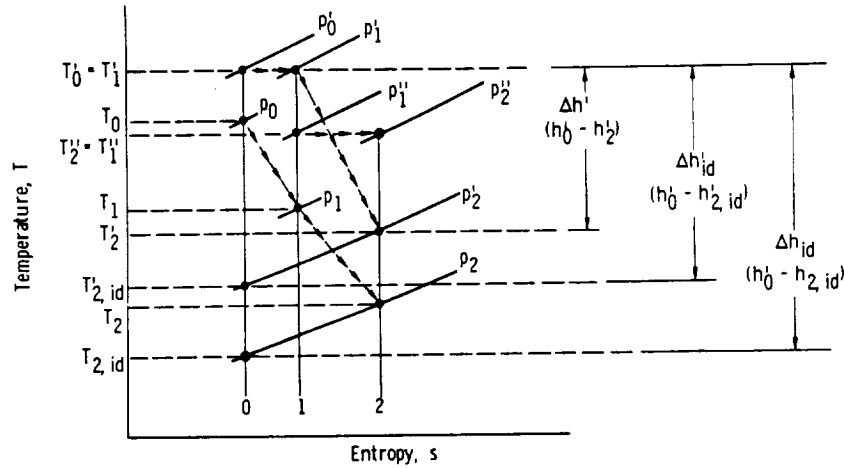


FIGURE 2-8.—Temperature-entropy diagram for a stage of an axial-flow turbine.

is, therefore, ambiguous but is commonly used in both senses. It is obvious from figure 2-8 that the work obtained from the real turbine process (as represented by $T_0' - T_2'$) is less than the work that could be obtained from an ideal turbine process (as represented by $T_0' - T_{2, id}$).

Blade-Row Efficiency

Since turbine blade rows do not operate isentropically, we need a parameter to express blade-row performance. One common parameter used for this purpose is blade-row efficiency, which is defined as the actual exit kinetic energy divided by the ideal exit kinetic energy of the blade row. For the stator,

$$\eta_{st} = \frac{V_1^2}{V_{1, id}^2} \quad (2-42)$$

where η_{st} is stator efficiency. The relation between V_1^2 and $V_{1, id}^2$ is indicated in figure 2-7(a). By applying equations (1-51), (1-52), and (1-55), we get

$$V_{1, id}^2 = 2gJc_p T_0' \left[1 - \left(\frac{p_1}{p_0} \right)^{(\gamma-1)/\gamma} \right] \quad (2-43)$$

For the rotor

$$\eta_{ro} = \frac{W_2^2}{W_{2, id}^2} \quad (2-44)$$

where η_{ro} is rotor efficiency. The relation between W_2^2 and $W_{2, id}^2$ is indicated in figure 2-7(c). For purely axial flow,

$$W_{2, id}^2 = 2gJc_p T_1'' \left[1 - \left(\frac{p_2}{p_1} \right)^{(\gamma-1)/\gamma} \right] \quad (2-45)$$

Thus, with inlet conditions and efficiency known for a given blade row, it is possible to calculate exit velocity for a specified exit static pressure. Blade-row performance in terms of kinetic energy is sometimes expressed as a loss rather than as an efficiency, as

$$e = 1 - \eta \quad (2-46)$$

where e is the kinetic-energy loss coefficient.

Blade-row performance also can be expressed in terms of a loss in total pressure. Several coefficients of this type have been used, each differing by the normalizing parameter used to make the coefficient dimensionless. Inlet total pressure, exit ideal dynamic head, and exit actual dynamic head have all been used for this purpose as follows:

Stator:	Axial rotor:	
$Y_{s, id} = \frac{p_0' - p_1'}{p_0}$	$Y_{r, id} = \frac{p_1'' - p_2''}{p_1''}$	(2-47a)

$Y_{s, a} = \frac{p_0' - p_1'}{p_0' - p_1}$	$Y_{r, a} = \frac{p_1'' - p_2''}{p_1'' - p_2}$	(2-47b)
---	--	---------

$Y_{s, o} = \frac{p_0' - p_1'}{p_1' - p_1}$	$Y_{r, o} = \frac{p_1'' - p_2''}{p_2'' - p_2}$	(2-47c)
---	--	---------

where Y , Y' , and Y'' are total-pressure loss coefficients. Relations between the kinetic-energy loss coefficient and the various total-pressure loss coefficients can be derived. These relations are not simply stated, and they involve a Mach number dependency.

Turbine and Stage Efficiencies

Turbine or stage energy transfer is maximum when the expansion process is isentropic. Since the process is never isentropic, we need a parameter for expressing turbine or stage performance. The parameter that we use is the turbine or stage efficiency, which is defined as the ratio of actual energy transfer to ideal (isentropic) energy transfer. This efficiency is known as the isentropic or adiabatic efficiency. The several different ways that we can apply the above definition are discussed in the sections to follow.

Overall efficiency.—Overall efficiency refers to the overall turbine or stage process. It is the ratio of actual energy transferred in the turbine or stage to the ideal energy transfer based on isentropic flow from the turbine or stage inlet condition to the exit pressure. Note that we are discussing aerodynamic efficiency and are not, at present,

considering mechanical inefficiencies due to items such as bearing and seal friction.

We will define actual energy transfer as the shaft work done by the turbine. This definition is the one used by most people; occasionally, however, actual energy transfer is defined as shaft work plus exit kinetic energy. Actual energy transfer as defined herein is the decrease in absolute total enthalpy across the turbine or stage, and this is indicated in figure 2-8.

Now we must consider whether to define the ideal energy available to do work on the basis of static or total conditions. At the inlet, the total state is always used because the inlet kinetic energy is available for conversion to shaft work. At the turbine or stage exit, static conditions are sometimes used and total conditions are sometimes used. If the turbine exhaust-flow kinetic energy is dissipated, as in a plenum, then the exit kinetic energy is just wasted. This wasted kinetic energy could have been put to use if it could have been converted to shaft work in the turbine. In such a case, we use the exit static state for the computation of ideal work because it would be desirable to expand down to the exit static state with zero exit kinetic energy. In this desirable ideal case, the exit total state would equal the exit static state.

If we were considering a multistage turbine in the above situation, the kinetic energy from only the last stage would be considered as a loss. The kinetic energies leaving the other stages are not wasted, but are carried over to the next stage, where they may be converted to shaft work. Thus, the last stage is rated on the basis of its exit static condition, while the other stages are rated on the basis of their exit total conditions.

In cases where the turbine-exit kinetic energy serves a useful purpose, the entire turbine is rated on the basis of ideal work computed from the exit total state conditions. The most obvious example of this case is the jet-engine turbine. Here the gas must be expanded to a high velocity before leaving the engine, and, therefore, a high velocity leaving the turbine is not a waste.

The efficiency based on the ideal work available between the inlet total and exit static conditions is called the static efficiency. The efficiency based on the ideal work available between the inlet total and exit total conditions is called the total efficiency. The conditions represented by the ideal enthalpy decrease for each of these cases are indicated in figure 2-8. It can be seen that the ideal work based on the exit total condition must be less (as long as there is some exit kinetic energy) than that based on the exit static condition. Thus, total efficiency is always higher than static efficiency, with the difference between the two increasing with increasing exit kinetic energy.

TURBINE DESIGN AND APPLICATION

Overall turbine efficiency $\bar{\eta}$ and stage efficiency η_{st} are defined by similar equations. The subscripts *in* and *ex* are used to denote turbine inlet and exit conditions, instead of the subscripts 0 and 2 used for the stage. Overall turbine static efficiency can be expressed as

$$\bar{\eta} = \frac{\overline{\Delta h'}}{\overline{\Delta h'_{id}}} = \frac{h'_{in} - h'_{ex}}{h'_{in} - h'_{id,ex}} \quad (2-48a)$$

For the ideal-gas-law and constant-heat-capacity assumptions, this reduces to

$$\bar{\eta} = \frac{T'_{in} - T'_{ex}}{T'_{in} \left[1 - \left(\frac{p'_{ex}}{p'_{in}} \right)^{(\gamma-1)/\gamma} \right]} \quad (2-48b)$$

Overall turbine total efficiency is expressed as

$$\bar{\eta}' = \frac{\overline{\Delta h'}}{\overline{\Delta h'_{id}}} = \frac{h'_{in} - h'_{ex}}{h'_{in} - h'_{id,ex}} \quad (2-49a)$$

For the ideal-gas-law and constant-heat-capacity assumptions, this reduces to

$$\bar{\eta}' = \frac{T'_{in} - T'_{ex}}{T'_{in} \left[1 - \left(\frac{p'_{ex}}{p'_{in}} \right)^{(\gamma-1)/\gamma} \right]} \quad (2-49b)$$

Stage total and static efficiencies are similarly defined but with the appropriate subscripts.

Relation of turbine efficiency to stage efficiency.—The overall turbine efficiency is useful as a measure of the overall performance of the turbine. However, it is not a true indication of the efficiency of the stages comprising the turbine. There is an inherent thermodynamic effect hidden in the overall turbine efficiency expression. If equation (2-48b) or (2-49b) were written for a stage, it could be seen that for a given stage pressure ratio and stage efficiency, the energy transfer, which for a stage would be $(T'_0 - T'_2)$, is proportional to the temperature of the gas entering the stage. For a turbine, as can be seen from figure 2-8, the losses of one stage appear in the form of a higher temperature gas entering the following stage ($T_2 > T_{2,id}$). This following stage is then capable of delivering additional work. Therefore, even though all the individual stages may have the same stage efficiency, the overall turbine efficiency still depends on the pressure ratio and the number of stages.

This effect can be shown by means of a temperature-entropy diagram, such as figure 2-9. The solid vertical line 0-2,*id* represents

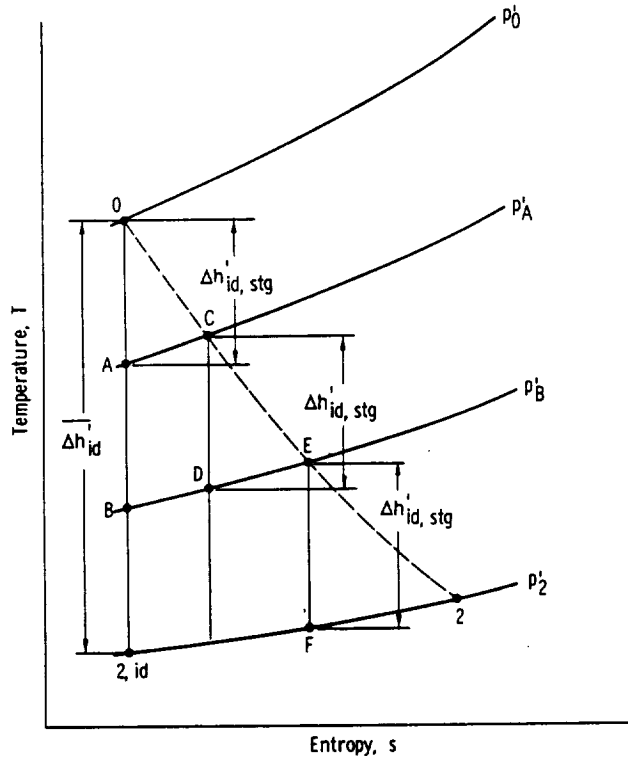


FIGURE 2-9.—Temperature-entropy diagram showing reheat effect in a multistage turbine.

isentropic expansion from inlet pressure p'_0 to exit pressure p'_2 . The dashed line 0-2 represents the process of overall turbine efficiency $\bar{\eta}'$ taking place in three stages, each having the same stage efficiency η'_{stg} .

The actual work obtained from each stage is $\eta'_{stg} \Delta h'_{id, stg}$, where $\Delta h'_{id, stg}$ is the ideal work for a stage. As mentioned previously, the difference of temperature between lines of constant pressure increases with increasing values of entropy. Hence, for the second stage (p'_A to p'_B), the isentropic work represented by the line C-D is greater than that represented by A-B. Thus, the isentropic work for this stage is greater by virtue of the inefficiency of the previous stage and, for constant stage efficiency, the actual work will be greater. Similarly, E-F is greater than B-2,*id*. With lines 0-A, C-D, and E-F representing the ideal work for the three stages, and $\Sigma \Delta h'_{id, stg}$ representing the sum of these, it can be seen that $\Sigma \Delta h'_{id, stg}$ is greater than $\bar{\Delta h}'_{id}$, which is the turbine ideal work represented by the sum of 0-A, A-B, and B-2,*id*.

The total actual turbine work obtained from the expansion from p'_0 to p'_2 can be represented by either $\bar{\eta}' \bar{\Delta h'_{id}}$ or $\eta'_{stg} \Sigma \Delta h'_{id, stg}$, and these two values must be equal. Thus,

$$\bar{\eta}' \bar{\Delta h'_{id}} = \eta'_{stg} \Sigma \Delta h'_{id, stg} \quad (2-50)$$

or

$$\frac{\bar{\eta}'}{\eta'_{stg}} = \frac{\Sigma \Delta h'_{id, stg}}{\bar{\Delta h'_{id}}} \quad (2-51)$$

Since $\Sigma \Delta h'_{id, stg} > \bar{\Delta h'_{id}}$, the turbine overall isentropic efficiency is greater than the stage isentropic efficiencies, or $\bar{\eta}' > \eta'_{stg}$.

This effect in turbines is called the "reheat" effect. This must not be confused with the process of adding heat from an external source between stages, which is also called "reheat".

The equation for calculating overall turbine efficiency for several stages of constant stage pressure ratio p'_2/p'_0 and constant stage efficiency η'_{stg} is

$$\bar{\eta}' = \frac{1 - \left\{ 1 - \eta'_{stg} \left[1 - \left(\frac{p'_2}{p'_0} \right)^{(\gamma-1)/\gamma} \right] \right\}^n}{1 - \left(\frac{p'_2}{p'_0} \right)^{n(\gamma-1)/\gamma}} \quad (2-52)$$

where n is the number of stages. The derivation of this equation can be found in reference 1.

The fact that stage efficiency differs from turbine efficiency, depending on the pressure ratio, raises an important consideration. A comparison of turbine efficiencies of two machines of different pressure ratios is not a true comparison of their aerodynamic behavior, as the one of higher pressure ratio is helped by the reheat effect. It would be desirable to be able to express a true aerodynamic efficiency for a turbine. In order to eliminate all reheat effect, this would have to be the efficiency of an infinitesimally small stage.

Infinitesimal-stage efficiency.—Starting from pressure p and temperature T , suppose a gas is expanded to pressure $(p-dp)$ and temperature $(T-dT)$, where dT is the increment of temperature for an infinitesimal stage of isentropic efficiency η_p . By using the isentropic-efficiency definition, we write

$$dT = \eta_p T \left[1 - \left(\frac{p-dp}{p} \right)^{(\gamma-1)/\gamma} \right] \quad (2-53)$$

and

$$\frac{dT}{T} = \eta_p \left[1 - \left(1 - \frac{dp}{p} \right)^{(\gamma-1)/\gamma} \right] \quad (2-54)$$

These equations are not quite rigorously in accord with the isentropic-efficiency definition. Some authors ignore the fact that the actual work differential should be proportional to the total-temperature differential rather than the static-temperature differential. Other authors make the assumption that there is no change in kinetic energy across the infinitesimal stage, so that $dT' = dT$. However, it always seems to be the static temperature that is used in the infinitesimal-efficiency expression.

Using the series expansion approximation $(1+x)^n = 1+nx$ for evaluation of equation (2-54) yields

$$\frac{dT}{T} = \eta_p \frac{\gamma-1}{\gamma} \frac{dp}{p} \quad (2-55)$$

Integrating between the turbine inlet and exit yields

$$\eta_p = \frac{\ln \frac{T_{in}}{T_{ex}}}{\frac{\gamma-1}{\gamma} \ln \frac{p_{in}}{p_{ex}}} \quad (2-56)$$

Equation (2-56) can be written as

$$\frac{T_{in}}{T_{ex}} = \left(\frac{p_{in}}{p_{ex}} \right)^{\eta_p [(\gamma-1)/\gamma]} \quad (2-57)$$

The infinitesimal-stage efficiency η_p is supposedly the true aerodynamic efficiency, exclusive of the effect of pressure ratio. This efficiency is also known as the polytropic efficiency. This name arises from the method of expressing an irreversible process path as $pv^n = \text{constant}$, where n is called the polytropic exponent, and the process is called a polytropic process. Substituting for v from the ideal gas law, we get for the polytropic process

$$\frac{T_{in}}{T_{ex}} = \left(\frac{p_{in}}{p_{ex}} \right)^{(n-1)/n} \quad (2-58)$$

Equations (2-57) and (2-58) are very similar, and if the turbine process were to be expressed as a polytropic process, then we could relate polytropic efficiency and the polytropic exponent as

$$\frac{n-1}{n} = \eta_p \frac{\gamma-1}{\gamma} \quad (2-59)$$

If we neglect inlet and exit kinetic energies for the overall turbine

TURBINE DESIGN AND APPLICATION

process, we can relate turbine overall efficiency to polytropic efficiency. Actual temperature drop could be expressed as

$$T_{in} - T_{ex} = \bar{\eta} T_{in} \left[1 - \left(\frac{p_{ex}}{p_{in}} \right)^{(\gamma-1)/\gamma} \right] \quad (2-60)$$

or

$$T_{in} - T_{ex} = T_{in} \left\{ 1 - \left(\frac{p_{ex}}{p_{in}} \right)^{\eta_p^{(\gamma-1)/\gamma}} \right\} \quad (2-61)$$

Equating (2-60) with (2-61) then yields

$$\bar{\eta} = \frac{1 - \left(\frac{p_{ex}}{p_{in}} \right)^{\eta_p^{(\gamma-1)/\gamma}}}{1 - \left(\frac{p_{ex}}{p_{in}} \right)^{(\gamma-1)/\gamma}} \quad (2-62)$$

This relation is illustrated in figure 2-10. The two efficiencies approach each other as pressure ratio and efficiency each approach unity. However, at higher pressure ratios, especially at lower efficiency levels, the two efficiencies can differ significantly.

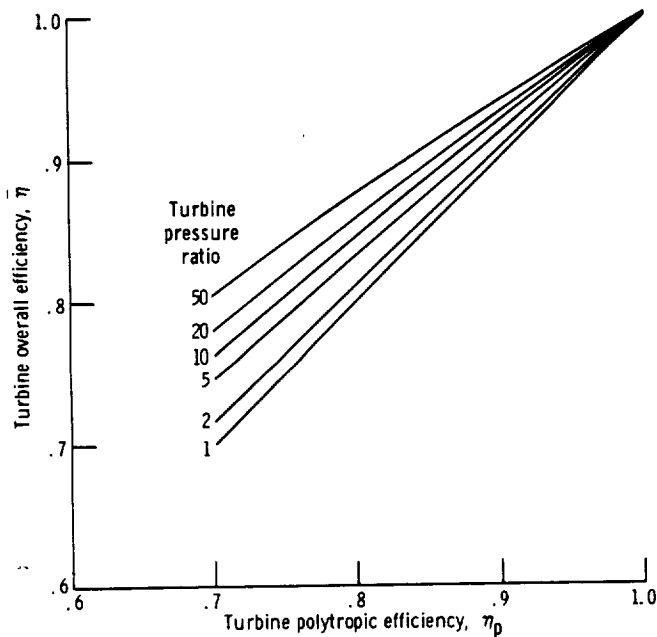


FIGURE 2-10.—Relation between turbine overall and polytropic efficiencies. Specific heat ratio γ , 1.4.

DIMENSIONLESS PARAMETERS

Dimensionless parameters serve to classify velocity diagrams, classify turbine geometry, and correlate turbine performance. A number of the more commonly used dimensionless parameters are introduced and discussed in this section. The basis for the use of dimensionless parameters is dimensional analysis.

Dimensional Analysis

Dimensional analysis is a procedure that allows a group of variables comprising a physical relation to be arranged so that they throw some light on the nature of the relation. It is a procedure for grouping the variables into a smaller number of dimensionless groups, each containing two or more variables. The number of such groups will be the minimum necessary to include all the variables at least once and to represent the physical relation between them. The basis of dimensional analysis as a formal procedure is the π -Theorem, which states that a complete physical equation may be expressed in the form of a number of terms, each term representing a product of powers of some of the variables and forming a dimensionless group. The formal procedure for obtaining the dimensionless groups from the pertinent variables is presented in many texts, including reference 1, which served as the basis for this discussion.

Application of dimensional analysis to the general problem of fluid flow yields considerable insight into the nature of the basic physical relations. The resultant dimensionless terms represent ratios of dimensions, ratios of forces, and ratios of velocities. The geometrical term implies that shape (as a ratio of linear dimensions), rather than the actual magnitude of each linear dimension by itself, is a controlling factor. Another term expresses the ratio of the force due to the change of pressure in the fluid to the inertia force due to the motion of the fluid. This is a basic flow parameter characteristic of an analysis based on an ideal fluid. There are other dimensionless groups, based on various attributes of a real fluid, that modify the ideal relations. These include the Reynolds number, which expresses the effect of viscous forces; the Weber number, which expresses surface-tension effects; an elasticity parameter (which for a gas reduces to the Mach number), which expresses compressibility effects; and the Froude number, which expresses gravitational effects. Of these terms expressing real fluid effects, in general, the Reynolds and Mach numbers are the significant parameters for gas flow.

The concept of dimensionless groups as ratios of geometric, kinematic, and dynamic quantities leads to the idea of similarity or similitude. If two operating conditions are such that all the dimen-

sionless terms have the same value, regardless of the individual values of the separate variables, then exactly similar physical conditions are obtained. Complete physical similarity implies (1) geometric similarity, which means that the linear dimension ratios are everywhere the same; (2) kinematic similarity, which means that the velocity ratios are the same; and (3) dynamic similarity, which means that the ratios of the different forces are the same. It is doubtful whether complete physical similarity is ever attained, but for most practical purposes it can be approached sufficiently closely to be of great utility. One use of similarity is the operation of models of smaller linear scale so that relatively inexpensive experiments can be performed with the results applicable to the full-size machine. Another use of similarity involves the operation of machines with the fluid at or near ambient conditions rather than at some severe design condition.

Turbomachine Operational Parameters

Application of dimensional analysis to the general problem of fluid flow results in the previously mentioned set of parameters. These parameters are important for the detailed examination of flow within the blade rows of turbomachines. In addition, dimensional analysis has great utility in the analysis of the overall operational characteristics. For any turbomachine, we are interested in the relation of head (for compressible flow, this relates to ideal work), flow rate, and power in conjunction with size, speed, and the properties of the fluid. The following variables are used to demonstrate some of the more important relations:

Volume flow rate, Q , m³/sec or ft³/sec

Head, H , J/kg or (ft)(lbf)/lbfm

Power, P , W or Btu/sec

Rotative speed, N , rad/sec or rev/min

Characteristic linear dimension, D , m or ft

Fluid density, ρ , kg/m³ or lb/ft³

Fluid viscosity, μ , (N)(sec)/m² or lbfm/(ft)(sec)

Fluid elasticity, E , N/m² or lbf/ft²

From these variables, five dimensionless groups can be formed. If we drop the dimensional conversion constants in order to ease the manipulation, the five dimensionless groups can be expressed as

$$\frac{Q}{ND^3} = f_{cn} \left(\frac{H}{N^2 D^2}, \frac{P}{\rho N^3 D^3}, \frac{\rho N D^2}{\mu}, \frac{E}{\rho N^2 D^2} \right) \quad (2-63)$$

The capacity, or flow rate, is expressed in dimensionless form by Q/ND^3 , which is called the capacity coefficient. It can be further

represented as

$$\frac{Q}{ND^3} \propto \frac{VA}{ND^3} \propto \frac{VD^2}{ND^3} \propto \frac{V}{ND} \propto \frac{V}{U} \quad (2-64)$$

Thus, the capacity coefficient is equivalent to V/U , and a given value of Q/ND^3 implies a particular relation of fluid velocity to blade speed or, in kinematic terms, similar velocity diagrams.

The head is expressed in dimensionless form by H/N^2D^2 , which is called the head coefficient. This can be represented as

$$\frac{H}{N^2D^2} \propto \frac{H}{U^2} \quad (2-65)$$

Thus, a given value of H/N^2D^2 implies a particular relation of head to rotor kinetic energy, or dynamic similarity.

The term $P/\rho N^3D^5$ is a power coefficient. It represents the actual power and thus is related to the capacity and head coefficients, as well as to the efficiency.

The term $\rho ND^2/\mu$ is the Reynolds number, or viscous effect coefficient. Its effect on overall turbine performance, while still important, can be regarded as secondary. The Reynolds number effect will be discussed separately later in this chapter.

The term $E/\rho N^2D^2$ is the compressibility coefficient. Its effect depends on the level of Mach number. At low Mach number, where the gas is relatively incompressible, the effect is negligible or very secondary. As Mach number increases, the compressibility effect becomes increasingly significant.

Velocity-Diagram Parameters

We have seen that the ratio of fluid velocity to blade velocity and the ratio of fluid energy to blade energy are important factors required for achieving similarity in turbomachines. Since completely similar machines should perform similarly, these factors become important as a means for correlating performance. Since the factors V/U and H/U^2 are related to the velocity diagrams, factors of this type are referred to as velocity-diagram parameters.

Several velocity-diagram parameters are commonly used in turbine work. Most of these are used primarily with respect to axial-flow turbines. One of these parameters is the speed-work parameter

$$\lambda = \frac{U^2}{gJ\Delta h'} \quad (2-66)$$

The reciprocal of the speed-work parameter is also often used, and it

TURBINE DESIGN AND APPLICATION

is referred to as the loading factor or loading coefficient

$$\psi = \frac{1}{\lambda} = \frac{gJ\Delta h'}{U^2} \quad (2-67)$$

For an axial-flow turbine, we can write

$$\Delta h' = \frac{U\Delta V_u}{gJ} \quad (2-68)$$

Therefore, equations (2-66) and (2-67) can be expressed as

$$\lambda = \frac{1}{\psi} = \frac{U}{\Delta V_u} \quad (2-69)$$

Another parameter often used is the blade-jet speed ratio

$$\nu = \frac{U}{V_j} \quad (2-70)$$

where V_j is the jet, or spouting, velocity, in m/sec or ft/sec. The jet, or spouting, velocity is defined as the velocity corresponding to the ideal expansion from inlet total to exit static conditions across the stage or turbine. That is,

$$V_j^2 = 2gJ\Delta h_{id} \quad (2-71)$$

Substitution of equation (2-71) back into equation (2-70) yields

$$\nu = \frac{U}{\sqrt{2gJ\Delta h_{id}}} \quad (2-72)$$

A relation between the blade-jet speed ratio and the speed-work parameter can be obtained by use of equations (2-66) and (2-72) and the static efficiency definition

$$\eta = \frac{\Delta h'}{\Delta h_{id}} \quad (2-73)$$

The resultant relation is

$$\nu = \sqrt{\frac{\lambda\eta}{2}} \quad (2-74)$$

This shows that if efficiency is a function of one of these parameters it must also be a function of the other. While the speed-work parameter is directly related only to the actual velocity diagram, the blade-jet speed ratio is related to the velocity diagram and to the efficiency.

Another frequently used velocity-diagram parameter is the flow

factor, or flow coefficient

$$\phi = \frac{V_z}{U} \quad (2-75)$$

The flow coefficient can be related to the loading coefficient as follows:

$$\phi = \frac{V_z}{U} = \left(\frac{V_r}{V_{u,1}} \right) \left(\frac{V_{u,1}}{\Delta V_u} \right) \left(\frac{\Delta V_u}{U} \right) \quad (2-76)$$

By using equation (2-69) and the velocity-diagram geometry, we get

$$\phi = \psi \cot \alpha_1 \left(\frac{V_{u,1}}{\Delta V_u} \right) \quad (2-77)$$

The term $V_{u,1}/\Delta V_u$ cannot be completely generalized. However, for specific types of velocity diagrams, such as will be discussed in the next chapter, this term becomes a function of loading coefficient alone (a different function for each type of velocity diagram). Therefore, for each of the different types of velocity diagrams, the flow coefficient can be expressed in terms of the loading coefficient and the stator exit angle.

It is thus seen that these four velocity-diagram parameters are related to each other. In addition, efficiency can be related to these parameters. This will be shown for an idealized specific case in the next section and for a somewhat more general real case in the next chapter. Where a particular type of velocity diagram is specified, only one of the velocity-diagram parameters is required for correlating efficiency. We at Lewis generally use the speed-work parameter or the blade-jet speed ratio. For a more general efficiency correlation, two of these parameters are required. One parameter must be the flow coefficient, and the other is usually the loading coefficient.

Relation of Efficiency to Velocity-Diagram Parameters

We will now show for an idealized specific case how static efficiency can be related mathematically to the blade-jet speed ratio. Assume that we have a single axial-flow ($U_1 = U_2$) impulse ($W_1 = W_2$) stage with constant axial velocity ($V_{z,1} = V_{z,2}$). A velocity diagram for a stage of this type is shown in figure 2-11. Further assume that flow through this turbine stage is isentropic (total efficiency $\eta' = 1$). The only loss, therefore, is exit kinetic energy. The static efficiency definition is

$$\eta = \frac{h'_0 - h'_2}{h'_0 - h'_{2, id}} = \frac{\Delta h'}{\Delta h'_{id}} \quad (2-78)$$

Substitution of equation (2-68) into equation (2-78) yields

TURBINE DESIGN AND APPLICATION

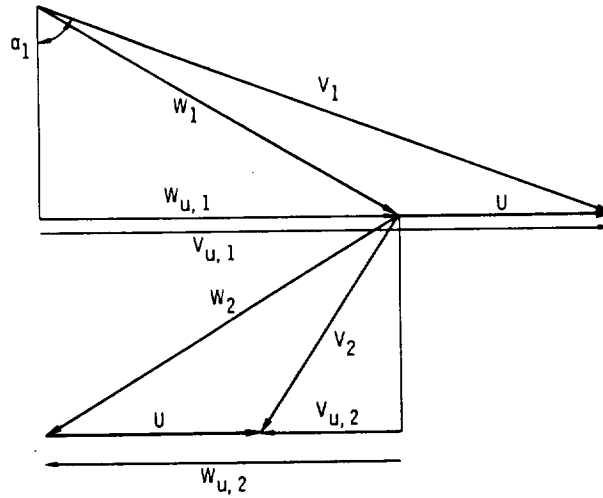


FIGURE 2-11.—Velocity-vector diagram for an axial-flow, impulse stage.

$$\eta = \frac{U \Delta V_u}{gJ \Delta h_{id}} \quad (2-79)$$

The change in fluid tangential velocity is

$$\Delta V_u = V_{u,1} - V_{u,2} \quad (2-80)$$

From the assumptions ($W_1 = W_2$) and ($W_{x,1} = W_{x,2}$) and the sign convention we adopted,

$$W_{u,2} = -W_{u,1} \quad (2-81)$$

From equations (2-6), (2-81), and (2-80), we get

$$V_{u,2} = W_{u,2} + U = -W_{u,1} + U = -(V_{u,1} - U) + U = -V_{u,1} + 2U \quad (2-82)$$

and

$$\Delta V_u = V_{u,1} - V_{u,2} = V_{u,1} - (-V_{u,1} + 2U) = 2V_{u,1} - 2U \quad (2-83)$$

From the velocity-diagram geometry

$$V_{u,1} = V_1 \sin \alpha_1 \quad (2-84)$$

Since flow is isentropic and the turbine stage is of the impulse type ($h_{2, id} = h_2 = h_1$),

$$V_1 = \sqrt{2gJ \Delta h_{id}} \quad (2-85)$$

Substitution of equations (2-84) and (2-85) into equation (2-83)

yields

$$\Delta V_u = 2 \sin \alpha_1 \sqrt{2gJ\Delta h_{id}} - 2U \quad (2-86)$$

Substitution of equation (2-86) back into equation (2-79) yields

$$\eta = \frac{4U \sin \alpha_1}{\sqrt{2gJ\Delta h_{id}}} - \frac{4U^2}{2gJ\Delta h_{id}} \quad (2-87)$$

Now using the definition of blade-jet speed ratio from equation (2-72) finally yields

$$\eta = 4\nu \sin \alpha_1 - 4\nu^2 \quad (2-88)$$

Equation (2-88) shows that for this particular case and any constant stator exit angle, static efficiency is a function of blade-jet speed ratio only. The variation is parabolic and is illustrated in figure 2-12 for an example with a stator exit angle of 70° . A maximum efficiency of 0.88 is reached at a blade-jet speed ratio of 0.47. The optimum blade-jet speed ratio can be found mathematically by differentiating equation (2-88) and setting the derivative equal to zero:

$$\nu_{opt} = \frac{\sin \alpha_1}{2} \quad (2-89)$$

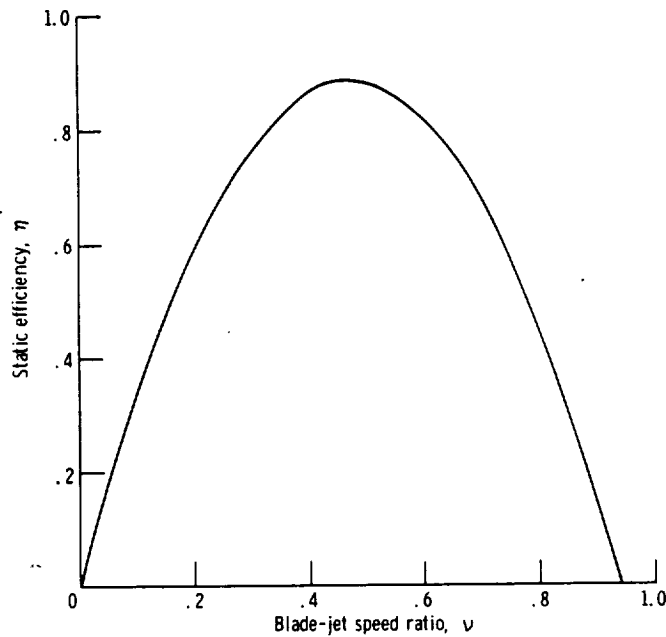


FIGURE 2-12.—Effect of blade-jet speed ratio on static efficiency of an isentropic, axial-flow, impulse stage. Stator exit angle, 70° .

Since the stator exit angle is normally in the range of 60° to 80°, where the sine of the angle does not vary greatly, the optimum blade-jet speed ratio for most cases of interest with a turbine of this type would be in the range of 0.4 to 0.5.

Equation (2-88) and figure 2-12 are, of course, very idealized and specific. While the levels and values for a real case will differ from the ideal case, the basic parabolic trend should remain the same; and, indeed, it does. We find that for a real case, blade-jet speed ratio is a very good correlating parameter for both static and total efficiency. Likewise, so are the other velocity-diagram parameters.

Design Parameters

The operation of dimensional analysis on the variables relating to turbomachines led to the dimensionless parameters shown in equation (2-63). This does not, however, exhaust the number of dimensionless parameters that are possible. A parameter not having the linear dimension D would be desirable because values of the remaining variables would apply to a range of geometrically similar turbomachines of all sizes. Also, a parameter not having rotative speed N would be desirable because, in this case, values of the remaining variables would apply to a turbomachine at all rotative speeds.

Such parameters can be found by combining two of the previous groups. The parameter that excludes D is known as the specific speed N_s , and is found as

$$N_s = \left(\frac{Q}{ND^3} \right)^{1/2} \left(\frac{N^2 D^2}{H} \right)^{3/4} = \frac{NQ^{1/2}}{H^{3/4}} \quad (2-90)$$

When used for a turbine, the volume flow rate is taken at the stage exit or turbine exit. Thus,

$$N_s = \frac{NQ_{t2}^{1/2}}{H^{3/4}} \quad (2-91)$$

The parameter that excludes N is known as the specific diameter D_s , and is found as

$$D_s = \left(\frac{H}{N^2 D^2} \right)^{1/4} \left(\frac{ND^3}{Q} \right)^{1/2} = \frac{DH^{1/4}}{Q^{1/2}} \quad (2-92)$$

With the volume flow rate taken at the stage exit or turbine exit,

$$D_s = \frac{DH^{1/4}}{Q_{t2}^{1/2}} \quad (2-93)$$

Commonly, but not exclusively, the values for these parameters are quoted with rotative speed N in revolutions per minute, exit

volume flow rate Q_{ex} in cubic feet per second, ideal work, or head, H in foot-pounds per pound, and diameter D in feet. With this set of units, specific speed and specific diameter are not truly dimensionless because the units are not consistent. The head H is usually taken to be the total-to-total value ($\Delta h'_{id}$), but sometimes, for convenience, it is specified as the total-to-static value (Δh_{id}).

Specific speed and specific diameter can be related to the previously presented velocity diagram parameters. The blade speed is

$$U = \frac{\pi ND}{K} \quad (2-94)$$

where K is the dimensional constant (2π rad/rev or 60 sec/min). The head is

$$H = J\Delta h'_{id} = J\Delta h_{id} \left(\frac{\eta}{\eta'} \right) \quad (2-95)$$

Combining equations (2-91), (2-93), and (2-72) with equations (2-94) and (2-95) yields

$$N_s D_s = \frac{K}{\pi} \sqrt{\frac{2g\eta'}{\eta}} \nu \quad (2-96)$$

The ratio of total efficiency to static efficiency appears because of the differing definitions of ideal work used in defining the various parameters. Some authors prefer to use the same ideal work definition in all cases, thus eliminating the efficiency ratio from equation (2-96).

The parameter interrelation can be expressed in terms of the speed-work parameter by substituting equation (2-74) into equation (2-96)

$$N_s D_s = \frac{K}{\pi} \sqrt{g\eta'\lambda} \quad (2-97)$$

Specific speed and specific diameter can also be related to the flow coefficient. The exit volume flow rate is

$$Q_{ex} = A_{ex} V_x \quad (2-98)$$

where A_{ex} is the exit flow area, in m^2 or ft^2 . Combining equations (2-91), (2-93), (2-94), and (2-75) with equation (2-98) yields

$$N_s D_s^3 = \frac{KD^2}{\pi\phi A_{ex}} \quad (2-99)$$

Since specific speed and specific diameter are related to the velocity-diagram parameters, which can be used to correlate efficiency, then

specific speed and specific diameter can also be used to correlate efficiency.

Specific speed and specific diameter contain variables that the velocity-diagram parameters do not. These are diameter and volume flow rate, and their use leads to terms, such as D^2/A_{ex} appearing in equation (2-99), that imply shape. Thus, specific speed and specific diameter are sometimes referred to as shape parameters. They are also sometimes referred to as design parameters, since the shape will often dictate the type of design to be selected.

Overall Parameters

The dimensionless parameters that we have been discussing can be applied to a stage or to the entire turbine. When applied to a stage, these are the similarity parameters that represent similar conditions for equal values and thus can be used to correlate efficiency. When applied to the overall turbine, some of these parameters help identify the type of design that might be most appropriate and serve as a rapid means for estimating the number of required stages.

The following are the most commonly encountered overall parameters:

Overall specific speed

$$\bar{N}_s = \frac{NQ_{ex}^{1/2}}{\bar{H}^{3/4}} \quad (2-100)$$

Overall specific diameter

$$\bar{D}_s = \frac{D_{av}\bar{H}^{1/4}}{Q_{ex}^{1/2}} \quad (2-101)$$

Overall speed-work parameter

$$\bar{\lambda} = \frac{U_{av}^2}{gJ\Delta h'} \quad (2-102)$$

Overall blade-jet speed ratio

$$\bar{v} = \frac{U_{av}}{(2gJ\Delta h_{id})^{1/2}} \quad (2-103)$$

The subscript *av* refers to some average condition, and the superscript (—) refers to the value for the entire turbine.

Of these overall parameters, specific speed perhaps is most significant because its value is almost always determined by application considerations only, while the values for the other parameters generally depend on the nature of the evolved geometry. Equation (2-100) for overall specific speed can be restated to show the considerations that contribute to the value of overall specific speed. Let

$$Q_{ex} = wv_{ex} \quad (2-104)$$

BASIC TURBINE CONCEPTS

where v_{ex} is specific volume at exit, in m^3/sec or ft^3/lb . Also, let mass flow rate be expressed as

$$w = \frac{J\bar{P}}{\eta\bar{H}} \quad (2-105)$$

Then, substitution of equations (2-104) and (2-105) into equation (2-100) yields

$$\bar{N}_s = \frac{1}{\eta} \left(\frac{v_{ex}}{\bar{H}^{5/2}} \right)^{1/2} (N\sqrt{J\bar{P}}) \quad (2-106)$$

Thus, the overall specific speed can be expressed as the product of three terms. The first term reflects expected performance, which can be reasonably estimated. The second term depends only on the specified gas and the thermodynamic cycle conditions. This second term is useful for evaluating the effects that different fluids (in cases where a choice is available) have on the turbine. The third term is dictated by the application. Often, both rotative speed and power are specified; in other cases, the product $N\sqrt{J\bar{P}}$, rather than the individual values of N and \bar{P} , is established by the application.

The manner in which the overall specific speed influences the tur-

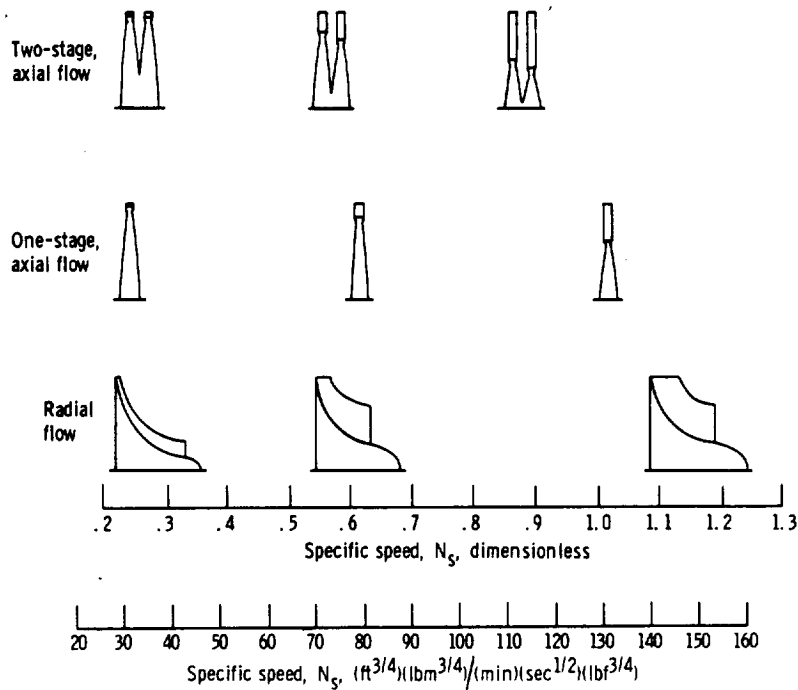


FIGURE 2-13.—Effect of specific speed on turbine-blade shape.

TURBINE DESIGN AND APPLICATION

bine passage shape is illustrated in figure 2-13 for a radial-flow turbine and for one- and two-stage, axial-flow, example turbines. The ratio of hub radius to tip radius decreases with increasing specific speed. For the axial-flow turbines, increasing the number of stages decreases the radius ratio. Thus, the overall specific speed for any application indicates the type or types of design that will be required.

The values of some of the overall parameters give us a rapid approximation of the number of stages required for a given application. Dividing equation (2-100) for overall specific speed by equation (2-91) for stage specific speed yields

$$\frac{\bar{N}_s}{N_s} = \left(\frac{Q_{ex}}{Q_{ex, stag}} \right)^{1/2} \left(\frac{H}{\bar{H}} \right)^{3/4} \quad (2-107)$$

If we neglect the reheat effect, which is small, and assume equal head change per stage, we can write

$$\bar{H} = nH \quad (2-108)$$

Further, if the expansion ratio is not too large, we can neglect the compressibility effect and assume that $Q_{ex} = Q_{ex, stag}$. Substitution of these last two conditions into equation (2-107) and rearrangement yields

$$n = \left(\frac{N_s}{\bar{N}_s} \right)^{4/3} \quad (2-109)$$

Since stage specific speed is a correlating parameter for efficiency, experience can tell us a reasonable value of stage specific speed to assume in order to achieve a given level of efficiency. Thus, with stage specific speed assumed and overall specific speed known from the application requirement, equation (2-109) gives us an estimate for number of stages. The effect of compressibility on this estimate is discussed in reference 2, where a compressibility correction is presented.

A similar type of estimate for number of stages is often obtained from the overall speed-work parameter and an assumed value for the stage speed-work parameter. Knowledge of a value for the overall speed-work parameter, however, requires a knowledge of the blade speed. Often, a reasonable value of blade speed can be selected on the basis of stress considerations. Or, blade speed may be varied parametrically if desired. Dividing equation (2-66) for stage speed-work parameter by equation (2-102) for overall speed-work parameter, assuming a constant blade speed for the turbine ($U^2 = U_{av}^2$), and assuming equal work per stage,

$$\bar{\Delta h}' = n\Delta h' \quad (2-110)$$

yields

$$n = \frac{\lambda}{\lambda} \quad (2-111)$$

Equations (2-109) and (2-111) are particularly useful for parametric studies associated with preliminary system analyses.

Performance Specification Parameters

The turbomachinery parameters presented in equation (2-63) are perfectly correct for compressible flow machines. Another choice of variables, however, is often preferred for expressing nondimensional performance. The mass flow rate w is preferred to the volume flow rate Q because for any significant degree of expansion, Q changes considerably throughout the turbine, while w remains constant. Change of pressure expressed as pressure ratio is preferred to H , which for compressible flow depends on both pressure ratio and initial temperature. Instead of power P , the preferred term to express actual work is the specific work or drop in total enthalpy $\Delta h'$. Since ideal work depends on the initial temperature as well as on the pressure ratio, we include initial temperature as another variable. Since Mach number depends on temperature, introduction of temperature is equivalent to introducing elasticity. Rotative speed N and a characteristic dimension D are still of interest. The fluid properties are included as gas constant R , which implies a molecular weight, and viscosity μ . For simplicity here, the specific heat ratio γ is assumed constant.

Now, operating with the variables

$$w = \text{fcn}(\Delta h', p'_{in}, p'_{ex}, T'_{in}, N, D, R, \mu) \quad (2-112)$$

dimensional analysis produces the following:

$$\frac{w\sqrt{RT'_{in}}}{p'_{in}D^2} = \text{fcn}\left(\frac{\Delta h'}{RT'_{in}}, \frac{ND}{\sqrt{RT'_{in}}}, \frac{p'_{in}}{p'_{ex}}, \frac{w}{\mu D}\right) \quad (2-113)$$

If the specific heat ratio had not been assumed constant, there would be some complicated, but second-order, terms modifying the flow, work, and speed terms.

Let us operate on some of the above terms to see what significance we can get out of them. The mass-flow parameter may be transformed by using the continuity equation, the ideal-gas law, and the proportionality $A \propto D^2$, so that

$$w = AV\rho = AV \frac{p}{RT} \propto D^2 V \frac{p}{RT} \propto D^2 V \frac{p'_{in}}{RT'_{in}} \quad (2-114)$$

TURBINE DESIGN AND APPLICATION

Substitution of this relation into the mass flow parameter of equation (2-113) yields

$$\frac{w\sqrt{RT'_{in}}}{p'_i D^2} \propto \frac{D^2 V p'_{in} \sqrt{RT'_{in}}}{RT'_{in} p'_{in} D^2} \propto \frac{V}{\sqrt{RT'_{in}}} \propto \frac{V}{a_{cr}} \quad (2-115)$$

Thus, the mass flow rate is represented nondimensionally by the ratio of actual mass flow rate to the mass flow rate when the velocity equals the critical, or sonic, velocity.

The speed parameter may be transformed as

$$\frac{ND}{\sqrt{RT'_{in}}} \propto \frac{U}{\sqrt{RT'_{in}}} \propto \frac{U}{a_{cr}} \quad (2-116)$$

Thus, the rotative speed is represented nondimensionally by the ratio of rotor-blade velocity to critical velocity, which is a kind of rotor Mach number. Division of the mass-flow parameter by the speed parameter gives V/U , the kinematic condition of similarity. The implication of this analysis is that for similarity, not only must the fluid have a certain Mach number, but the rotor must also have a certain fixed velocity with respect to the critical velocity. For a given machine of fixed dimensions, therefore, the rotative speed is not a singular variable as for incompressible flow, but becomes associated with the temperature of the fluid. All variables must be expressed in dimensionless form in order for the effect of varying inlet temperature to be correlated.

For a given gas, the dimensionless parameters presented as equation (2-113) can be expressed as

$$\frac{w\sqrt{T'_{in}}}{p'_{in} D^2} = \text{fcn} \left(\frac{\Delta h'}{T'_{in}}, \frac{ND}{\sqrt{T'_{in}}}, \frac{p'_{in}}{p_{ez}}, \frac{w}{\mu D} \right) \quad (2-117)$$

For a given gas in a given turbine, the parameters further reduce to

$$\frac{w\sqrt{T'_{in}}}{p'_{in}} = \text{fcn} \left(\frac{\Delta h'}{T'_{in}}, \frac{N}{\sqrt{T'_{in}}}, \frac{p'_{in}}{p_{ez}}, \frac{w}{\mu} \right) \quad (2-118)$$

Depending on the particular case, the parameters presented in equations (2-113), (2-117), or (2-118) can be used to express turbine performance.

Equivalent Conditions

It is very useful to report performance under standard conditions of temperature and pressure and sometimes of fluid molecular weight and specific heat ratio. This is done in order that results obtained at

different conditions may be directly and readily compared and also easily used to determine performance for any condition we desire. The following are the standard conditions usually used: atmospheric pressure, 101 325 N/m² abs or 14.696 psia; temperature, 288.2 K or 518.7° R; molecular weight, 29.0; and specific heat ratio, 1.4. These are known as NACA standard conditions, or NACA standard air. The performance variables of flow, work, and speed expressed on the basis of these standard conditions are known as equivalent conditions.

Let us use the parameters of equation (2-113) but with diameter constant. With the subscript *std* denoting standard conditions and the subscript *eq* denoting equivalent conditions, the similarity conditions can then be expressed as

$$\frac{w\sqrt{RT'_{in}}}{p'_{in}} = \frac{w_{eq}\sqrt{R_{std}T'_{std}}}{p'_{std}} \quad (2-119)$$

$$\frac{\Delta h'}{RT'_{in}} = \frac{\Delta h'_{eq}}{R_{std}T'_{std}} \quad (2-120)$$

$$\frac{N}{\sqrt{RT'_{in}}} = \frac{N_{eq}}{\sqrt{R_{std}T'_{std}}} \quad (2-121)$$

Rearrangement of these equations then yields for the equivalent conditions

$$w_{eq} = w \frac{\sqrt{RT'_{in}}}{\sqrt{R_{std}T'_{std}}} \frac{p'_{std}}{p'_{in}} \quad (2-122)$$

$$\Delta h'_{eq} = \Delta h' \frac{R_{std}T'_{std}}{RT'_{in}} \quad (2-123)$$

$$N_{eq} = N \frac{\sqrt{R_{std}T'_{std}}}{\sqrt{RT'_{in}}} \quad (2-124)$$

As you may recall, we started off the discussion of these parameters by assuming constant specific heat ratio for all conditions. This is not always the case, since specific heat ratio can change with temperature and fluid. Let us now add a specific-heat-ratio effect into the above parameters. The specific-heat-ratio corrections that are commonly used do not yield similarity under all conditions, but only at critical (sonic) velocity. However, the terms that are left out depend on both specific heat ratio and Mach number, are cumbersome to work with, and have only a very small effect on equivalent conditions. With the commonly used specific-heat-ratio terms, the equivalent conditions are expressed as

$$w_{eq} = w \sqrt{\left(\frac{V_{cr}}{V_{cr, std}}\right)^2 \left(\frac{p'_{std}}{p'_{in}}\right) \epsilon} \quad (2-125)$$

$$\Delta h'_{eq} = \Delta h' \left(\frac{V_{cr, std}}{V_{cr}}\right)^2 \quad (2-126)$$

$$N_{eq} = N \sqrt{\left(\frac{V_{cr, std}}{V_{cr}}\right)^2} \quad (2-127)$$

where

$$\epsilon = \frac{\gamma_{std} \left(\frac{2}{\gamma_{std} + 1}\right)^{\gamma_{std}/(\gamma_{std} - 1)}}{\gamma \left(\frac{2}{\gamma + 1}\right)^{\gamma/(\gamma - 1)}} \quad (2-128)$$

and, as you recall,

$$V_{cr}^2 = \frac{2\gamma}{\gamma + 1} gRT' \quad (2-129)$$

Therefore, for constant specific heat ratio, equations (2-125) to (2-127) reduce to equations (2-122) to (2-124).

Finally, we define

$$\theta = \left(\frac{V_{cr}}{V_{cr, std}}\right)^2 \quad (2-130)$$

and

$$\delta = \frac{p'_{in}}{p'_{std}} \quad (2-131)$$

The equivalent conditions are then expressed as

$$w_{eq} = w \frac{\sqrt{\theta}}{\delta} \epsilon \quad (2-132)$$

$$\Delta h'_{eq} = \frac{\Delta h'}{\theta} \quad (2-133)$$

$$N_{eq} = \frac{N}{\sqrt{\theta}} \quad (2-134)$$

One point that can be seen from these similarity equations is that operation at temperatures greater than standard will cause a reduction of both actual mass flow and equivalent speed. Both of these factors reduce the output of a powerplant. A well-known example of this effect is the reduction in takeoff performance of jet aircraft on hot days.

Reynolds Number Effect

The effect of viscosity in the form of Reynolds number was shown to be one of the dimensionless parameters affecting turbomachine

performance. While its effect is secondary, it is still important. The effect of Reynolds number on turbine efficiency is usually correlated in the following manner:

Expressing efficiency as

$$\eta' = \frac{\Delta h'_{id} - \Delta h'_{loss}}{\Delta h'_{id}} = 1 - \frac{\Delta h'_{loss}}{\Delta h'_{id}} \quad (2-135)$$

we can write

$$1 - \eta' = \frac{\Delta h'_{loss}}{\Delta h'_{id}} \quad (2-136)$$

If we assume that the only loss is friction loss,

$$\Delta h'_{loss} \propto f \left(\frac{L}{D} \right) V^2 \quad (2-137)$$

where f is the friction factor, and L is the characteristic flow-path length. For turbulent flow,

$$f \propto \frac{1}{Re^{0.2}} \quad (2-138)$$

where Re is the Reynolds number. Substituting equations (2-138) and (2-137) into equation (2-136) yields

$$1 - \eta' \propto \frac{1}{Re^{0.2}} \left(\frac{L}{D} \right) \left(\frac{V^2}{\Delta h'_{id}} \right) \quad (2-139)$$

Adding subscripts for conditions 1 and 2 to equation (2-139) and dividing the equation for condition 1 by the equation for condition 2 yield

$$\frac{1 - \eta'_1}{1 - \eta'_2} = \frac{\left(\frac{1}{Re_1^{0.2}} \right) \left(\frac{L_1}{D_1} \right) \left(\frac{V_1^2}{\Delta h'_{1, id}} \right)}{\left(\frac{1}{Re_2^{0.2}} \right) \left(\frac{L_2}{D_2} \right) \left(\frac{V_2^2}{\Delta h'_{2, id}} \right)} \quad (2-140)$$

Since for geometric similarity $L_1/D_1 = L_2/D_2$ and for dynamic similarity $V_1^2/\Delta h'_{1, id} = V_2^2/\Delta h'_{2, id}$, equation (2-140) reduces to

$$\frac{1 - \eta'_1}{1 - \eta'_2} = \left(\frac{Re_2}{Re_1} \right)^{0.2} \quad (2-141)$$

This is an ideal correlation. Actually, it has been found that the exponent for this type of correlation is not 0.2, but usually varies in the range of 0.1 to 0.2, depending on the machine. This occurs because all the losses are not viscous losses, and the fraction of total loss attributable to viscous loss varies between machines. In view of this, another suggested type of correlation is

TURBINE DESIGN AND APPLICATION

$$\frac{1-\eta_1'}{1-\eta_2} = A + B \left(\frac{Re_2}{Re_1} \right)^{0.2} \quad (2-142)$$

where A and B are fractions such that $A + B = 1$. In equation (2-142) the exponent is maintained at 0.2 to reflect the viscous loss exponent, and the coefficients A and B serve to represent the fact that not all loss is viscous loss. Recent turbine tests here at Lewis, as well as the discussion presented in reference 1, indicate that values of about 0.3 to 0.4 for A and corresponding values of 0.7 to 0.6 for B seem to be a good compromise for correlating Reynolds number effects.

REFERENCES

1. SHEPHERD, D. G.: Principles of Turbomachinery. Macmillan Co., 1956.
2. GLASSMAN, ARTHUR J.; AND STEWART, WARNER L.: Use of Similarity Parameters for Examination of Geometry Characteristics of High-Expansion-Ratio Axial-Flow Turbines. NASA TN D-4248, 1967.

SYMBOLS

A	{ flow area, m^2 ; ft^2 Reynolds number correlation coefficient in eq. (2-142)
a	speed of sound, m/sec ; ft/sec
B	Reynolds number correlation coefficient in eq. (2-142)
c_p	heat capacity at constant pressure, $J/(kg)(K)$; $Btu/(lb)(^\circ R)$
D	diameter, m ; ft
D_s	specific diameter, dimensionless; $(sec^{1/2})(lb^{1/4})/(ft^{1/4})(lbm^{1/4})$
E	modulus of elasticity, N/m^2 ; lb/ft^2
e	kinetic energy loss coefficient, defined by eq. (2-46)
F	force, N ; lb
f	friction factor
g	conversion constant, 1; $32.17 (lbm)(ft)/(lbf)(sec^2)$
H	head, J/kg ; $(ft)(lbf)/lbm$
h	specific enthalpy, J/kg ; Btu/lb
J	conversion constant, 1; $778 (ft)(lb)/Btu$
K	conversion constant, 2π rad/rev; 60 sec/min
L	characteristic length, m ; ft
M	Mach number
N	rotative speed, rad/sec ; rev/min
N_s	specific speed, dimensionless; $(ft^{3/4})(lbm^{3/4})/(min)(sec^{1/2})(lbf^{3/4})$
n	{ number of stages polytropic exponent
P	power, W ; Btu/sec
p	absolute pressure, N/m^2 ; lb/ft^2
Q	volume flow rate, m^3/sec ; ft^3/sec
R	{ gas constant, $J/(kg)(K)$; $(ft)(lbf)/(lbm)(^\circ R)$ reaction
Re	Reynolds number
r	radius, m ; ft
T	absolute temperature, K ; $^\circ R$
U	blade speed, m/sec ; ft/sec
V	absolute velocity, m/sec ; ft/sec
V_j	ideal jet speed (defined by eq. (2-71)), m/sec ; ft/sec
v	specific volume, m^3/kg ; ft^3/lb
W	relative velocity, m/sec ; ft/sec
w	mass flow rate, kg/sec ; lb/sec
Y	total-pressure loss coefficient, defined by eqs. (2-47)
Y'	
Y''	
α	fluid absolute angle measured from axial or radial direction, deg
β	fluid relative angle measured from axial or radial direction, deg

TURBINE DESIGN AND APPLICATION

γ	ratio of heat capacity at constant pressure to heat capacity at constant volume
δ	ratio of inlet total pressure to NACA standard pressure
ϵ	function of specific heat ratio, defined by eq. (2-128)
η	efficiency
θ	squared ratio of critical velocity based on turbine inlet temperature to critical velocity based on NACA standard temperature
λ	speed-work parameter, defined by eq. (2-66)
μ	viscosity, (N)(sec)/m ² ; lb/(ft)(sec)
ν	blade-jet speed ratio, defined by eq. (2-72)
ρ	density, kg/m ³ ; lb/ft ³
τ	torque, N-m; lb-ft
φ	flow coefficient, defined by eq. (2-75)
ψ	loading coefficient, defined by eq. (2-67)
ω	angular velocity, rad/sec

Subscripts:

<i>av</i>	average
<i>cr</i>	critical condition ($M=1$)
<i>eq</i>	equivalent
<i>ex</i>	exit
<i>id</i>	ideal
<i>in</i>	inlet
<i>loss</i>	loss
<i>opt</i>	optimum
<i>p</i>	polytropic
<i>r</i>	radial component
<i>rel</i>	relative
<i>ro</i>	rotor
<i>st</i>	stator
<i>std</i>	NACA standard condition
<i>stg</i>	stage
<i>u</i>	tangential component
<i>x</i>	axial component
0	at stator inlet
1	at stator exit or rotor inlet
2	at rotor exit

Superscripts:

→	vector quantity
—	overall turbine
'	absolute total state
''	relative total state

GLOSSARY

The terms defined herein are illustrated in figure 2-14.

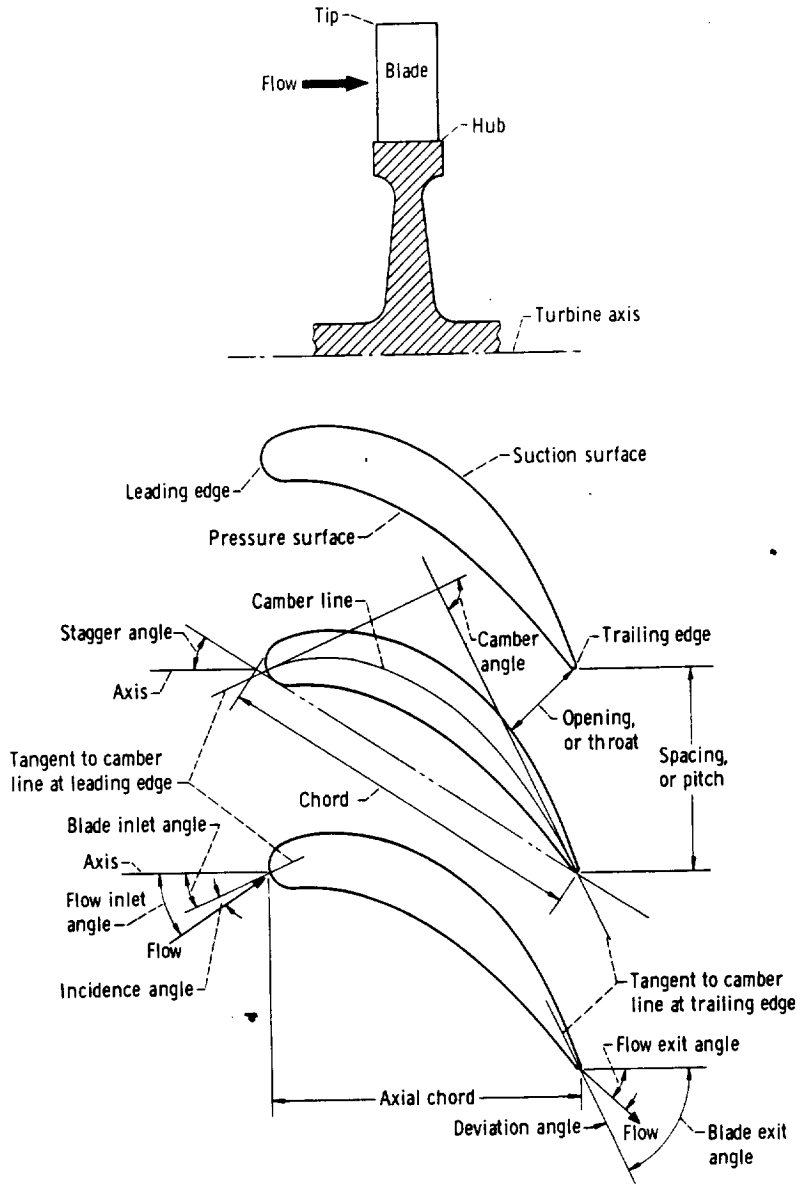


FIGURE 2-14.—Blade terminology.

TURBINE DESIGN AND APPLICATION

aspect ratio. The ratio of the **blade height** to the **chord**.

axial chord. The length of the projection of the blade, as set in the turbine, onto a line parallel to the turbine axis. It is the axial length of the blade.

axial solidity. The ratio of the **axial chord** to the **spacing**.

blade exit angle. The angle between the tangent to the **camber line** at the **trailing edge** and the turbine axial direction.

blade height. The radius at the **tip** minus the radius at the **hub**.

blade inlet angle. The angle between the tangent to the **camber line** at the **leading edge** and the turbine axial direction.

bucket. Same as **rotor blade**.

camber angle. The external angle formed by the intersection of the tangents to the **camber line** at the **leading** and **trailing edges**. It is equal to the sum of the angles formed by the **chord line** and the **camber-line** tangents.

camber line. The mean line of the blade profile. It extends from the **leading edge** to the **trailing edge**, halfway between the **pressure surface** and the **suction surface**.

chord. The length of the perpendicular projection of the blade profile onto the **chord line**. It is approximately equal to the linear distance between the **leading edge** and the **trailing edge**.

chord line. If a two-dimensional blade section were laid convex side up on a flat surface, the **chord line** is the line between the points where the front and the rear of the blade section would touch the surface.

deflection. The total turning angle of the fluid. It is equal to the difference between the **flow inlet angle** and the **flow exit angle**.

deviation angle. The **flow exit angle** minus the **blade exit angle**.

flow exit angle. The angle between the fluid flow direction at the blade exit and the turbine axial direction.

flow inlet angle. The angle between the fluid flow direction at the blade inlet and the turbine axial direction.

hub. The innermost section of the blade.

hub-tip ratio. Same as **hub- to tip-radius ratio**.

hub- to tip-radius ratio. The ratio of the hub radius to the tip radius.

incidence angle. The **flow inlet angle** minus the **blade inlet angle**.

leading edge. The front, or nose, of the blade.

mean section. The blade section halfway between the **hub** and the **tip**.

nozzle blade. Same as **stator blade**.

pitch. The distance in the direction of rotation between corresponding points on adjacent blades.

pressure surface. The concave surface of the blade. Along this surface, pressures are highest.

radius ratio. Same as **hub- to tip-radius ratio**.

BASIC TURBINE CONCEPTS

root. Same as **hub**.

rotor blade. A rotating blade.

solidity. The ratio of the **chord** to the **spacing**.

spacing. Same as **pitch**.

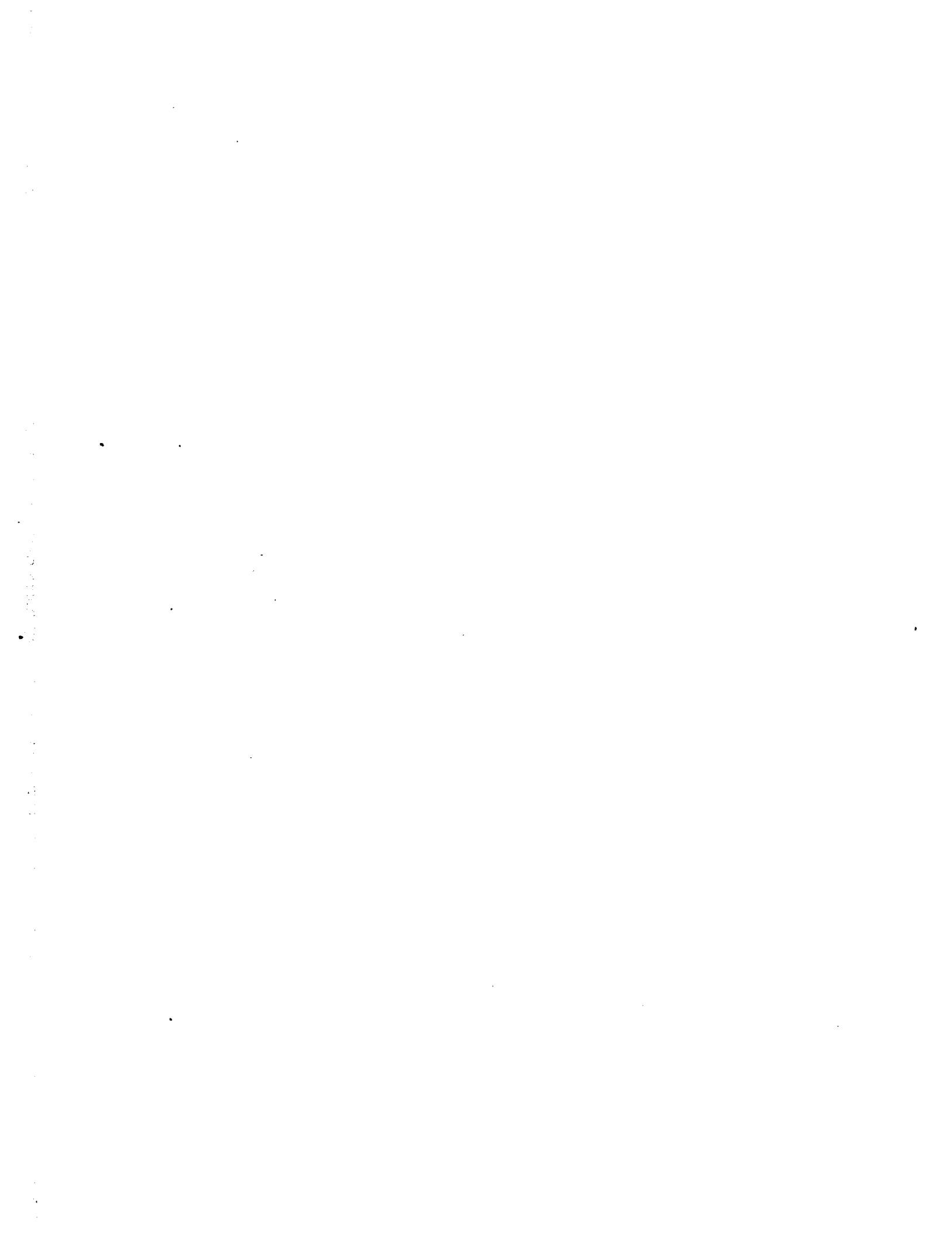
stagger angle. The angle between the **chord line** and the turbine axial direction.

stator blade. A stationary blade.

suction surface. The convex surface of the blade. Along this surface, pressures are lowest.

tip. The outermost section of the blade.

trailing edge. The rear, or tail, of the blade.



CHAPTER 3

Velocity Diagrams

By Warren J. Whitney and
Warner L. Stewart

As indicated in chapter 2, one of the most important variables to be considered in the design or analysis of turbines is the velocity of the fluid as it passes from one blade row to the next. The absolute and relative velocities and their relation to the speed of the blade row are universally described through the use of velocity diagrams. Once the overall design requirements of flow, work, and rotative speed are established, the next step is the evolution of the velocity diagrams. Their relation to the required blading geometry is very important in that these diagrams specify the flow angles and velocities that the blading is required to produce. In addition, the velocity diagrams significantly affect the efficiency level expected from the turbine.

The general methods for constructing velocity diagrams and relating them to the work and flow capacity of the turbine were discussed in chapter 2. Various dimensionless parameters associated with the velocity diagram were also presented in chapter 2, and their relation to turbine efficiency was illustrated by an idealized case. This chapter is devoted entirely to the subject of velocity diagrams. The first part of this chapter concerns a single diagram that can be considered representative of the average flow conditions for the stage. Usually, the conditions at the blade mean radius are used. The second part of this chapter is devoted to the radial variations in the diagrams that result from the balance of forces in the radial direction and from the variation in blade speed with radius. Only axial-flow turbines are considered in this chapter.

MEAN-SECTION DIAGRAMS

In this section, the velocity diagrams occurring at the mean section (halfway between hub and tip) are assumed to represent the average conditions encountered by the turbine. The different types of diagrams, their relation to stage efficiency, and their selection when staging is required are discussed.

In review, figure 3-1 shows an illustrative stage velocity diagram indicating the vector relations described in chapter 2 and the nomenclature. Assuming no change in mean radius through the stage, equation (2-14) can be written as

$$\Delta h' = \frac{U \Delta V_u}{gJ} \quad (3-1)$$

where

- h' total enthalpy, J/kg; Btu/lb
- U blade speed, m/sec; ft/sec
- V_u tangential component of velocity, m/sec; ft/sec
- g conversion constant, 1; 32.17 (lbm)(ft)/(lbf)(sec²)
- J conversion constant, 1; 778 (ft)(lb)/Btu

This equation relates the stage specific work to the velocity diagram. The axial component of the velocity vector is related to the flow rate, state conditions, and the area by the relation

$$V_z = \frac{w}{\rho A_{an}} \quad (3-2)$$

where

- V_z axial component of velocity, m/sec; ft/sec
- w mass flow rate, kg/sec; lb/sec
- ρ density, kg/m³; lb/ft³
- A_{an} annulus area, m²; ft²

Flow angles are key velocity-diagram parameters because they not only link the axial and swirl velocities (the tangential component of the absolute velocity is often referred to as the swirl velocity) but also affect the expected efficiency and blading geometry. In addition, dimensionless parameters are used in association with velocity-diagram studies because the parameter values can be related to the diagram shape. Such parameters were discussed in chapter 2 and include the speed-work parameter, which can be expressed in several ways, such as

$$\lambda = \frac{U^2}{gJ\Delta h'} = \frac{U}{\Delta V_u} = \frac{gJ\Delta h'}{\Delta V_u^2} \quad (3-3)$$

The speed-work parameter is used in this chapter because diagram

VELOCITY DIAGRAMS

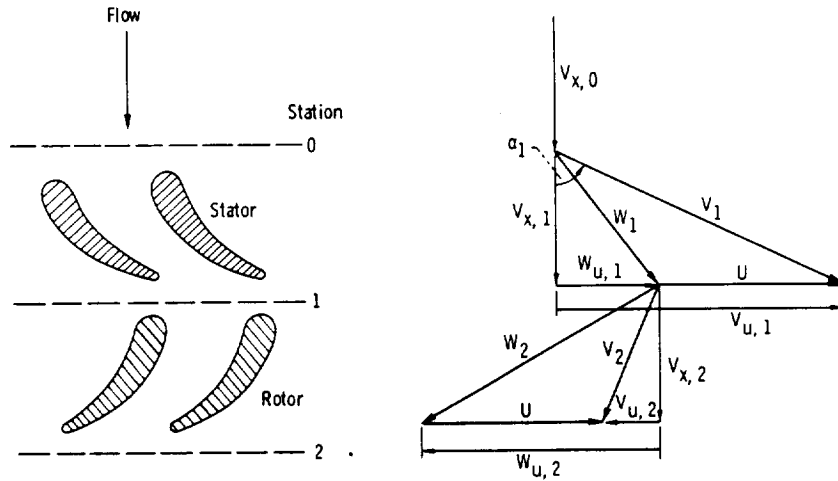


FIGURE 3-1.—Velocity-vector diagrams and nomenclature.

types are related to the swirl distribution and it is convenient to normalize the diagram velocities by ΔV_u .

Velocity-Diagram Types

After the overall design requirements are established, the velocity diagrams can be evolved. Velocity diagrams have different sizes and shapes depending on the diagram type and the value of the speed-work parameter. Diagram type refers to some physical constraint imposed on the diagram. Diagram shape determines the values of performance-related parameters, such as stage reaction and swirl split between the stator exit ($V_{u,1}$) and the rotor exit ($V_{u,2}$). The following three common types of diagrams and their reaction and swirl characteristics are discussed in this section:

- (1) Zero-exit-swirl diagram ($V_{u,2}=0$)
- (2) Rotor-impulse diagram ($W_1=W_2$)
- (3) Symmetrical diagram ($V_1=W_2$ and $V_2=W_1$)

These three diagrams for several values of speed-work parameter are shown in figure 3-2.

Zero-exit-swirl diagram.—In many cases, either the entire exit velocity head or the swirl component thereof represents a loss in efficiency. The zero-exit-swirl diagram, where

$$\frac{V_{u,1}}{\Delta V_u} = 1 \quad (3-4a)$$

and

TURBINE DESIGN AND APPLICATION

Speed-work parameter	Diagram type		
	Zero exit swirl	Impulse	Symmetrical
0.25			
0.5			
1.0			

FIGURE 3-2.—Effects of speed-work parameter and diagram type on shape of stage velocity-vector diagram.

$$\frac{V_{u,2}}{\Delta V_u} = 0 \quad (3-4b)$$

can be used to reduce such loss.

For an axial-flow rotor ($U_1 = U_2$) having constant axial velocity ($V_{z,1} = V_{z,2}$), the definition of stage reaction presented in equation (2-39) reduces to

$$R_{st} = \frac{W_{u,2}^2 - W_{u,1}^2}{V_{u,1}^2 - V_{u,2}^2 + W_{u,2}^2 - W_{u,1}^2} \quad (3-5)$$

where

R_{st} stage reaction

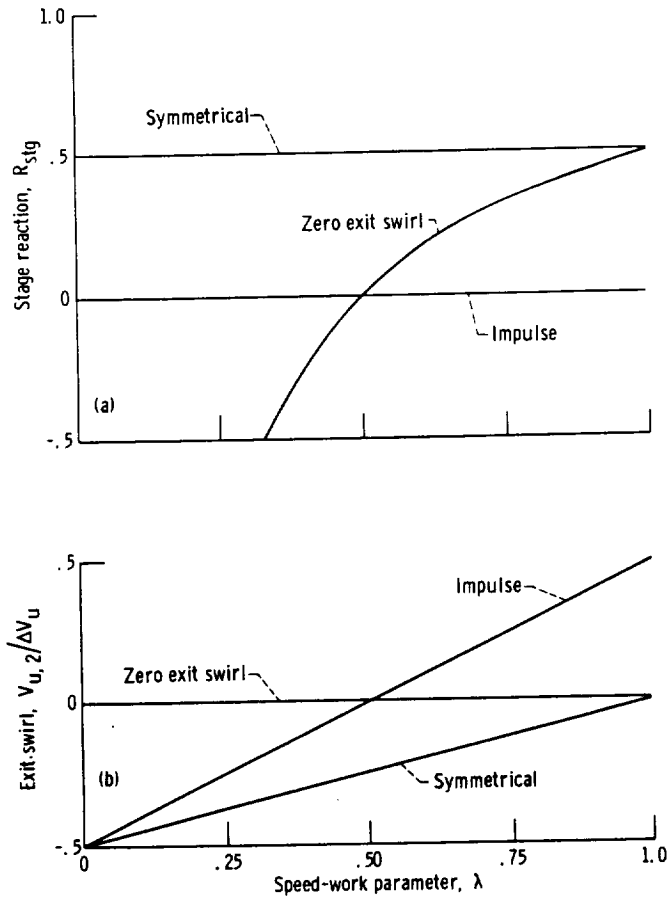
W_u tangential component of relative velocity, m/sec; ft/sec

By using equation (2-6) and equations (3-3) and (3-4), equation (3-5) can be expressed as

$$R_{st} = 1 - \frac{1}{2\lambda} \quad (3-6)$$

This equation is plotted in figure 3-3(a). At $\lambda = 1$, the reaction is 0.5, which indicates a conservative diagram. At $\lambda = 0.5$, the reaction is zero, which indicates an impulse rotor. Below $\lambda = 0.5$, negative reaction is encountered. For example, at $\lambda = 0.33$, the reaction is -0.5 , which, as can be shown, represents a substantial decrease in velocity and increase in static pressure across the rotor. Because of

VELOCITY DIAGRAMS



(a) Reaction.
 (b) Exit swirl.

FIGURE 3-3.—Effects of speed-work parameter and velocity-vector diagram type on reaction and exit swirl.

potentially high losses, such high negative reactions are usually avoided; therefore, zero-exit-swirl diagrams are seldom used for $\lambda < 0.5$. Figure 3-2 presents the zero-exit-swirl diagrams for the positive-reaction, impulse, and negative-reaction cases.

Impulse diagram.—For this case, $W_1 = W_2$ and the equation for stage reaction reduces to

$$R_{stg} = 0 \tag{3-7}$$

From equation (2-6), equation (3-3), and the assumption of constant axial velocity, the rotor inlet and exit swirl velocities can be expressed

TURBINE DESIGN AND APPLICATION

as

$$\frac{V_{u,1}}{\Delta V_u} = \lambda + 0.5 \quad (3-8a)$$

and

$$\frac{V_{u,2}}{\Delta V_u} = \lambda - 0.5 \quad (3-8b)$$

The exit swirl characteristics are shown in figure 3-3(b). Positive swirls are encountered at λ values greater than 0.5, and negative swirls are obtained at λ values less than 0.5. At $\lambda=0.5$, the impulse and zero-exit-swirl cases coincide. These effects are illustrated in figure 3-2. Because swirl velocity leaving a turbine is a loss and because positive swirl decreases stage work, impulse diagrams are seldom, if ever, used when λ is greater than 0.5.

Symmetrical diagram.—A third type of diagram commonly used is one in which the stator-exit- and rotor-exit-velocity triangles are specified to have the same shape. In terms of velocities,

$$V_1 = W_2 \quad (3-9a)$$

and

$$V_2 = W_1 \quad (3-9b)$$

Under this condition, the equation for stage reaction reduces to

$$R_{st} = \frac{1}{2} \quad (3-10)$$

From equation (2-6), equation (3-3), and the assumption of constant axial velocity, the swirl velocity components can be expressed as

$$\frac{V_{u,1}}{\Delta V_u} = \frac{\lambda + 1}{2} \quad (3-11a)$$

and

$$\frac{V_{u,2}}{\Delta V_u} = \frac{\lambda - 1}{2} \quad (3-11b)$$

These reaction and swirl characteristics are shown in figure 3-3, with typical diagrams illustrated in figure 3-2. The symmetrical diagram is the same as the zero-exit-swirl diagram at $\lambda=1$. As the value of λ decreases, the exit swirl increases, but the reaction remains constant at 0.5. This good reaction is conducive to high total efficiency, making this type of diagram attractive for stages where exit swirl is not a loss (e.g., the front and middle stages of a multistage turbine).

Stage Efficiency

A significant aspect of a turbine design is the expected efficiency.

The efficiency is an important function of, among other things, the type of velocity diagram used and the pressure distribution on the blade surface. Therefore, the diagram selection is greatly dependent on the efficiency requirements of the intended application. Some basic relations between diagram parameters and efficiency are presented and used herein to point up some of the more important effects. References 1 and 2 are used as a basis for this development.

As presented in chapter 2, turbine stage static efficiency can be written as

$$\eta = \frac{\Delta h'}{\Delta h_{id}} \quad (3-12)$$

where

η stage static efficiency

$\Delta h'$ stage work, J/kg; Btu/lb

Δh_{id} stage ideal work based on ratio of inlet total pressure to exit static pressure, J/kg; Btu/lb

Expressing ideal work in terms of actual work plus losses yields

$$\eta = \frac{\Delta h'}{\Delta h' + L_{st} + L_{ro} + \frac{V_2^2}{2gJ}} \quad (3-13)$$

where

L_{st} stator loss, J/kg; Btu/lb

L_{ro} rotor loss, J/kg; Btu/lb

$V_2^2/2gJ$ stage leaving loss, J/kg; Btu/lb

The equation for total efficiency η' is the same except for the elimination of the stage leaving loss, $V_2^2/2gJ$. Substituting equation (3-3) into equation (3-13) yields

$$\eta = \frac{\lambda}{\lambda + \frac{gJ(L_{st} + L_{ro})}{\Delta V_u^2} + \frac{1}{2} \frac{V_2^2}{\Delta V_u^2}} \quad (3-14)$$

In relating the stator and rotor losses to the diagram parameters, it was assumed that the losses were proportional to the average kinetic energy across the blade rows. That is,

$$L_{st} = K_{st} \frac{V_0^2 + V_1^2}{2gJ} \quad (3-15a)$$

and

$$L_{ro} = K_{ro} \frac{W_1^2 + W_2^2}{2gJ} \quad (3-15b)$$

where K is constant of proportionality.

Equations (3-14) and (3-15) serve as the basis for estimating efficiency. The exact nature of the assumptions and equations can be found in references 1 and 2. Briefly, the procedure for estimating efficiency is as follows:

- (1) The velocities are expressed in terms of their tangential and axial components.
- (2) The tangential components are expressed in terms of the speed-work parameter according to the diagram type being considered (eq. (2-6) and eq. (3-4), (3-8), or (3-11)).
- (3) The axial components are evaluated by means of an application-related mass-flow assumption or by relating them to the tangential components by an angle assumption.
- (4) The values for the constant of proportionality are selected on the basis of previous test experience.
- (5) Efficiency curves can then be generated over a range of speed-work parameter for the various diagram types.

The total- and static-efficiency characteristics as obtained from reference 2 by the above method are presented in figure 3-4. The curves presented for the symmetrical diagram are actually for the diagram that analytically yields maximum total efficiency. This diagram, as determined in reference 2, approximates the symmetrical diagram, and the associated efficiency characteristics are representative of those for a symmetrical diagram. The curves for the zero-exit-swirl diagram were not obtained for λ values less than 0.5 because of the undesirable negative reaction in that region.

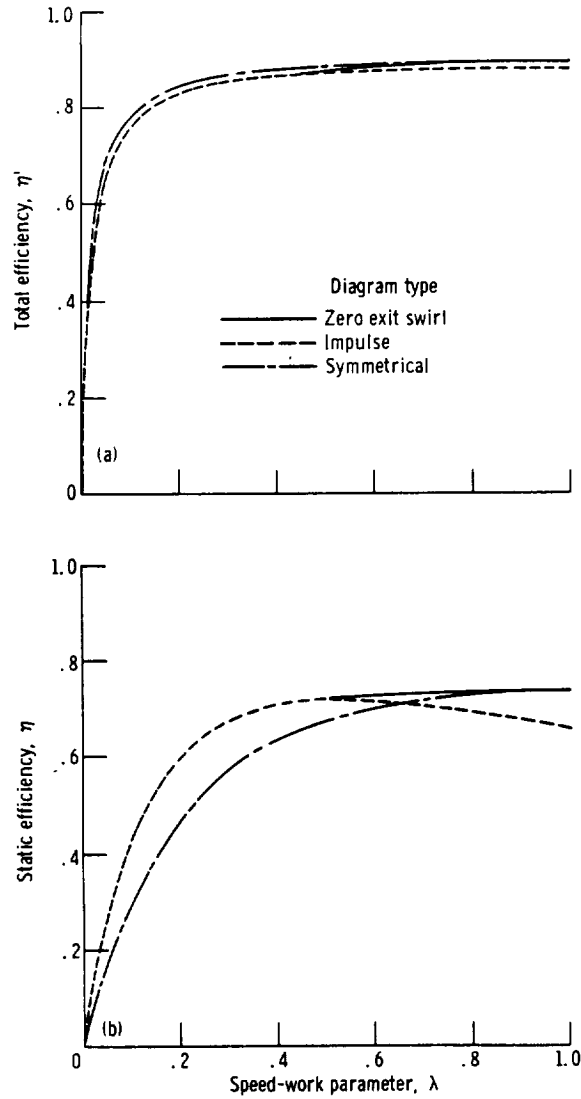
The total efficiency characteristics are presented in figure 3-4(a). For each diagram type, the highest efficiency occurs at a speed-work parameter, λ , value of 1. The symmetrical-diagram efficiency is slightly higher than the impulse-diagram efficiency for all values of λ . The zero-exit-swirl-diagram efficiency is equal to the symmetrical-diagram efficiency at $\lambda=1$, is equal to the impulse-diagram efficiency at $\lambda=0.5$, and, although not shown, becomes less than either of the other two for λ values less than 0.5. Between $\lambda=1$ and $\lambda=0.5$, the efficiency curves are rather flat. As λ is reduced below 0.5, efficiency decreases more rapidly.

High total efficiencies, therefore, are achievable with any of these diagram types for λ values greater than about 0.5. Even where total, rather than static, efficiency is the criterion of merit, however, the designer must still consider aspects such as the previously discussed exit swirls and the three-dimensional effects, to be discussed later in this chapter, before a diagram type is selected.

The static efficiency characteristics are presented in figure 3-4(b). The static efficiency is substantially lower than the total efficiency because the exit velocity head represents a loss. The highest static

VELOCITY DIAGRAMS

efficiency for λ values less than 0.5 is obtained with the impulse diagram, and for λ values greater than 0.5, with the zero-exit-swirl diagram. For the impulse diagram, the efficiency is a maximum at $\lambda=0.5$, where there is no exit swirl. For the symmetrical diagram, $\lambda=0.5$, where there is no exit swirl. For the symmetrical diagram,



- (a) Total efficiency.
- (b) Static efficiency.

FIGURE 3-4.—Effects of speed-work parameter and velocity-vector diagram type on efficiency. (Curves from ref. 2.)

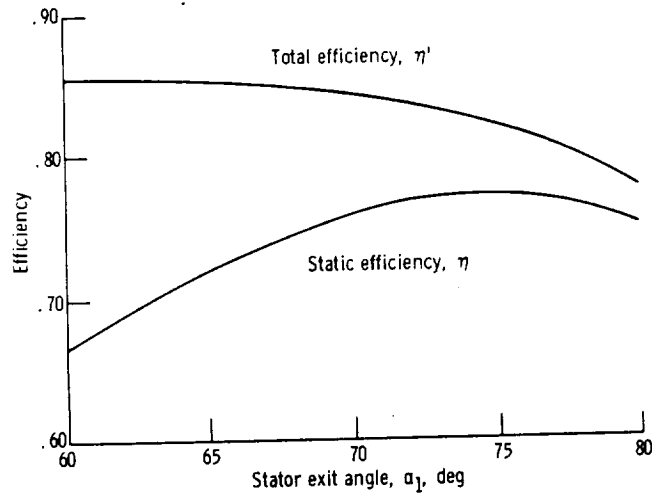


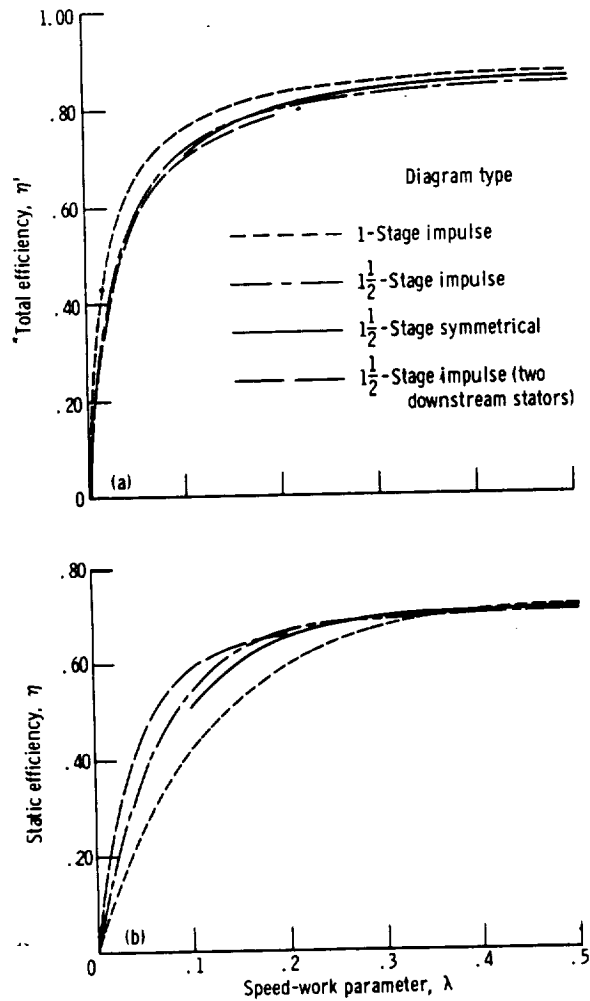
FIGURE 3-5.—Effect of stator exit angle on stage efficiency. Speed-work parameter λ , 0.5. (Curves from ref. 1.)

the efficiency is a maximum at $\lambda=1$, where there is no exit swirl. The zero-exit-swirl-diagram efficiency is highest at $\lambda=1$, but decreases very little as λ is reduced to 0.5.

Efficiency is affected not only by the speed-work parameter and diagram type but also by the velocity through-flow component V_z , which is related to the flow angles. An example of this effect can be obtained from reference 1. Figure 3-5, which is taken from reference 1, shows the total and static efficiencies as functions of stator exit angle. It is evident that the best angle depends upon which efficiency is to be maximized. If maximum total efficiency is desired, the stator exit angle should be about 60° . If maximum static efficiency is desired, a stator exit angle of about 75° is indicated. However, complete freedom of selection of this angle does not always exist since it affects the through-flow component of velocity and, therefore, the annulus area. The rotor stress level is also influenced by the annulus area and, hence, could influence the angle selection.

It has been shown that at low values of speed-work parameter, large exit swirls are encountered, with associated reductions in static efficiency. One means of increasing the static efficiency is through the use of downstream stators, which remove the swirl and diffuse the flow back to axial. The efficiency characteristics of such turbines (ref. 3) are presented in figure 3-6. In this figure, the turbines with downstream stators are referred to as $1\frac{1}{2}$ -stage turbines. Figure 3-6(a) shows that the total efficiencies of the $1\frac{1}{2}$ -stage turbines are lower

than those of the 1-stage impulse turbines. These lower total efficiencies are due to the additional friction losses of the downstream stators. Because of this additional friction loss, the $1\frac{1}{2}$ -stage turbine achieves no gain in static efficiency over that of the 1-stage turbine until the value of λ is below approximately 0.35 (fig. 3-6(b)). For λ values below about 0.35, substantial gains in static efficiency can be achieved through use of downstream stators.

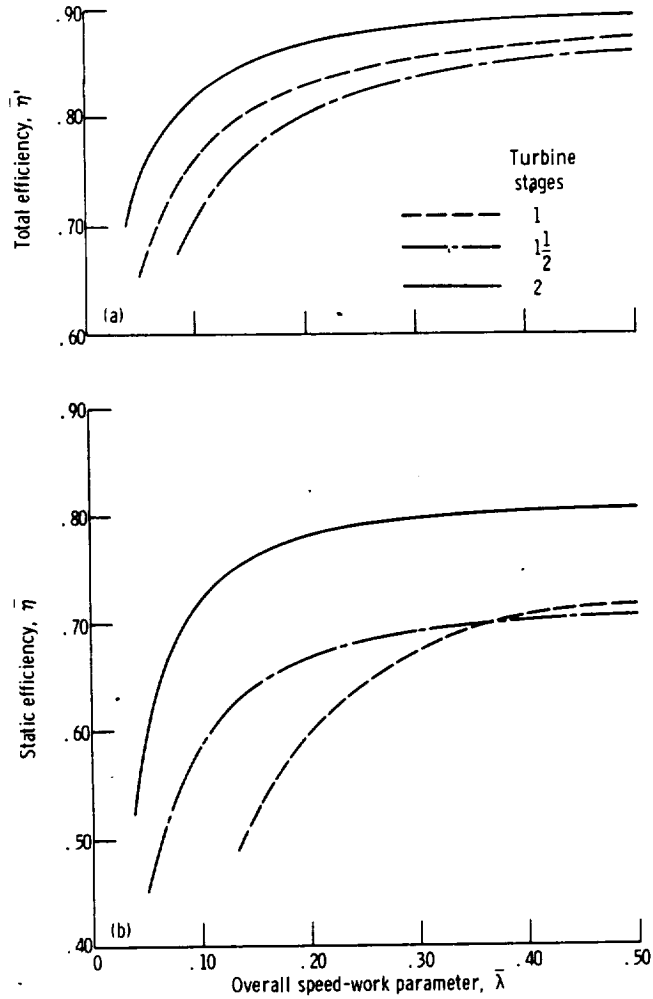


(a) Total efficiency.
 (b) Static efficiency.

FIGURE 3-6.—Effect of downstream stator on efficiency. (Curves from ref. 3.)

Multistage Turbine Efficiency

When the turbine requirements are such that the speed-work parameter is quite low and high efficiencies are still desired, multistage turbines are used, and the required work is split amongst the various stages.



(a) Total efficiency.
(b) Static efficiency.

FIGURE 3-7.—Comparison of efficiencies of 1-, 1½-, and 2-stage turbines. (Curves from ref. 4.)

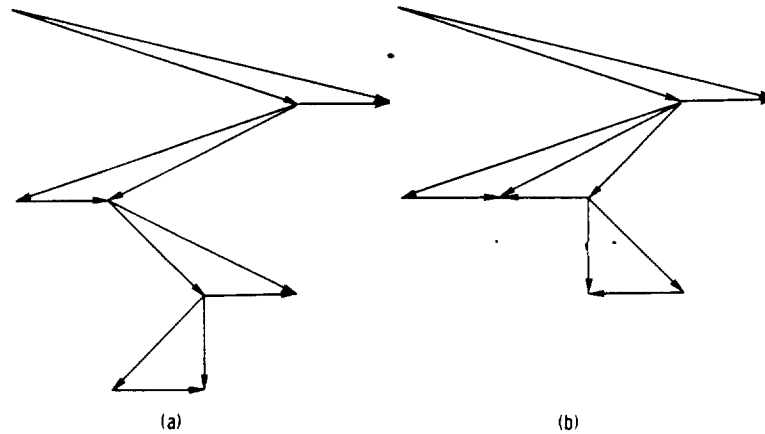
Two-stage turbines.—The addition of a second stage to a 1-stage turbine results in about doubling the average stage λ value through the reduction of stage work. As shown previously, an increase in stage λ is accompanied by an increase in stage efficiency. In addition, with two stages it becomes possible to adjust the stage work split and the exit swirls so as to maximize efficiency.

A study of the efficiency characteristics of 2-stage turbines is presented in reference 4. The efficiencies of 1-, 1½-, and 2-stage turbines (from ref. 4) are compared in figure 3-7. At an overall speed-work parameter, $\bar{\lambda}$, of 0.50, the 2-stage turbine has a 2-percentage-point-higher total efficiency and a 9-percentage-point-higher static efficiency than the 1-stage turbine. As $\bar{\lambda}$ is reduced to 0.15, the difference between the 2- and 1-stage efficiencies increases to 5 percentage points for total efficiency and 24 percentage points for static efficiency. The smaller difference between total and static efficiencies for the 2-stage turbine than for the 1-stage turbine occurs because the leaving loss for the 2-stage turbine is a much smaller fraction of the total work output.

The 2-stage turbine efficiencies presented in figure 3-7 are the maximum values obtained by varying stage work split and exit swirl while imposing good diagram criteria of no positive exit swirl and no negative reaction. At $\bar{\lambda}=0.5$, efficiency is maximized with a 50:50 work split and symmetrical zero-exit-swirl diagrams for each stage. As $\bar{\lambda}$ is reduced, maximum efficiency is achieved with zero exit swirl maintained in the second stage and an increasing fraction of the work produced by the first stage. At $\bar{\lambda}=0.125$, the optimum work split has increased to 75:25. The associated diagram features impulse first and second stages as well as an impulse second-stage stator. This type of diagram is illustrated in figure 3-8(a) and represents a type of turbine known as velocity compounded. In general, a velocity-compounded turbine is a two-stage (or three-stage) turbine in which all expansion (fluid velocity increase) is achieved in the first stator and all subsequent blade rows merely turn the flow with no change in velocity. As $\bar{\lambda}$ is reduced below 0.125, the velocity-compounded condition is maintained, but with increasing exit swirl and decreasing first-stage work fraction.

Figure 3-8(b) illustrates the velocity diagram for another type of two-stage turbine, the counterrotating turbine without a second-stage stator. The diagram shown is again for the $\bar{\lambda}=0.125$ case with zero exit swirl and with both blade speeds equal. A study of the efficiency characteristics of this type of turbine was made in reference 5. Efficiencies higher than those for conventional two-stage turbines were obtained because of the elimination of one blade row. Because the second-stage work depends upon the swirl leaving the first stage, the

TURBINE DESIGN AND APPLICATION



(a) Velocity-compounded turbine. (b) Counterrotating turbine.
 FIGURE 3-8.—Velocity-vector diagrams for special types of 2-stage turbines.
 Overall speed-work parameter $\bar{\lambda}$, 0.125.

second stage, in general, would be a low-work stage (work split is 75:25 for the illustrated diagram). The efficiencies and work splits are also functions of the blade-speed ratio. Because of their high efficiency potential at low $\bar{\lambda}$ levels and their compactness due to the lack of a blade row, counterrotating turbines are being utilized in such advanced applications as direct-lift engines for V/STOL aircraft.

n-stage turbines.—In many applications the combination of work and speed requirements dictates the use of turbines in which considerably more than two stages are required. Such applications include fan-drive turbines, vapor turbines used for power production, and turbopump turbines for nuclear hydrogen rockets.

The efficiency characteristics of multistage turbines composed of impulse stages (for $\lambda \leq 0.5$) or zero-exit-swirl stages (for $\lambda \geq 0.5$) are examined in reference 6. Equal stage work and constant stage blade speed were assumed. Overall and stage speed-work parameters are related (derived as eq. (2-111)) as

$$\lambda = n\bar{\lambda} \quad (3-16)$$

where n is the number of stages. Total efficiency for a first stage (stator-inlet velocity is axial) and total and static efficiencies for a general stage (intermediate or last stage, where stator inlet velocity is equal to stage exit velocity) were obtained as functions of λ . Overall efficiencies were then obtained from the stage efficiencies. For overall static efficiency, neglecting the reheat effect discussed in chapter 2,

$$\bar{\eta} = \frac{n\Delta h'}{\Delta h'_{i,a} + (n-2)\Delta h'_{i,t} + \Delta h_{i,t}} \quad (3-17)$$

where

$\Delta h'_{i,a}$ first-stage ideal work based on ratio of inlet total pressure to exit total pressure, J/kg; Btu/lb

$\Delta h'_{i,t}$ general-stage ideal work based on ratio of inlet total pressure to exit total pressure, J/kg; Btu/lb

$\Delta h_{i,t}$ general-stage ideal work based on ratio of inlet total pressure to exit static pressure, J/kg; Btu/lb

This equation neglects the reheat effect, which reference 6 shows to be small. By using the stage-efficiency definition, equation (3-17) becomes

$$\bar{\eta} = \frac{n}{\frac{1}{\eta_a} + \frac{n-2}{\eta_i} + \frac{1}{\eta_t}} \quad (3-18)$$

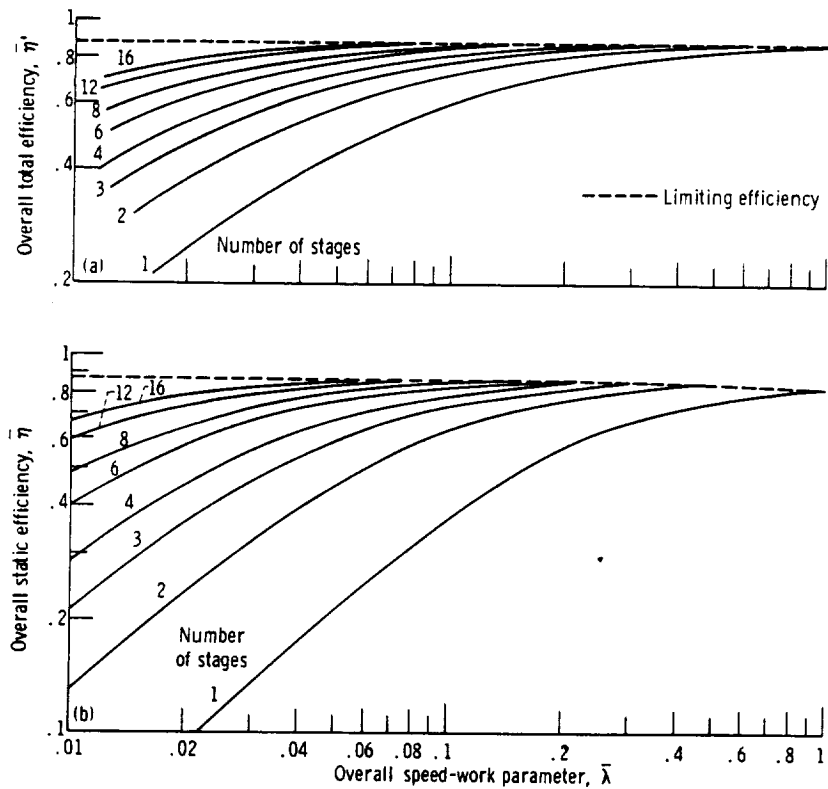
Overall total efficiency differs only in that the last stage is evaluated on the basis of stage total efficiency. Therefore,

$$\bar{\eta}' = \frac{n}{\frac{1}{\eta'_a} + \frac{n-1}{\eta'_i}} \quad (3-19)$$

The multistage efficiency characteristics obtained in this manner are presented in figure 3-9, which was obtained from reference 6. Figure 3-9(a) shows total efficiency as a function of $\bar{\lambda}$. The limiting efficiency (in this case, 0.88) is reached when all stages are at $\lambda=1$. This level of efficiency, as well as all those described herein, is a function of many other factors (stator angle, Reynolds number, blade aspect ratio, blade solidity, etc.) in addition to diagram shape and may vary upward or downward from the indicated value. The variations in efficiency with varying diagrams are, however, the concern here. This figure illustrates that at low $\bar{\lambda}$ values (0.1 or less), either large increases in the number of stages are required to achieve high total efficiencies or, if some restriction on the number of stages is imposed, lower efficiencies must be expected. The static efficiencies shown in figure 3-9(b) show similar trends, although at lower levels because of the leaving loss.

Another commonly used method of presenting turbine performance in terms of diagram parameters is to plot efficiency as a function of overall blade-jet speed ratio. This parameter was described in chapter 2 (eq. (2-72)) as the ratio of the blade speed to a velocity corresponding to the kinetic energy associated with the total-to-static pressure ratio across the turbine. Blade-jet speed ratio is related to speed-work

TURBINE DESIGN AND APPLICATION



(a) Total efficiency.

(b) Static efficiency.

FIGURE 3-9.—Overall efficiency characteristics. (Curves from ref. 6.)

parameter and efficiency according to equation (2-74).

From the discussions in this section, it is clear that the selections of the number of stages and velocity diagram type have an important effect on the expected efficiency level and are very dependent upon the specific work (actual or ideal) imposed and blade speed utilized. In an actual design, the final selection of the turbine diagrams must represent a compromise among such design goals as performance (dictated by the cycle requirements), structural integrity (related to component life), compactness, and weight.

RADIAL VARIATION OF DIAGRAMS

In the first half of this chapter, a single velocity diagram was assumed to represent average conditions over the entire blade span. In a turbine having a relatively high hub- to tip-radius ratio (about

0.85 or greater), such an assumption is reasonable. In the case of lower hub- to tip-radius ratios, however, substantial variations in the velocity diagrams are encountered, and the mean-section diagrams may or may not represent the average flow conditions for the entire blade span. The radial variations in diagrams are due to the radial variation in blade speed and the balance of forces that must exist in the flow. The considerations that were described for the mean section diagrams must also be applied to the end regions, which become very important in the final diagram selection. This section will consider the radial variations in flow conditions and their effect on the velocity diagrams.

Radial Equilibrium

Consider an element of fluid in the turbine flow field, as in figure 3-10(a). When there is a tangential component of velocity, the resulting circumferential flow (fig. 3-10(b)) must be maintained by a pressure force. The pressure force serves to balance the centrifugal force acting on the fluid and to keep the fluid moving along its curved path. When the through-flow path (streamline) is curved (fig. 3-10(c)), the force required to maintain the flow along this curved path must be accounted for as part of the net pressure force. Any linear acceleration of the flow must have an associated pressure force, part of which is in the radial direction if the streamline is inclined from horizontal. The balance of forces required to account for these factors is termed radial equilibrium.

The radial equilibrium will now be formulated mathematically. The pressure forces acting on an element of fluid are indicated in figure 3-10(b). Fluid weight is neglected. If unit length is assumed in the x direction, the net pressure force (directed radially inward) is

$$F_{p, net} = (p + dp)(r + dr)d\theta - prd\theta - 2 \left(p + \frac{dp}{2} \right) dr \sin \frac{d\theta}{2} \quad (3-20a)$$

where

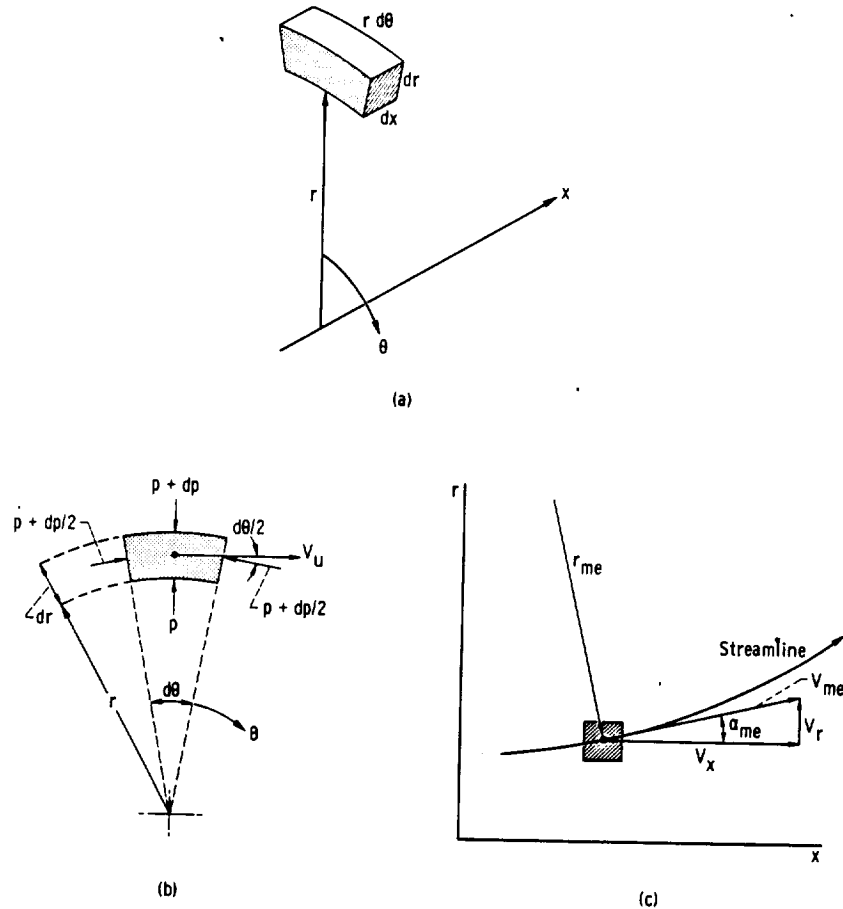
- $F_{p, net}$ net inward pressure force, N; lb
- p static pressure, N/m²; lb/ft²
- θ angle of rotation, rad
- r radius of rotation, m; ft

Neglecting higher-order terms (product of three differentials) and setting $\sin (d\theta/2) = d\theta/2$ yields

$$F_{p, net} = rdpd\theta \quad (3-20b)$$

The mass m of the fluid being acted on by the pressure force is

TURBINE DESIGN AND APPLICATION



(a) Element of fluid in turbine flow field. (b) Rotation plane ($r-\theta$). (c) Meridional plane ($r-x$).
 FIGURE 3-10.—Radial equilibrium factors.

$$m = \rho [\pi(r+dr)^2 - \pi r^2] \frac{d\theta}{2\pi} \quad (3-21a)$$

which reduces to

$$m = \rho r dr d\theta \quad (3-21b)$$

The net pressure force results from the three factors mentioned previously. To balance the centrifugal force associated with circumferential flow, the radial pressure force is

$$F_{p,c} = \frac{m}{g} \frac{V_u^2}{r} = \frac{\rho r dr d\theta}{g} \frac{V_u^2}{r} = \frac{\rho}{g} V_u^2 dr d\theta \quad (3-22)$$

VELOCITY DIAGRAMS

The radial component of the pressure force required to balance the centrifugal force associated with flow along the meridional streamline is

$$F_{p,r} = -\frac{m}{g} \frac{V_{me}^2}{r_{me}} \cos \alpha_{me} = -\frac{\rho r dr d\theta}{g} \frac{V_{me}^2}{r_{me}} \cos \alpha_{me} \quad (3-23)$$

where

V_{me} velocity along meridional streamline, m/sec; ft/sec

r_{me} radius of curvature of meridional streamline, m; ft

α_{me} angle of inclination of meridional streamline, deg

The positive directions for streamline curvature and inclination angle are as indicated in figure 3-10(c). The minus sign in equation (3-23) indicates that the balancing pressure force is directed outward in this case. The radial component of the pressure force required to produce the linear acceleration along the meridional streamline is

$$F_{p,t} = -\frac{m}{g} \frac{dV_{me}}{dt} \sin \alpha_{me} = -\frac{\rho r dr d\theta}{g} \frac{dV_{me}}{dt} \sin \alpha_{me} \quad (3-24)$$

Setting the net radial pressure force (eq. (3-20(b)) equal to the various components (eqs. (3-22), (3-23), and (3-24)) yields

$$\frac{g}{\rho} \frac{dp}{dr} = \frac{V_z^2}{r} - \frac{V_{me}^2}{r_{me}} \cos \alpha_{me} - \frac{dV_{me}}{dt} \sin \alpha_{me} \quad (3-25)$$

Equation (3-25) is the radial equilibrium equation and includes all contributing factors. It is, however, not convenient to use in its complete form. For axial flow (or near-axial flow), the meridional streamline curvatures ($1/r_{me}$) and inclination angles (α_{me}) are both quite small. Therefore, the last two terms on the right side of equation (3-25) are small as compared to the first (rotational) term and can often be neglected. Thus, we can write

$$\frac{g}{\rho} \frac{dp}{dr} = \frac{V_z^2}{r} \quad (3-26)$$

The approximation represented by equation (3-26) has become known as "simple" radial equilibrium.

Radial Variations in Velocity

In order to illustrate the nature of the radial variations in velocity, those effects that are usually second order will be neglected, and certain other simplifying assumptions will be made. If streamline slope is assumed to be zero, there is no radial component of velocity, and the total enthalpy definition (eq. (1-49)) can be written as

$$h' = h + \frac{V_u^2}{2gJ} + \frac{V_z^2}{2gJ} \quad (3-27)$$

Differentiating with respect to radius and using equation (1-8) to substitute for dh (and since $\rho = 1/v$) yields

$$\frac{dh'}{dr} = T \frac{ds}{dr} + \frac{1}{J\rho} \frac{dp}{dr} + \frac{1}{2gJ} \frac{d(V_u^2)}{dr} + \frac{1}{2gJ} \frac{d(V_z^2)}{dr} \quad (3-28)$$

If the flow entering the turbine is radially uniform, then the total enthalpy at the first-stator exit is radially constant. Further, if the stator loss is radially constant, then the entropy at the first-stator exit is also radially constant. The rotor, as will be discussed later in this chapter, may or may not have radially constant work (total enthalpy) extraction and probably does not have radially constant loss. At any place in the turbine, therefore, radial gradients in total enthalpy and entropy depend on the uniformity of the inlet flow, the gradients imposed by the various blade rows, and the gradient damping due to radial mixing.

For simplicity, it is here assumed that the total enthalpy and the entropy are radially constant. With these assumptions and with equation (3-26), the "simple" radial equilibrium expression, substituted into equation (3-28), we get

$$\frac{V_u^2}{r} + \frac{1}{2} \frac{d(V_u^2)}{dr} + \frac{1}{2} \frac{d(V_z^2)}{dr} = 0 \quad (3-29)$$

In order to solve this equation, it is necessary to independently specify a relation between V_u or V_z and r or between V_u and V_z . Most often, a variation of swirl velocity with radius has been specified as

$$V_u = Kr^N \quad (3-30a)$$

or, in terms of mean-section conditions,

$$\frac{V_u}{V_{u,m}} = \left(\frac{r}{r_m}\right)^N \quad (3-30b)$$

Substituting equation (3-30b) and its differential form into equation (3-29) and then integrating between the limits of r_m and r yields

$$\frac{V_z}{V_{z,m}} = \left\{ 1 - \tan^2 \alpha_m \left(\frac{N+1}{N}\right) \left[\left(\frac{r}{r_m}\right)^{2N} - 1 \right] \right\}^{1/2} \quad (3-31)$$

where α_m is the absolute flow angle at the mean radius. Equation (3-31) is not valid for the special case of $N=0$ (constant V_u). For this

special case, integration of equation (3-29) yields

$$\frac{V_z}{V_{z,m}} = \left[1 - 2 \tan^2 \alpha_m \ln \frac{r}{r_m} \right]^{1/2} \quad (3-32)$$

A case of interest not covered by equation (3-30b) is that where the absolute flow angle is radially constant. In this case, $V_u = V_z \tan \alpha$, and equation (3-29) integrates to

$$\frac{V_u}{V_{u,m}} = \frac{V_z}{V_{z,m}} = \left(\frac{r}{r_m} \right)^{-\sin^2 \alpha} \quad (3-33)$$

The radial variations in swirl velocity, axial velocity, and flow angle, as computed from the above equations, are presented in figure 3-11 for a mean radius flow angle of 60° . The radial variations in axial velocity and flow angle are largely dependent on the specified swirl

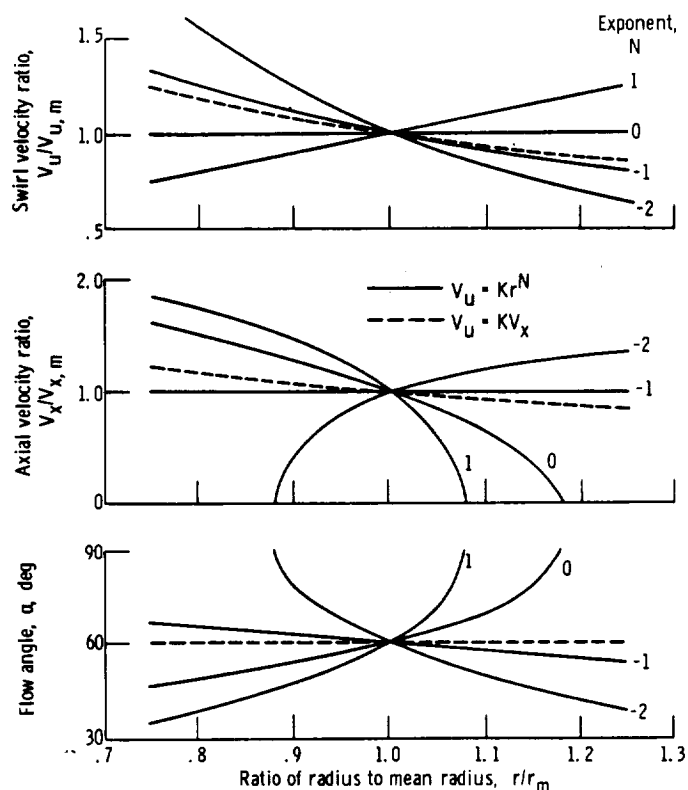


FIGURE 3-11.—Radial variations of velocity and flow angle. Mean-section flow angle α_m , 60° .

velocity variation (value of N). As the swirl distribution exponent N increases or decreases from a value of -1 , the changes in axial velocity and flow angle with changing radius become more pronounced. As seen, the axial velocities and flow angles associated with certain values of N cannot be obtained with all blade lengths. The range of N that can be used for design purposes becomes larger as the blades become shorter (values of r_h/r_m and r_t/r_m closer to 1). The effects of the radial variations illustrated in figure 3-11 on stage velocity diagrams are discussed in subsequent sections of this chapter.

Free-Vortex Diagrams

When a value of -1 is used for the exponent N in equation (3-30a), then

$$rV_u = K \quad (3-34)$$

This is the condition for flow in a free vortex, and a turbine designed for such a swirl distribution is referred to as a free-vortex design, or a free-vortex turbine.

The free-vortex design is used in the vast majority of axial-flow turbines in which radial variation of the diagram is accounted for. If this condition is specified at both the stator and rotor outlets, then there is no radial variation in specific work, $\Delta(UV_u)$, because the UV_u products both entering and leaving the rotor are radially constant. Thus, the specific work computed from the mean-section diagram is valid for the entire flow. Further, if $N = -1$ in equation (3-31), the axial velocity V_z is radially constant. Thus, the radial variation in mass flow per unit area (ρV_z) is small, and the mass flow rate obtained from the mean-section velocity diagram can be used to represent the entire flow within an accuracy of 0.1 percent in most cases. This design simplicity is one of the main reasons for the wide use of free-vortex designs for axial-flow turbines.

An example set of velocity diagrams for a free-vortex design is shown in figure 3-12 for the hub, mean, and tip sections of a blade with a radius ratio of 0.6. The radial variation in the diagram shape is considerable. The mean-section diagram for this example is a symmetrical zero-exit-swirl diagram having a speed-work parameter λ_m of 1. The associated hub diagram is nearly an impulse diagram ($\lambda_h = 0.56$), while the tip diagram is very conservative, with high reaction ($\lambda_t = 1.56$). Thus, for a free-vortex swirl distribution, the hub section is the critical section from an aerodynamic standpoint (lowest efficiency). Therefore, special care must be taken when selecting the mean-section diagram, especially for low-radius-ratio blades, in order to ensure satisfactory diagrams at the hub section. A

VELOCITY DIAGRAMS

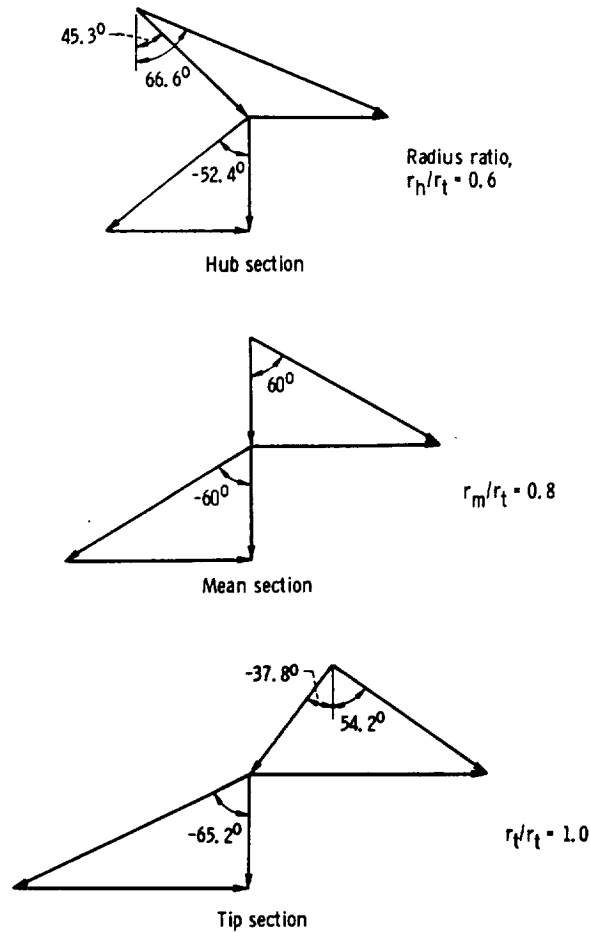


FIGURE 3-12.—Radial variation of velocity-vector diagrams for free-vortex flow. Stator mean-section exit angle α_m , 60° ; mean-section speed-work parameter λ_m , 1.

very high reaction tip diagram can also be troublesome because it increases leakage across the blade tip clearance space.

Another potential problem is that of rotor-blade twist. There is a considerable radial variation in rotor inlet angle. For the case illustrated in figure 3-12, the rotor inlet angle varies from 45° at the hub to -38° at the tip, a variation of 83° . This results in a blade having an overhanging tip section, thus causing some fabrication problems and bending stresses. The positioning of the hub and tip sections of such a blade is illustrated in figure 3-13.

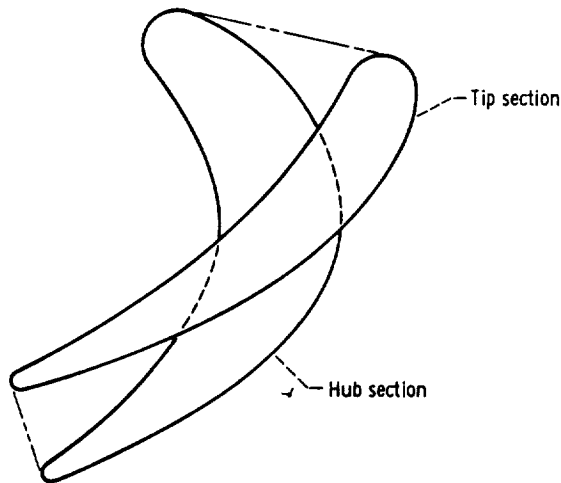


FIGURE 3-13.—Relative positioning of hub and tip sections of free-vortex turbine.

Non-Free-Vortex Diagrams

Free-vortex designs are so commonly used that all other designs are often classified under the common heading of non-free vortex. The non-free-vortex designs are used in an attempt to alleviate some of the potential disadvantages associated with the free-vortex design. Illustrated in figure 3-14 are the radial variations in diagrams for the cases having the velocity variations illustrated in figure 3-11. The super-vortex ($N=-2$) design, the constant-swirl ($N=0$) design, the wheel-flow, or solid-rotation, ($N=1$) design, and the constant-flow-angle design are compared with the free-vortex ($N=-1$) design. The mean-section diagrams, which are at a radius ratio r/r_m of 1, are the same for all cases. Also shown are diagrams at radius ratios r/r_m of 0.75, 0.889, 1.111, and 1.25. For a blade with a hub- to tip-radius ratio of 0.6, the r/r_m values of 0.75 and 1.25 correspond to the hub and tip sections, respectively. For a blade with a hub- to tip-radius ratio of 0.8, the r/r_m values of 0.889 and 1.111 correspond to the hub and tip sections, respectively. As the blade hub- to tip-radius ratio decreases, any particular value of r/r_m corresponds to a blade section relatively closer to the mean section. There are, of course, no diagrams to show in figure 3-14 for those particular cases for which, as shown in figure 3-11, no real values exist for axial velocity.

At any radius ratio, the rotor exit diagrams are the same for all the swirl distributions. This is due to the selected mean-section diagram having zero exit swirl ($\alpha_{2,m}=0$).

The constant-flow-angle diagrams are quite similar to the free-

VELOCITY DIAGRAMS

Ratio of radius to mean radius, r/r_m	Radial swirl distribution				
	Super vortex ($N = -2$)	Free vortex ($N = -1$)	Constant swirl ($N = 0$)	Wheel flow ($N = 1$)	Constant flow angle
1.250			(a)	(a)	
1.111				(a)	
1.000					
0.889					
0.750	(a)				

^aNo real value for axial velocity.

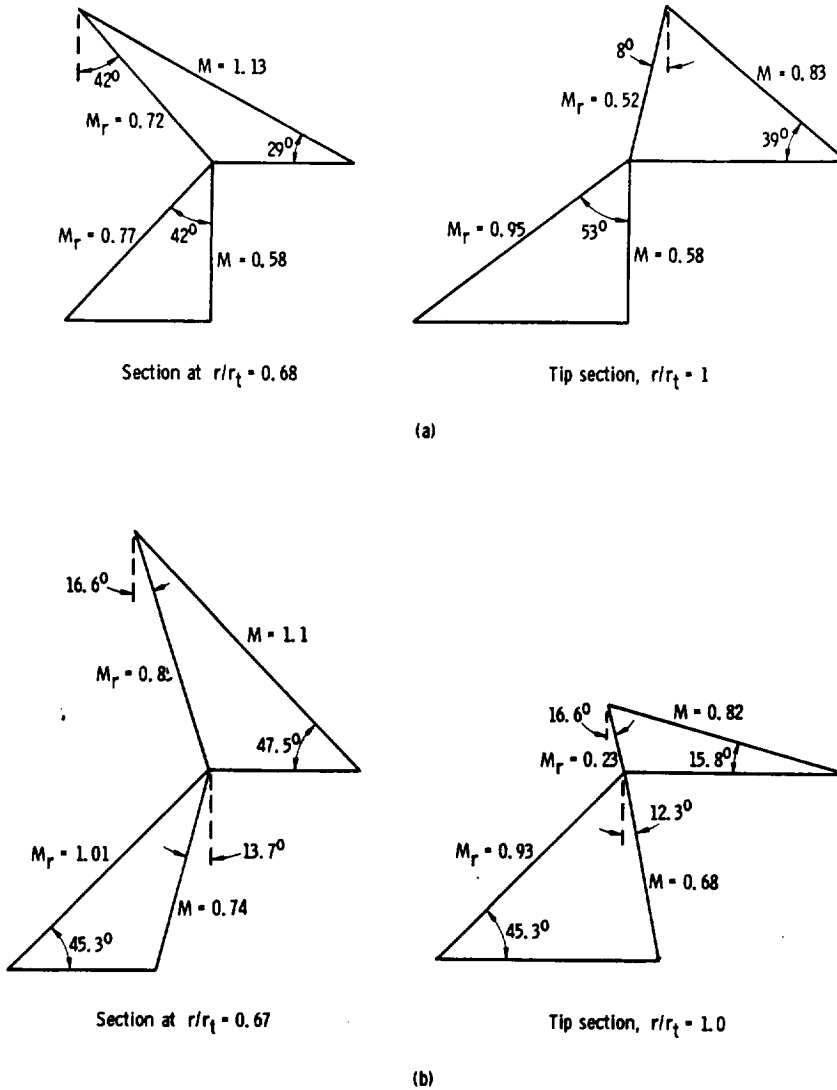
FIGURE 3-14.—Radial variation of velocity-vector diagrams for various swirl distributions.

vortex diagrams and, therefore, present the same problems of high rotor-blade twist and low hub reaction. A possible advantage is that the constant-flow-angle stator has no twist, while the free-vortex stator has a small amount of twist (about 12°).

The super-vortex ($N = -2$) diagrams appear to have no advantage of any sort. The blade twist is more severe than for the free-vortex case. The radial variation of stator-exit axial velocity is large and cannot be sustained (V_z becomes imaginary) on blades with hub- to tip-radius ratios much below 0.8.

The constant-swirl ($N = 0$) and wheel-flow ($N = 1$) diagrams do alleviate the blade-twist and hub-reaction problems of the free-vortex design. However, here too the radial variation in axial velocity is large and cannot be sustained on blades with hub- to tip-radius ratios below about 0.70 for the constant-swirl ($N = 0$) design and below about 0.85 for the wheel-flow ($N = 1$) design. In addition, the hub absolute and relative velocities at the stator exit are higher for these designs than for the free-vortex design. For relatively high Mach number turbines, these higher flow velocities could cause higher losses than those of a free-vortex design.

TURBINE DESIGN AND APPLICATION



(a) Free-vortex turbine.
 (b) Nontwisted turbine.
 FIGURE 3-15.—Comparison of velocity-vector diagrams of free-vortex and nontwisted turbines. (Diagrams from ref. 9.)

A design procedure for rotor blades of constant inlet and exit angle, termed a "nontwisted" design, is presented in reference 7. Such a design completely eliminates twist in the rotor, which, therefore, should be easy to fabricate. References 8 and 9 contain experimental results comparing free-vortex designs with nontwisted designs. The design velocity diagrams used for the study of reference 9 are shown in figure 3-15. A large radial variation in axial velocity at the stator exit is also present in this nontwisted design. The stator-exit conditions correspond closely to a swirl-distribution-exponent (N) value of $\frac{1}{4}$. Although rotor twist is eliminated, stator twist has increased from 10° for the free-vortex design to more than 30° for the nontwisted design. At the rotor exit, the swirl is negative at the hub and positive at the tip. The relative blade-inlet Mach number at the hub is higher for the nontwisted design (0.85) than for the free-vortex design (0.72). However, the reaction at the hub of the nontwisted design is improved over that of the free-vortex turbine. The two turbines have about the same efficiency.

The non-free-vortex designs all feature radial variation in specific work and, because of the radial gradient in axial velocity, radial variation in mass flow rate per unit area. Thus, the mean-section conditions may not represent true average conditions, and considerable error may occur if such a turbine is designed on the basis of the mean-section flow conditions. A non-free-vortex turbine should be designed by integrating the flow conditions between hub and tip in order to compute work and flow rate. The proper design of a non-free-vortex turbine is, therefore, much more complex than the design of a free-vortex turbine. With computerized design procedures, however, this additional complexity is no real disadvantage.

As seen from this discussion, the use of non-free-vortex designs to alleviate the rotor-twist and hub-reaction problems associated with free-vortex designs results in other problems such as higher hub Mach numbers, increased stator twist, and increased design complexity. It has been shown that large deviations from free-vortex designs cannot be sustained over all blade spans. However, small deviations from free-vortex designs, as reported in reference 10, have been used to obtain improved turbine performance.

COMPUTER PROGRAMS FOR VELOCITY-DIAGRAM STUDIES

This chapter has presented some of the basic aspects of velocity-diagram selection, including diagram types, their relation to efficiency, staging, and radial variations. It is evident that the determination of the best diagrams and number of stages for a given application requires

many considerations. If it is desired to include non-free-vortex designs, meridional-streamline curvature effects, and radial variation in efficiency, then such analyses are out of the realm of hand calculation. Therefore, computer programs have been evolved to perform such tasks.

One such computer program is described in references 11 and 12. The program includes consideration of streamline-curvature effects in the radial equilibrium equation and radial gradients in enthalpy and entropy in determining radial variations in flow. In addition, it not only allows for blade loss as an input but also includes an internal loss correlation using the information from reference 13 as a basis. This program uses stator exit swirl distribution and rotor work (which reflects rotor exit swirl) distribution as inputs. However, for many values and combinations of these input specifications, either there is no real solution for meridional velocity ($V_{m0} = V_z / \cos \alpha_{m0}$) or the computer cannot find the solution because of a large variation in dependent variable (meridional velocity) with small variations in independent variable (swirl velocity). The existence of these conditions is indicated by figure 3-11.

This problem has resulted in a program modification, as reported in reference 14, wherein the radial variation in meridional velocity instead of swirl velocity is used as input. The modified program has proven very successful and shows that valid turbine designs can be generated with any reasonable variation in meridional velocity.

REFERENCES

1. STEWART, WARNER L.: A Study of Axial-Flow Turbine Efficiency Characteristics in Terms of Velocity Diagram Parameters. Paper 61-WA-37, ASME, Dec. 1961.
2. STEWART, WARNER L.: Analytical Investigation of Single-Stage-Turbine Efficiency Characteristics in Terms of Work and Speed Requirements. NACA RM E56G31, 1956.
3. WINTUCKY, WILLIAM T.; AND STEWART, WARNER L.: Analysis of Efficiency Characteristics of a Single-Stage Turbine with Downstream Stators in Terms of Work and Speed Requirements. NACA RM E56J19, 1957.
4. STEWART, WARNER L.; AND WINTUCKY, WILLIAM T.: Analysis of Two-Stage-Turbine Efficiency Characteristics in Terms of Work and Speed Requirements. NACA RM E57F12, 1957.
5. WINTUCKY, WILLIAM T.; AND STEWART, WARNER L.: Analysis of Two-Stage Counterrotating Turbine Efficiencies in Terms of Work and Speed Requirements. NACA RM E57L05, 1958.
6. STEWART, WARNER L.: Analytical Investigation of Multistage-Turbine Efficiency Characteristics in Terms of Work and Speed Requirements. NACA RM E57K22b, 1958.

VELOCITY DIAGRAMS

7. SLIVKA, WILLIAM R.; AND SILVERN, DAVID H.: Analytical Evaluation of Aerodynamic Characteristics of Turbines with Nontwisted Rotor Blades. NACA TN 2385, 1951.
8. HEATON, THOMAS R.; SLIVKA, WILLIAM R.; AND WESTRA, LEONARD F.: Cold-Air Investigation of a Turbine with Nontwisted Rotor Blades Suitable for Air Cooling. NACA RM E52A25, 1952.
9. WHITNEY, WARREN J.; STEWART, WARNER L.; AND MONROE, DANIEL E.: Investigation of Turbines for Driving Supersonic Compressors. V-Design and Performance of Third Configuration with Nontwisted Rotor Blades. NACA RM E53G27, 1953.
10. DORMAN, T. E.; WELNA, H.; AND LINDLAUF, R. W.: The Application of Controlled-Vortex Aerodynamics to Advanced Axial Flow Turbines. J. Eng. Power, vol. 90, no. 3, July 1968, pp. 245-250.
11. CARTER, A. F.; PLATT, M.; AND LENHERR, F. K.: Analysis of Geometry and Design Point Performance of Axial Flow Turbines. I-Development of the Analysis Method and the Loss Coefficient Correlation. NASA CR-1181, 1968.
12. PLATT, M.; AND CARTER, A. F.: Analysis of Geometry and Design Point Performance of Axial Flow Turbines. II-Computer Program. NASA CR-1187, 1968.
13. SMITH, S. F.: A Simple Correlation of Turbine Efficiency. J. Roy. Aeron. Soc., vol. 69, no. 655, July 1965, pp. 467-470.
14. CARTER, A. F.; AND LENHERR, F. K.: Analysis of Geometry and Design-Point Performance of Axial-Flow Turbines Using Specified Meridional Velocity Gradients. NASA CR-1456, 1969.

SYMBOLS

<i>A</i>	flow area, m ² ; ft ²
<i>F_p</i>	pressure force, N; lb
<i>g</i>	conversion constant, 1; 32.17 (lbm)(ft)/(lbf)(sec ²)
<i>h</i>	specific enthalpy, J/kg; Btu/lb
<i>J</i>	conversion constant, 1; 778 (ft)(lb)/Btu
<i>K</i>	proportionality constant
<i>L</i>	loss, J/kg; Btu/lb
<i>m</i>	mass, kg; lb
<i>N</i>	swirl distribution exponent
<i>n</i>	number of stages
<i>p</i>	pressure, N/m ² ; lb/ft ²
<i>R</i>	reaction
<i>r</i>	radius, m; ft
<i>s</i>	specific entropy, J/(kg)(K); Btu/(lb)(°R)
<i>T</i>	temperature, K; °R
<i>U</i>	blade speed, m/sec; ft/sec
<i>V</i>	absolute velocity, m/sec; ft/sec
<i>v</i>	specific volume, m ³ /kg; ft ³ /lb
<i>W</i>	relative velocity, m/sec; ft/sec
<i>w</i>	mass flow rate, kg/sec; lb/sec
<i>α</i>	fluid absolute flow angle, deg
<i>η</i>	efficiency
<i>θ</i>	angle of rotation, deg
<i>λ</i>	speed-work parameter
<i>ρ</i>	density, kg/m ³ ; lb/ft ³

Subscripts:

<i>a</i>	first stage
<i>an</i>	annulus
<i>c</i>	component due to circumferential flow
<i>h</i>	hub
<i>i</i>	general stage
<i>id</i>	ideal
<i>l</i>	component due to linear acceleration
<i>m</i>	mean section
<i>me</i>	meridional
<i>net</i>	net
<i>r</i>	radial component
<i>ro</i>	rotor
<i>s</i>	component due to streamline curvature
<i>st</i>	stator
<i>stg</i>	stage

VELOCITY DIAGRAMS

t tip
 u tangential component
 x axial component
0 at stator inlet
1 at stator exit or rotor inlet
2 at rotor exit

Superscripts:

— overall turbine
' absolute total state